7,8-Dihydroneopterin and its effect on the formation of foam cells.

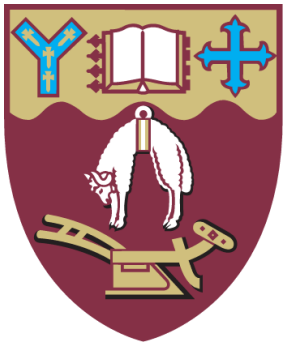

A thesis submitted in partial fulfilment of the requirements for the degree of Master of Science in Biochemistry at the University of Canterbury, New Zealand.

School of Biological Sciences
University of Canterbury

SIAN PATRICIA MARY DAVIES
2/1/2015

Contents

Figures……..…….Page

Abbreviations

7,8-NP	7,8-Dihydroneopterin
7KC	7-ketocholesterol
ɣ-IFN	Gamma interferon
ABC-A1/G1	ATP-binding cassette
AGE	Advanced glycated products
Apo-A1	Apolipoprotein-A1
BCA	Bicinchoninic acid
BHT	Butylated hydroxytoluene
c-DNA	Complementary deoxyribose nucleic acid
$CuCl_2$	Copper chloride
EDTA	Ethylene diamine tetracetic acid
FAK	Focal Adhesion Kinase
FFA	Free fatty acids
GMSCF	Granulocyte and monocyte colony-stimulating factor
GSH	Glutathione
GSSG	Glutathione disulphide
H_2O_2	Hydrogen peroxide
HDL	High density lipoprotein

HMDM	Human monocyte derived macrophage
HOCl	Hypochlorous acid
HPLC	High pressure liquid chromatography
KOH	Potassium hydroxide
LDL	Low density lipoprotein
MAP kinase	Mitogen-activated protein kinase
MCP-1	Monocyte chemotactic protein-1
MeOH	Methanol
MFI	Mean fluorescence intensity
MIF	Migration Inhibitory Factor
MPO	Myeloperoxidase
NADPH	Nicotinamide adenine dinucleotide phosphate
NaOH	Sodium hydroxide
NOX	NADPH oxidase
$O^{2-\cdot}$	Superoxide radical
oxLDL	Oxidised low density lipoprotein
PBS	Phosphate buffer saline
PMA	Phorbol 12-myristate 13-acetate
PPAR-ɣ	Peroxisome proliferator-activated receptor-ɣ
p/s	Penicillin/streptomycin
ROS	Reactive oxygen species
RPMI	Roswell Park Memorial Institute
SDS	Sodium Dodecyl sulfate
TAG	Triacylglycerides
VLDL	Very low density lipoprotein

Abstract

Atherosclerosis (Heart Disease) is an inflammatory disease caused by the formation of plaque within the arterial wall. In response to inflammation, monocytes enter the artery wall, differentiate into macrophages and take up altered low-density-lipoprotein (such as oxidised-LDL). This oxLDL is taken up into the phagocytotic macrophages via the action of the scavenger receptors. If more oxLDL is engulfed than the cell can process, they further differentiate into lipid-loaded foam cells. These are the main cell type found in atherosclerotic plaques. The scavenger receptor CD36 is responsible for 70% of oxLDL uptake by macrophages. Previous studies show that CD36 expression can be down regulated by the antioxidant, 7,8-dihydroneopterin. This research focuses on the effect of CD36 down regulation by 7,8-dihydroneopterin on foam cell formation.

Human macrophages prepared from monocytes purified from human blood were incubated with copper oxidised LDL for up to 48 hours. Macrophage accumulation of the sterols was measured using a high performance chromatograph (HPLC) method developed as part of this project. The HPLC analysis measured: cholesterol, cholesteryl-oleate and -palmitate and 7-ketocholesterol accumulation within human macrophages. A flow cytometry procedure was developed where the strongly adherent macrophages could be lifted from the tissue culture plates before immuno staining for CD36. Effect of incubating macrophages with 7,8-dihydroneopterin on the formation of foam cells was studied by measuring the lipid content by HPLC and flow cytometry measurement of CD36.

HPLC analysis showed non-cytotoxic levels of oxLDL produced a large accumulation of cholesterol and cholesteryl esters in the macrophages. Cholesterol, 7-ketocholesterol and cholesteryl-oleate and -palmitate concentrations in the cells rose significantly over the first 24 hours and stayed at a steady level for the following 24 hours. CD36 levels was further analysed on human macrophages. This study shows that foam cell formation can be measured using human macrophages. 7,8-Dihydroneopterin treatment resulted in a reduction of cholesterol and oxysterol uptake back to basal levels. It also reduced CD36 cell surface expression by a third. These results suggest that even a small reduction in CD36 cell surface expression may have a large effect on foam cell formation. This is another mechanism by which 7,8-dihydroneopterin protects against atherosclerosis developing.

1 Introduction

1.1 Overview

Though a huge amount of international effort has gone into researching the mechanism of atherosclerosis and general vascular disease, the actual mechanism driving the collection and growth within the artery wall proven to be difficult to define. Atherosclerosis is characterised by the collection of immune cells, mainly macrophages between the layers of the artery wall. With time this atherosclerotic plaque becomes a distinct growth which pushes the artery wall out into the flow of blood. This occlusion of the artery restricts the flow of blood generating many of the symptoms of vascular disease. Rupture of the plaque causes blood clots to enter the blood stream resulting in a heart attack or stroke. As atherosclerotic plaques take decades to develop, unravelling the underlying cause of the disease is analogous to turning up late at a brawl, tasked with investigating the reason for the disturbance. The order of events leading up to the first punch being thrown is crucial but just like in a street fight, the nuances of the initial interactions are complicated, subtle and difficult to determine.

The early stages of the disease cause changes in the cells which have been difficult to detect *in vivo*. These stages involve monocytes accumulating at the site of inflammation and differentiating into macrophages. Macrophages take up oxidised low density lipoprotein (oxLDL) via the CD36 scavenger receptor. Binding of oxLDL to CD36 results in interactions which allow the cell to uncontrollably accumulate cholesterol esters. This accumulation transforms the macrophages into foam cells. Foam cells amass between the intima and media of the artery wall and start to degrade via apoptosis and necrosis, forming a necrotic core. This necrotic core that develops between these sections of artery wall is the beginning of the atherosclerotic plaque that results in heart disease which is common in a third of the western world (Roger et al. 2012).

The research presented in this thesis examines the possibility of blocking the macrophage uptake of oxLDL with a specific macrophage antioxidant to prevent foam cell formation. The aim is by studying the interactions of the protein expression of scavenger receptor CD36 and its relation to ester uptake, a more complete understanding of the initial stages of plaque development will result. Macrophages

produce an antioxidant to protect themselves from the inflammatory environment that leads to foam cell formation. 7,8-Dihydroneopterin (7,8-NP) is a pterin found to scavenge free radicals (Baird et al. 2005; Oettl et al. 1997; Gieseg et al. 2001; Gieseg et al. 1995). Previous studies in this laboratory showed 7,8-dihydroneopterin down regulates the expression of CD36 in monocyte derived macrophages (HMDM) (Shchepetkina 2013). This was shown to decrease oxLDL uptake using 7-ketocholesterol as a marker of oxLDL uptake. It did not demonstrate whether the down regulation prevented foam cell formation as defined by Kritharides (L. Kritharides et al. 1993). This thesis specifically investigates the effects of 7,8-dihydroneopterin on CD36 cell surface expression and the effect CD36 down regulation has on cholesterol accumulation within macrophages. The addition of 7,8-dihydroneopterin to macrophages is postulated to prevent foam cell formation. It is hypothesised that this mechanism occurs *in vivo* and it is the failure of this mechanism that may lead to the development of atherosclerosis.

1.2 Atherosclerosis

Atherosclerosis is an inflammatory disease of the artery wall (Libby 2002). It involves chronic inflammatory responses without the benefit of the system fully returning to homeostasis. At bifurcations of the artery and other areas of turbulent blood movement, the wall of the artery is susceptible to inflammatory damage. This results in the tissue sending out chemo-attractants. These chemokines result in the recruitment of monocytes and other inflammatory cells (T-lymphocytes) to the area.

When monocytes are present a range of chemicals such as GMCSF (Granulocyte and Monocyte colony-stimulating factor) induce differentiation into Macrophages (Libby 2002). Macrophages are crucial in the healing of the artery intima as they are involved both in the reparation and remodelling of the tissue after the inflammatory episode (Gordon and Taylor 2005), as well as clearing debris from the area. Macrophages have been identified in atherosclerotic plaques in all stages of plaque development. Monocyte differentiated macrophages are therefore involved in atherosclerosis from the initiation of the disease (Saha et al. 2009; Fenyo and Gafencu 2013). Clearing debris from an area of infection or inflammation is a necessary and healthy process however exposure of the cell to oxidised low density lipoprotein (oxLDL) alters the normal cellular response.

During the inflammatory process, the scavenger receptor CD36 recognises and binds the oxLDL (Image 1). OxLDL particles were originally low density lipoprotein

particles that have been oxidised. It is not conclusively known where the oxidants come from that oxidise LDL. Oxidation of LDL at the site of inflammation (inside the artery wall) can occur via any of the cell types found in the artery wall, as well as through reactions involving free radicals and Reactive Oxygen Species (ROS).

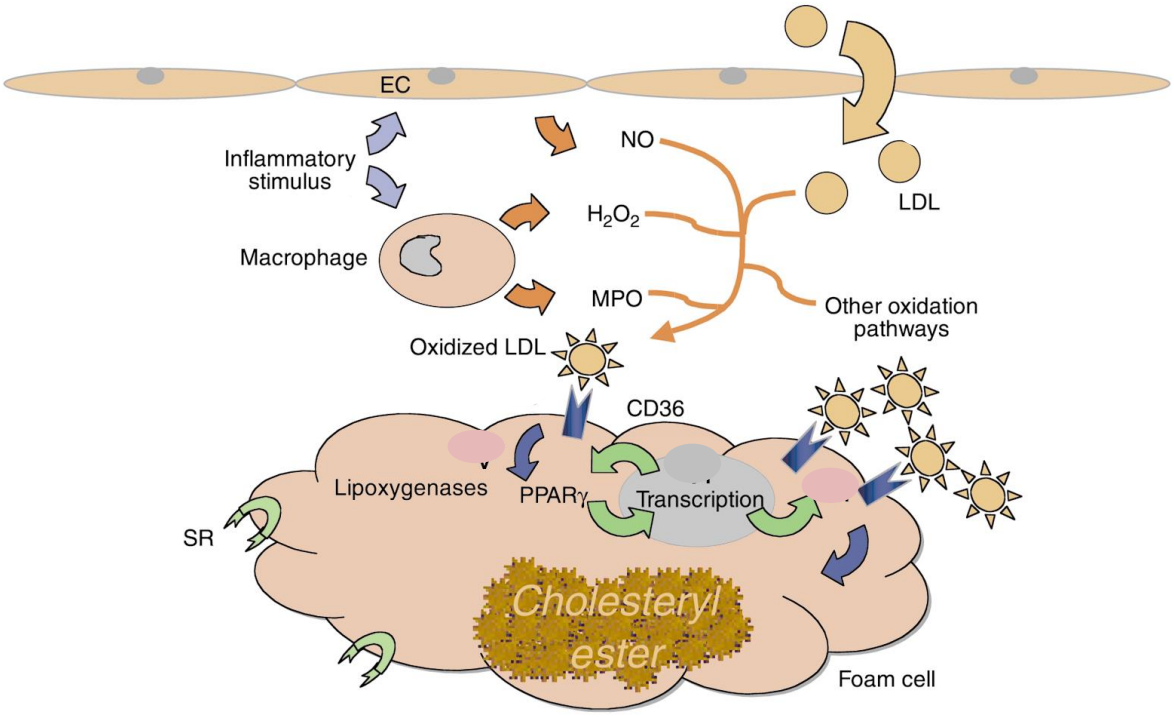

Image 1. Macrophage and LDL migration to the site of the inflammation. Once in the intima of the artery wall, the LDL is oxidised. OxLDL is internalised by the macrophage and the cell is transformed into a foam cell. Scavenger Receptor A is also depicted as SR and the Endothelial cells (EC) that are the barrier between the intima and artery interior are also present. Image adapted from Febbraio. (Febbraio, Hajjar, and Silverstein 2001)

Cells can oxidise LDL primarily through the over activation of NADPH oxidase (NOX). NOX is found in every cell type and is an enzyme that catalyses the electron transfer from NADPH to oxygen to form superoxide ($O_2^{\cdot-}$) (Lugrin et al. 2014). Superoxide either then reacts with superoxide dismutase or spontaneously forms H2O2 (Maxwell and Lip 2003). The reaction to hydrogen peroxide is very fast (Kerr, Bender, and Monti 1996). Hydrogen peroxide is turned into HOCl in order to break down foreign materials such as bacteria (Aviram 1992; Podrez et al. 1999).

Another source of LDL oxidation is free radicals. Free radicals are molecules with unpaired electrons, such as superoxide ($O_2^{\cdot-}$), which is also a ROS. It stabilises itself by removing electrons from surrounding molecules such as the proteins and lipids that make up LDL (Maxwell and Lip 2003). A major source of free radicals are leakages

from electron transport chains (Dean et al. 1997). Another source of free radical formation is when free copper or iron ions react with hydrogen peroxide to form hydroxyl radicals ($OH^{\cdot}$).

Lipids and proteins then react with the hydroxyl radical (image 2, equation1), via a carbon centred radical. Carbon centred radicals then rearrange to form conjugated dienes which react with oxygen to form peroxyl radicals, producing a lipid or protein hydroperoxyl radical through electron transfer (image 2, equation 2) (Kerr, Bender, and Monti 1996; Maxwell and Lip 2003). Lipid hydroperoxyls are unstable and degrade to secondary products such as cytotoxic alkanes and aldehydes.

Equation 1 - initiation phase of lipid peroxidation

$$LH + OH^{\bullet} \rightarrow L^{\bullet} + H_2O$$

$$L^{\bullet} + O_2 \rightarrow LOO^{\bullet}$$

Equation 2 - Propagation/Chain Reaction phase, oxygen independent stage

$$LOO^{\bullet} + LH \rightarrow LOOH + L^{\bullet}$$

Image 2 Free radical peroxidation of lipids. The process by which lipids and proteins can be altered into species such as oxLDL. Adapted from Dotan. (Dotan, Lichtenberg, and Pinchuk 2004)

Lipids are chemically structured in a manner that makes them vulnerable to peroxidation via their bis-allylic methylene groups (Maxwell and Lip 2003). Branching reactions then occur which result in other radical species being formed. Radicals interfere with normal cellular processes which result in the breakdown of cellular membranes, DNA and enzymatic processes. When radicals damage proteins, the result is often aggregation or degradation of the protein and loss of function. If LDL in the artery's intima is oxidised, the oxLDL binds to scavenger receptors on human monocyte derived macrophages (HMDMs).

Scavenger receptors are receptors that recognise altered LDL such as Scavenger Receptor A (SR-A) and CD36. SR-A is asserted to be responsible for the majority of acetylated LDL (acLDL) uptake into cells and CD36 is responsible for the majority of

oxLDL uptake, but they are not specific. Recognition of lipid moieties on the oxLDL has been attributed to the reaction between oxLDL and CD36 (Nicholson and Hajjar 2004). Recognition induces a rapid and uncontrolled uptake of cholesterol esters in concert with an up-regulation of cell surface CD36 receptor (Viana et al. 2005). Under other circumstances, the contents of an LDL particle are endocytosed through clatherin pits.

Cholesterol esters, free cholesterol, free fatty acids or triacylglycerides are transported into the cell as part of the LDL particle. LDL receptors are found on the surface of all cells but in highest quantities on the liver indicating that its main purpose is to deliver to the liver cholesterol and free fatty acids. When the peripheral cells' needs are met, the cholesterol gets returned to the liver. ABC-A1/G1 receptors work in concert with pre β-HDL (nascent) and lipid rich HDL to export cholesterol (Tiwari, Singh, and Barthwal 2008).

Failure of this process results in the cell developing an enlarged and foamy-looking morphology (Greig, Kennedy, and Spickett 2012)(Kruth, H.S. (2001). Such foam cells lose their motility as there is an increase in the expression of the cytokine: Migration Inhibitory Factor (MIF). Grieg *et al* discovered that the absence of this gene in mice models results in a reduction in atherosclerosis. Conclusions drawn from this data suggest lack of motility exacerbates the condition. Macrophages in the pro-inflammatory M1 state also produce increased levels of monocyte chemotactic protein-1 (MCP-1). MCP-1 attracts monocytes to the area which ultimately leads to further formation of foam cells (Greig, Kennedy, and Spickett 2012). These cells eventually become apoptotic or necrotic.

As part of the cellular cascade to the area, cytokines summon T-cells which in turn cause smooth muscle cells to migrate towards the site of inflammation. The influx of cells and retardation of normal function combined with the increase in cell mortality results in a necrotic lipid core. The lipid core develops into plaque which is always present in patients with atherosclerosis.

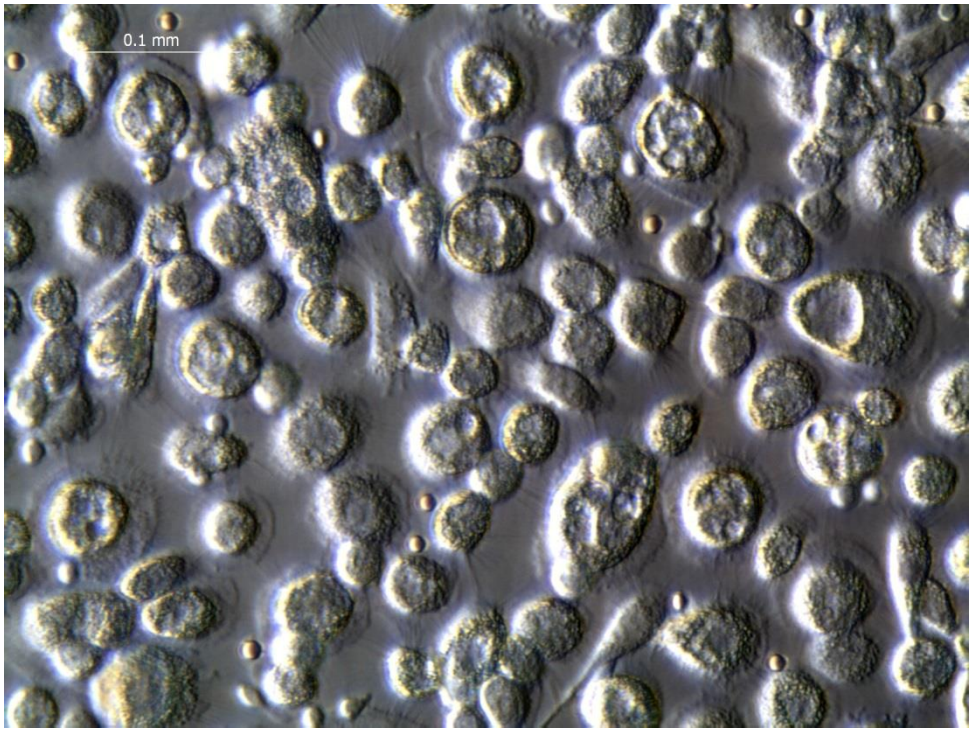

Image 3 Macrophage cell morphology before being treated. As can be seen there is a puffy, annulus morphology. The cells are healthy and in a cobblestone formation with no blebbing. Cells prepared by S. Davies 2014.

The formation of foam cells is commonly known as one of the crucial preliminary steps of heart disease (Cookson 1971; Yu et al. 2013). Foam cells develop as an overstimulated response to abnormal physiological actions (Image 3). It was postulated by several scientists such as F. Cookson and M. Mitchinson in the 70s and early 80s that this was a morphological change that the macrophage cells went through. Morphological changes take place which affects the cell's responses to altered LDL. During an inflammatory response, the monocyte differentiated macrophage cell is exposed to oxLDL. Phagocytotic macrophages take up cholesteryl esters, cholesterol, FFA, TAGs and oxysterols from the oxLDL particle.

Within the intima of the artery wall, the monocytes express lipoprotein-binding proteoglycans which increases the accumulation of altered LDL such as oxLDL (Legein et al. 2013). Transformation into foams cells is complete when uptake exceeds the cholesterol efflux. This results in a release of cytokines that conscript other monocytes in a continuous cycle. Despite scavenger receptors such as CD36 being responsible for 60% of oxLDL binding and cholesteryl ester uptake (Febbraio, Hajjar, and Silverstein 2001), some macrophages become foam cells without the presence of scavenger receptors. SR-A and CD36 deficiency studies (Moore et al. 2005) implicate other

scavenger receptor activity or pinocytosis as being a part of this disease process (Legein et al. 2013).

1.3 CD36

CD36 is a Class B scavenger receptor. It was originally discovered as binding to thrombospondin-1, a critical factor in clotting development (Febbraio, Hajjar, and Silverstein 2001). It has since been implicated in recognition of anionic phospholipids, apoptotic cells, fatty acid binding, collagen, *Plasmodium falciparum* malaria-parasitized erythrocytes, as well as altered LDL. During the differentiation from monocytes to macrophages, the CD36 cell surface expression increases (Alessio et al. 1996) and unlike LDL receptors, CD36 is up-regulated when exposed to oxLDL. Isolation of the protein is complicated as it is a transmembrane glycoprotein found on macrophages, microglia, microvascular endothelium, cardiac and skeletal muscle, adipocytes and platelets (Zamora et al. 2012).

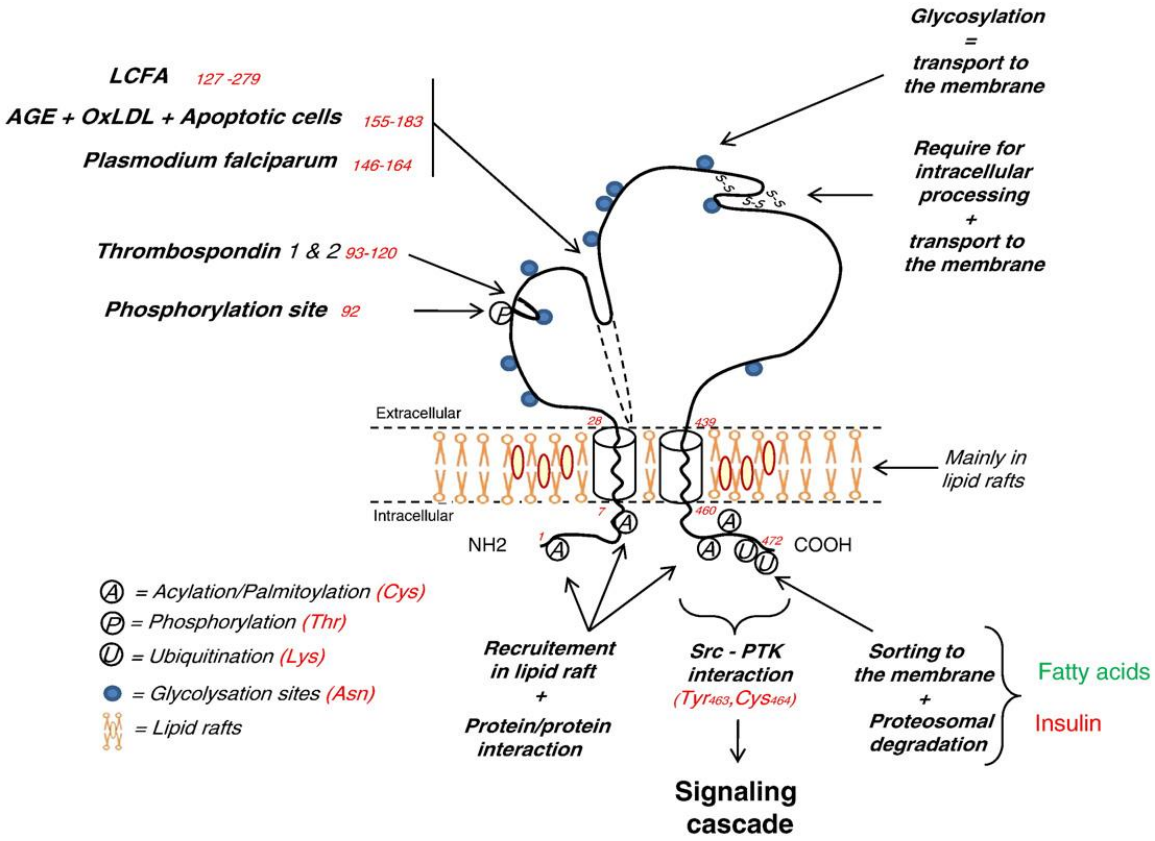

Image 4. The main structural features of human CD36. Identified are the intracellular, short -N terminal end of the protein, the C- terminal end of the protein, the CD36 binding site, the intramembrane anchoring sites, the extracellular loop and the 10 glycosylation sites. Image adapted from Martin. (Martin et al. 2011)

It is a hairpin shaped protein with two intramembrane domains that anchor on the cytosolic side and a long extracellular loop where the active site for CD36 is found (Image 4).

The gene for CD36 is found on chromosome 7 (Collot-Teixeira et al. 2007) and results in an 88 kDa, ditopically configured protein with multiple N-linked glycosylation sites. There are approximately 10 sites, as estimated from cDNA, along with multiple functional domains (image 4). Its ditopic nature allows polar and non-polar aspects of ligands to be accommodated within a single binding site. Due to the multiple N-linked glycosylation products, the receptor exhibits different molecular masses which correspond to different glycoforms in different cell types.

Alessio identified the THP-1 and U937 cells' ability to intracellularly process CD36 resulting in diverse differentiation. When treated with PMA, two monocyte-like cell lines were induced into morphological changes that mimicked differentiation into macrophages. During differentiation, western blotting revealed the appearance of a 74 kDa band that differed to the mature CD36 band at 94 kDa. Corresponding with the 74 kDa band decreasing after 6 hours, the intensity of the 94 kDa band increased, becoming a broad band of 90-105 kDa. The width of this band could be attributed to the different levels of glycosylation (Libby 2002; Gieseg et al. 2010). This concurs with work done by Huh and Yesner in 1996 who found that a moderate two times increase in surface expression of CD36 during differentiation resulted in a marked uptake of neutral lipid (Huh et al. 1996).

The intracellular N-terminal domain of the receptor is short and thought to be functional as an anchor, however the C-terminal domain is longer and has a CXCX5K motif known to be involved in signalling. The discovery of this motif prompted signalling studies which revealed that CD36-oxLDL interaction induced a signalling cascade crucial in the reduction of cell motility and oxLDL uptake (Silverstein et al. 2010). The oxLDL binding site is found in the domain between amino acids 155 to 183 and shares its binding domain with advanced glycated products (AGEs), apoptotic cells, thrombospondin, long chain fatty acids, *Plasmodium falciparum*, and collagen (Collot-Teixeira et al. 2007; Febbraio, Hajjar, and Silverstein 2001).

The reduction in cellular motility is not only attributed to cytokine release, but also CD36. CD36 signalling results in the increase in actin polymerisation and the oxidation of the tyrosine phosphatase responsible for stopping the polymerisation through Focal Adhesion Kinase (FAK). This resulted in the cell losing the ability to co-ordinate actin

activity and the loss of cell motility. In addition when CD36 is exposed to oxLDL, the protrusive lamellipodia that normally extend for motility retract by activating the kinase Vav. Vav activates Rac which inhibits phosphorylation of non-muscle myosin II. Therefore there is no tension on lamellipodia. This inhibits both random migration and chemotaxis through loss of cell polarity (Park et al. 2012).

The existence of this signalling pathway is beneficial when considering the other binding site ligands. As well as apoptotic cells the amino acid 155-183 binding site binds *Plasmodium falciparum*, AGEs and oxLDL (Martin et al. 2011). *Plasmodium falciparum* is the most lethal of the species of parasites that cause malaria (Gardner et al. 2002). AGEs are glycated proteins or lipids that form links between the extracellular matrix molecules which result in complications in the micro- and macro-vasculature. Therefore it is beneficial to remove them from a biological system. They also may form reactive oxygen species (ROS) and induce scavenger receptor A and CD36 expression through gene expression (Goldin et al. 2006). The apparent purpose of this receptor is removal of harmful products from the system. Consequently, it is deduced that the signalling cascade that prevents motility is due to the need for internalisation and degradation, either within the cell or of the cell that has engulfed the harmful ligand.

A complication arises when a ligand is oxLDL. OxLDL is taken up through CD36 which causes uncontrollable cholesteryl ester accumulation. When oxLDL attempts to bind to CD36, unusually HDL and oxHDL are sometimes already bound. HDL usually selectively binds to SRBI in the process of delivering cholesterol and free fatty acids to the liver during Reverse Cholesterol Transport. The role of SRB1 is to uptake cholesterol esters and free cholesterol from HDL and LDL particles. It then binds to receptors on the liver and its contents are recycled (Rhainds and Brissette 2004). SRBI, like CD36, is a scavenger receptor in Class B and this may contribute some idea as to why HDL would bind to CD36. HDL binding to CD36 does not contribute to atherosclerotic plaque development. Despite CD36 binding HDL, it is not taken up into the cell and consequently is poor at eliciting cholesterol esters. Plaque formation is prevented because this HDL binding limits the amount of CD36 receptors available for oxLDL binding without increasing the ester uptake (Thorne et al. 2007). In parallel, there is a decrease in the ability of HDL to stimulate the efflux of cholesterol (Nagano, Arai, and Kita 1991). Nagano *et al* attribute the degradation of ApoA1 due to oxidation. This ApoA1 oxidation likely occurred because HDL has effluxed the cholesterol and free

fatty acids from the foam cells in the environment in which the LDL was oxidised (Nagano, Arai, and Kita 1991).

A further complication is that free radicals are not specific about what they oxidise thus HDL will become oxidised to oxHDL. CD36 can also bind oxHDL. This is sufficient to enable cholesterol ester uptake to occur in the cell (Thorne et al. 2007). Despite the conflicting and sometimes negative outcomes of HDL in the system, Nicholson and Hajjar have shown that by stimulating MAP kinase and PPARɣ, HDL down-regulates CD36 expression in a dose-dependent manner. HDL increased the translocation of the PPARɣ from the cytoplasm to the nucleus as well as the PPARɣ phosphorylation by MAP kinase which inhibited CD36 gene expression (Nicholson and Hajjar 2004). HDL has many ways of decreasing foam cell formation, but currently the uncontrolled uptake of cholesteryl esters from oxLDL are overwhelming and results in a pro-atherogenic cell system. The normally efficient process of LDL uptake and HDL efflux is distorted due to exposure to free radicals.

1.4 Antioxidants

Antioxidants are compounds whose rate of reaction with free radicals is higher than a biological compounds rate of reaction with a free radical. It effectively neutralises the free radical because the resulting species isn't as reactive as a free radical, and so the damage is slowed. In this way antioxidants ameliorate the effect that is had on the macrophages by interfering with the free radical reaction and preventing peroxidation (Dotan, Lichtenberg, and Pinchuk 2004). The antioxidants of main interest are those that are commonly found in the diet or that are produced by cells, such as ascorbic acid (Vitamin C), alpha tocopherol (Vitamin E), 7,8-dihydroneopterin (7,8-NP) and glutathione (GSH). These compounds can be oxidised instead of the lipids or proteins that make up the LDL particle and often maintain their reduced form by reacting with glutathione.

When glutathione is oxidised to glutathione disulphide (GSSG), it has donated an H^+ or an e^- to an unstable compound such as a free radical or an oxidised antioxidant. GSSG then reacts with NADPH and glutathione reductase to re-protonate the GSSG and reform GSH. An antioxidant system can be overwhelmed by free radicals (Morris et al. 2013). This occurs when the cell binds oxLDL and superoxide is generated (Gieseg et al. 2010). As a previous student in this lab has shown, the oxidative stress caused by oxLDL results in 25% GSH loss within 3 hours (Gieseg et al. 2010). The presence of

other antioxidants in the system can relieve the oxidation burden for GSH and allow the protein levels to recover by affecting different pathways in the cell as well as mopping up the free radicals.

Though antioxidant activity is normally associated with radical scavenging, some have direct effects on specific gene expression. Alpha-tocopherol down regulates macrophage CD36 levels when it has been first upregulated by oxLDL via inhibition of tyrosine kinase phosphorylation so foam cell formation is diminished (Özer et al. 2006; Venugopal 2004). Ascorbic acid reduces the binding and uptake of when it is oxidised in the presence of ascorbic acid. This has been attributed to the antioxidant's ability to protect against protein oxidation (Aldred and Griffiths 2004). The macrophage antioxidant 7,8-dihydroneopterin not only prevents oxLDL formation but also decreases its uptake in macrophages by CD36 down regulation.

1.5 Action of 7,8-Dihydroneopterin

Human monocytes and macrophages produce the pterin, 7,8-dihydroneopterin, when stimulated by interferon-ɣ (IFN-ɣ). IFN-ɣ is released by activated T lymphocytes. GTP cyclohydrolase I is stimulated by IFN-ɣ which results in the production of 7,8-dihydroneopterin in monocytes and macrophages from guanosine triphosphate (GTP) (Sugioka et al. 2010). 7,8-NP is secreted out of the cell and scavenges free radicals which have been released by the cell (Berdowska and Zwirska-Korczala 2001). 7,8-NP is oxidised to neopterin when reacting with free radicals thus neopterin levels can be an indication of oxidants in the environment. Though 7,8-NP is a measure of inflammation currently there is no way to tell from which part of the body the 7,8-NP to neopterin release is occurring.

Because neopterin is an oxidative product of 7,8-dihydroneopterin and highly fluorescent it is a good marker of inflammation. This is true of all types of inflammatory diseases however in the case of atherosclerosis, studies have been done that correlate neopterin rise in plasma to atherosclerosis development. While neopterin levels are raised in patients with unstable angina pectoris, there is also a correlation between enhanced neopterin levels and the plaque instability that leads to unstable angina pectoris (Adachi et al. 2007). As the atherosclerotic burden develops towards plaque rupture, the plasma neopterin levels rise (Schumacher et al. 1997). Research done by this laboratory analysed plasma from patients with cardio heart disease undergoing an angioplasty from sites close to the plaque. Measurements analysed using HPLC

showed that the average 7,8-dihydroneopterin concentration was 55.59nM and the neopterin concentration was 14.37nM. This was significantly higher than the healthy donors whose plasma revealed neopterin concentrations of 6.83nM and 7,8-dihydroneopterin concentrations of 17.78nM (Genet 2010). This confirmed the ability of pterins to be used as indicators of high inflammatory stress with in the body, and as indicators of atherosclerosis.

In patients suffering from acute inflammation, pus samples were taken from the site of inflammation and total neopterin was measured as an indicator for inflammation directly from the source, rather than diluted in the serum. This produced an average of 0.54µM neopterin concentration for females and 0.45µM for males (Firth, Laing, et al. 2008). This is much higher than the nM concentrations seen in serum. The presence of neopterin due to inflammatory diseases other than atherosclerosis causes pause when stating that pterins can be used as an atherosclerosis marker. 7,8-dihydroneopterin is a potent inhibitor of oxLDL formation at low uM concentration through the scavenging of the lipid peroxyl radical (Gieseg et al. 1995). 7,8-dihydroneopterin also scavenges hydroxyl and water soluble peroxyl radicals generated with azo compound AAPH (Firth, Laing, et al. 2008; Gieseg et al. 1995). This scavenging has been shown to protect monocyte like and macrophage cells from a range of oxidants. This protection occurs by 7,8-NP not only reacting with the chain propagating lipid peroxyl radical on the oxLDL but also by interfering with cell mediated oxidation (Firth, Crone, et al. 2008; Gieseg et al. 2010). Oxidative loss of 7,8-NP occurs when macrophages and LDL (with protein hydroperoxides) are both present or due to reaction with hypochlorous acid released during the MPO reaction (Firth, Crone, et al. 2008; Widner et al. 2000). This protection is observed by a loss of 7,8-NP as it is oxidised to neopterin and 7, 8-dihydroxanthopterin (Gieseg et al. 2010; Firth, Crone, et al. 2008).

Surprisingly, 7,8-dihydroneopterin was found to reduced oxLDL uptake via the down regulation of CD36 (Gieseg et al. 2010). The decrease in oxLDL uptake was initially measured via DiI staining but was later confirmed to be occurring by measuring 7-ketocholesterol uptake. The CD36 down regulation by 7,8-NP was specifically of the 100kDa, cell membrane glycoform of CD36 where there was a 40% reduction after 24 hours (Shchepetkina 2013). RT-PCR studies showed that the down regulation was occurring at the mRNA expression of CD36. 200mM 7,8-NP caused a 40% decrease in CD36's mRNA expression. The CD36 down regulation failed to protect the cells from the acute cell death which occurs within 24 hours of oxLDL exposure, the study did not

examine the effect on foam cell formation at a non-toxic level of oxLDL (Shchepetkina 2013).

1.6 Aims of Research

As CD36 is thought to be the main scavenger receptor for oxidised low density lipoprotein uptake, and as 7,8-dihydroneopterin is able to reduce CD36 receptor levels, then the uptake of oxLDL lipids may be retarded by the action of 7,8-dihydroneopterin. This information was central to answering the question "Does 7,8-dihydroneopterin down-regulate foam cell formation?"

This thesis therefore aimed to study the formation of foam cells and to try to more accurately define their formation. However, the assay commonly used to determine the success of foam cell formation was flawed as the human cells recorded false positives due to their natural high triacylglyceride levels in tissue culture. Lipid dyes, such as Oil red O when used in conjunction with light microscopy, were used to determine foam cell formation but fluorescence is observed when the vacuoles contained TAGS and lipids. An increase in fluorescence was assumed to correspond to an increase in intracellular lipids. However the dyes are not actually cholesterol specific. DiI stains triacylglycerides in human macrophage primary cells. High Performance Liquid Chromatography (HPLC) provides a rigorous and informative technique for identifying foam cells compared to lipid dyes. Kritharides published an HPLC method for analysing lipids (L. Kritharides et al. 1993) and after adaption, this method was used to measure cholesterol, cholesteryl esters and 7-ketocholesterol (7KC) uptake in macrophages.

CD36 expression had responded to 7,8-dihydroneopterin with a decrease in cell protein levels measured using immunoblotting and CD36 mRNA levels measured by rtPCR (Shchepetkina 2013). Both these methods require a large number of cells and a considerable amount of time. Therefore this thesis also looked at CD36 cell surface expression using flow cytometry analysis of CD36 labelled macrophages.

Experimentally, foam cell formation was initiated by treating cells with oxLDL and measuring the uptake at the end of an allocated time. As cells needed to survive in order to become foam cells, the oxLDL concentration would not be toxic. The HPLC method quantified the cell's cholesterol uptake as a marker of foam cell formation. CD36 cell surface expression was to be measured at specific time points to see if 7,8-

dihydroneopterin down regulation was responsible for changes in the cells cholesterol content.

2 Materials and Methods

2.1 Materials

2.1.1 Reagents

All reagents used were of analytical grade or better. All solutions were prepared using MilliQ (Millipore) water.

7,8-Dihydroneopterin	Schircks Laboratory, Switzerland
Acetic acid	BDH Laboratory Supplies
Acetonitrile	Fisher Scientific
Accutase	Millipore.
Argon gas	BOC
Bicinchoninic acid (BCA) protein determination kit	Thermo Scientific
Bovine Serum Albumin (BSA)	Invitrogen Corporation
Butylated hydroxytoluene (BHT)	Sigma Chemical Co.
Chelex 100 resin	Bio-Rad Laboratories
Cholesterol reagent	Roche/Hitachi
Copper Chloride	Mallinckrodt Chemical Works
Dialysis tubing	Sigma-Aldrich Inc.
Diethyl ether	Thermo Fisher Scientific
Ethylenediaminetetraacetic acid (EDTA)	Sigma-Aldrich Co.
Ethanol	Merck
n-Hexane	BDH Laboratory Supplies
Hydrochloric acid (HCl)	Merck
Isopropanol (2-Propanol)	Fisher Scientific
Lymphoprep	Axis-Shield PoC
Nitrogen gas	BOC
Methanol	Fisher Scientific
3-[4,5-Dimethylthiazol-2-yl]-2,5-diphenyl-tetrazolium bromide (MTT)	Sigma Chemical Co.

Potassium Hydroxide	Sigma-Aldrich Co.
Sodium Bicarbonate	Sigma-Aldrich Co.
Sodium Dihydrogen Phosphate monohydrate	Scharlab
Sodium Hydroxide	Sharlau Chemie
Trypan Blue Solution (0.4%)	Sigma-Aldrich Co.
Ultra-membrane tubing	Sigma-Aldrich Co.

2.1.2 Antibodies

Purified mouse IgM k isotype control	BD Biosciences
Purified Mouse Anti-Human CD36	BD Biosciences
Polyclonal Goat Anti-Mouse Immunoglobulins/ R-phycoerythrin Goat F(ab')2	DAKO

2.1.3 Media, Buffers and General Solutions

Foetal Calf serum (FCS)	Invitrogen
Penicillin/Streptomycin (10,000U of penicillin G and 10,000µg of streptomycin /ml)	Gibco BRL
Roswell Park Memorial Institute 1640 (RPMI 1640)	Gibco BRL
RPMI 1640 without phenol red.	Sigma-Aldrich

Cell culture media

RPMI 1640 medium powder was dissolved in MilliQ water, sodium bicarbonate was added and the pH was adjusted to 7.1. Sterilization was completed using Millipore 0.22µm filter in the Scanlaf Mars Class II sterility cabinet under vacuum. It was then transferred to sterile bottles and stored at 4°C. It was warmed to 35°C before use.

RPMI 1640 cell media

Each 500ml bottle of RPMI 1640 media had 10,000U of penicillin G and 10,000µg of streptomycin (p/s) /ml added when opened from storage at 4°C. RPMI 1640 was further supplemented with 10% human serum (v/v) for human monocyte derived macrophages or 5% foetal calf serum for U937 cells before addition to cells.

PBS

Phosphate Buffered Saline (3M Sodium Chloride and 250mM Sodium dihydrogen phosphate, pH 7.4) was vacuum filtered through a 0.45µm filter membrane. When required for cell culture, the PBS was autoclaved at 121°C for 20 minutes and stored at room temperature. It was warmed to 35°C before use.

7,8-Dihydroneopterin (7,8-NP) solution

A 100µM stock solution was prepared fresh prior to each treatment by dissolving in RPMI 1640 no phenol red using a 10 minute sonication. The solution was sterilized by filtration through a 0.22 µm filter membrane.

Washed Chelex

Chelex 100 resin was stirred with MilliQ water for 30 minutes. After resting for 30 minutes, the chelex was washed three times. The Chelex was then dried under vacuum using a 0.45 µm filter membrane.

2.2 Methods

2.2.1 Preparation of Human monocyte derived macrophages (HMDMs)

HMDM cells are one of the cell types available for use as a model when studying atherosclerosis. They are preferred because they offer much of the variability that is faced when studying the human body. In treating them with GM-CSF, their differentiation is directed towards becoming a M1, pro-atherogenic macrophage. 470ml of autologous blood is collected from hemochromatosis patients at the NZ blood bank. This is blood that has had an anticoagulant added. Once back at the Free Radical Biochemistry Laboratory, using aseptic technique, the blood was transferred into 50ml

falcon tubes. The blood is centrifuged at 1000g for 20 minutes with the brake off and the buffy coat (the layer of cells between the red blood cell layer and the plasma layer) is transferred into new falcon tubes. An equal amount of warmed PBS is mixed with the buffy coat and warmed lymphoprep is deposited at the bottom of the tubes. The cell preparations are centrifuged at 1000g for 20 minutes with the brake on. This results a monocyte/T- and lymphocyte cell layer which is isolated and washed 3 or 4 times with 45ml PBS. Between each wash is a 10 minute centrifuge at 500g. The cells are re-suspended in 30mls of warmed RPMI 1640 and 6mls are plated in 6 well suspension plates and placed in the Sanyo incubator for 40 hours. During this time the T cells die off and the lymphocytic cells adhere to the plate. This leaves the monocytes in suspension and they are re-suspended in a new mix of RPMI1640 supplemented with 10% human serum and p/s. The cell concentration is adjusted to $5x10^6$ cells/ml and 2uL of 25ug/ml of Granulocyte and Monocyte Colony Stimulation Factor (GMCSF) is added per ml of 5 million cells. The cell suspension can then be adjusted to whichever concentration required, plated in adherent tissue culture plates at 1ml/ well and moved to the 37°C/ 5% Sanyo CO_2 incubator. New RPMI 1640 supplemented with 10% human serum and p/s was exchanged every 3-4 days, and experiments were executed when the differentiation process finished at day 11 after seeding. The cells were recognised as differentiated when the majority of the monocytes had conformationally changed to macrophages.

2.2.2 U937 culturing

U937 cells were grown and maintained in suspension culture in a $75cm^2$ tissue culture flasks. The media used was RPMI 1640 medium with phenol red, supplemented with 5% foetal bovine serum, penicillin (100 U/mL) and streptomycin (100 µg/mL) at 37°C in a humidified atmosphere containing 5% CO_2 (Sanyo incubator). The cell media was changed every 3 days and cell concentrations were maintained between 0.2 and 1 million cells per ml through passages.

2.2.3 Human Serum

470ml of dry blood is collected from hemochromatosis patients at the NZ blood bank. This is blood with no anticoagulant added. After sitting overnight at 4°C, the clotting cascade was complete and the serum had separated from the clot. Under aseptic conditions in the Scanlaf Mars Class II sterility cabinet, the serum was transferred into

50ml falcon tubes. The serum underwent centrifugation at 1000g for 10 minutes, with the brake on. This pelleted the remaining red blood cells and allowed for the serum to be isolated, combined and aliquoted into new falcon tubes. The serum was frozen at -20°C on an angle and stored in the Sanyo -80°C freezer.

2.2.4 HPLC analysis of Cholesterol, Cholesteryl esters and 7-ketocholesterol

This method was adapted from Zunika Amit's thesis (Amit 2008). The original method was described by Kritharides (L. Kritharides et al. 1993) who elucidated cholesterol and other compounds on the HPLC. The cholesteryl esters and oxysterols eluted in an Acetonitrile: Isopropanol mobile phase using a C18 reverse phase column. The acetonitrile improves the resolution of the peaks (Flavall et al. 2008) measured at 210nm and 234nm.

Cholesteryl Ester Measurement

Lipids were extracted from 3 wells containing $5x10^6$ cells/ml and pooled before being injected onto the HPLC. After removal of the RPMI 1640 media, cells were washed with ice cold PBS. Lipids were harvested by treatment with 0.6ml of ice cold 0.2mol/L sodium hydroxide at 4°C for 15minutes. Lysate was pooled and 1.2ml was aliquoted into centrifuge tubes. The remainder of the lysate was set aside for protein determination. 0.5ml cold nanopure water, 20 µL of 20mg/ml EDTA pH7.4, 20 µL of 100mg/ml BHT in methanol and 1ml of ice cold methanol was added to the lysate. The tubes were vortexed briefly and 5ml of hexane was added. After a 1 minute vortex, the tubes were centrifuged for 2 minutes at 1000g in 4°C. 4 ml of the top hexane layer was removed into drying tubes and dried under nitrogen gas. 100uL of Acetonitrile: Isopropanol (30:70 v/v) mobile phase is added to the lipid residue and dissolved. The samples were run through the Shimadzu HPLC on a reverse phase Phenosphere-NEXT 5u C18 column at 20µL. The lipids eluted isocratically at 1ml/min with mobile phase and detected by absorbance at 210nm. Identification and quantification of sample lipids was carried out by using known concentrations of cholesteryl ester standards (Cholesterol, cholesteryl arachidonate, cholesteryl linoleate, cholesteryl oleate and cholesteryl palmitate made up in mobile phase).

Free Cholesterol and 7-Ketocholesterol

Cholesterol and 7-Ketocholesterol determination was modified further from the cholesterol ester method as cholesterol and 7KC are released by the potassium hydroxide hydrolysis of the esters. After removal of the RPMI 1640 media, cells were washed with ice cold PBS. Lipids were harvested by treatment with 0.6ml of ice cold 0.2mol/L sodium hydroxide at 4°C for 15minutes. Lysate from 3 wells were pooled and 1.2ml was aliquoted into centrifuge tubes. The remainder of the lysate was set aside for protein determination. 0.5ml cold nanopure water, 20 µL of 20mg/ml EDTA pH7.4, 20 µL of 100mg/ml BHT in methanol and 1ml of ice cold methanol was added to the lysate. The tubes were vortexed briefly and 5ml of hexane was added. After a 1 minute vortex, the tubes were centrifuged for 2 minutes at 1000g in 4°C. 4 ml of the top hexane layer was removed into new centrifuge tubes and dried under nitrogen gas. Hydrolysis occurred by adding 2.5ml diethyl ether and 2ml 20% KOH in MeOH to the dried lipid residue. Once the samples had been briefly vortexed, argon gas was used to flush the tubes before a 3 hour incubation on ice during which ester hydrolysis occurred. This was helped along by a 30 second vortex every half hour of the incubation. Hydrolysis was stopped with 2ml of 20% acetic acid and a 30 second vortex. 2.5ml of hexane was added, the samples were vortexed for 1 minute and centrifuged at 200g for 10 minutes at 4°C. The top 80% (3.6ml) of the hexane layer was removed into drying tubes and dried under nitrogen gas. The dried lipid residue was then re-solubilised into Acetonitrile: Isopropanol: MilliQ water (44:54:02 v/v) mobile phase and run through the Shimadzu HPLC on The samples were run through the Shimadzu HPLC on a reverse phase Phenosphere-NEXT 5u C18 column at 20µL. The lipids eluted isocratically at 1ml/min and detected at 210nm for the cholesterol and 234nm for the 7-ketocholesterol. Identification and quantification of sample lipids was carried out by using known concentrations of cholesterol and oxysterol standards (Cholesterol and 3β-hydroxy-cholest-5-en-7-one made up in acetonitrile: isopropanol (9:11v/v) mobile phase).

2.2.5 Plasma and LDL preparation

Plasma collection

With Ethics Approval from the Upper South A Regional Ethics Committee: Ethics approval number 98/07/069, 200ml of blood was collected from 5-7 volunteers. The blood was collected into 50ml falcon tubes containing 0.5ml of 10% (w/v) EDTA pH7.4 and centrifuged at 4100g for 20 minutes at 4°C.. The plasma was transferred to

centrifuge tubes and centrifuged using an Eppendorf 5810R fixed angle rotor at 11, 000 rpm for 30 minutes at 4°C. This second centrifugation ensures the plasma has no cell remnants. The plasma from each donor is pooled and aliquoted into 30 ml portions to minimise inter-person variation. The aliquots were stored at -80°C for up to six months.

LDL isolation

LDL was purified by a single step ultracentrifugation using a Beckman NVTi65 rotor (Gieseg and Esterbauer 1994). To isolate the LDL from the plasma, the thawed plasma was centrifuged at 4700 rpm for 10 minutes at 4°C to remove precipitation. The plasma has 0.3816g of Potassium Bromide (KBr)/ml dissolved in it to adjust the LDL's density to 1.24. Into 8 ultracentrifuge tubes, 5-6ml of 1mg/ml EDTA ph7.4 was added. A long needle was used to underlay 3.75ml of the adjusted plasma to the bottom of each tube. The ultra-centrifuge was run at 60,000 rpm for 2 hours at 10°C with a slow acceleration and slow deceleration (brakes on) to isolate the LDL. After centrifugation, the upper yellow layer of VLDL was removed and disposed of. The LDL sample was removed from the ultracentrifuge tubes using a syringe needle bent to 90°. The cholesterol content of the LDL layer was measured using the Roche/Hitachi CHOL reagent and the spectrophotometer UVProbe 2.01 program. The LDL and CHOL reagent was incubated for 10 minutes before the absorbance was measured at 500nm using a Shimadzu 1601 spectrophotometer. The remainder of the sample is stored in the dark, under argon, at 4°C. The LDL concentration was determined using an equation accounting for the molecular mass of cholesterol, its mass and the estimation that cholesterol is 31.64% of the LDL particle's weight (Gieseg and Esterbauer 1994).

2.2.5.1 OxLDL preparation

Once the LDL was isolated, ultra-membrane tubes from Sigma-Aldrich were used to concentrate the LDL to 8mg/ml. PBS was added to the LDL and it was centrifuged at 3000g for 30 minutes at 10°C. The LDL in the inner membrane had PBS added and a second centrifugation occurred. Once there was the correct concentration of LDL, the solution had 50mM $CuCl_2$ stock solution added to it to make a final concentration of 0.5mM $CuCl_2$. The mixture was incubated in dialysis tubing in 37°C PBS also with a final concentration of 0.5mM $CuCl_2$ for 24 hours. The completion of LDL oxidation was indicated with a colour change to colourless. The copper ions were then removed

by incubating the oxLDL in PBS and washed chelex for 2 hours at 4°C. The chelex and PBS was replaced for another two hours before being replaced again and incubating overnight. The oxLDL was filter sterilised under aseptic conditions through a 0.22um filter membrane and stored at 4°C.

2.2.6 MTT cell viability assay

The MTT assay is a viability assay that measures NADH dehydrogenase activity. This allows living cells to metabolise the solution of 3-[4,5-Dimethylthiazol-2-yl]-2,5-diphenyl-tetrazolium bromide (MTT) into MTT-formazan. This is an insoluble compound which is purple in colour, measured on the spectrophotometer at 570nm. The 5mg/ml MTT reagent is made up in RPMI1640 with no phenol red to prevent false colour readings. The adherent cells were washed twice with warm PBS. 900uL of RPMI 1640 with no phenol red was added to the wells and 100uL of yellow MTT reagent was added. The plates were incubated for one hour at 37°. This allowed the purple crystals to form. 1ml of 10% SDS (in 0.01M HCl) was added to each well to dissolve the crystals. After gentle pipetting, the absorbance was measured at 570nm using the UV-1601PC Shimadzu Spectrophotometer against a MTT and RPMI blank. The results were calculated as a percent of the control cell value.

2.2.7 Protein determination assay, BCA.

The BCA protein determination measures the reaction between Bicinchoninic acid with copper ions and peptide bonds. The resultant purple colour is due to the protein reducing the copper and the reduced copper subsequently being chelated by the Bicinchoninic acid. This gives a correlation between the Purple colour formed and the amount of protein. This technique is not influenced by differing protein composition, as other dyes can be, because it relies not only on the protein residues but also the peptide backbone. This evens out the variability resultant of protein composition and which allows comparison to other protein samples.

The cell samples from the NaOH extraction method were diluted 1/10 so their absorbance fell within the range of the protein standards. A total volume of 50uL of the diluted sample was transferred to an Eppendorf. The protein analysis was achieved using a BCA protein determination kit from Thermo Scientific. 50 parts of Reagent A (Sodium carbonate/bicarbonate buffer, Bicinchoninic acid and Sodium tartrate in 0.1M NaOH) was mixed with 1 part Reagent B (4% $CuSO_4.5H_2O$). 1 ml of this working

solution was mixed with the diluted samples for 30minutes at 60°C on a heated shaking block. The reaction ceased when the samples were placed on ice and their absorbances were measured on the UV-1601PC Shimadzu spectrophotometer at 562nm. Protein concentration was determined from the slope and the y-intercept of a standard curve created from a series of five protein standards: 0ug/ml, 25ug/ml, 50ug/ml, 100ug/ml and 250ug/ml of 2mg/ml Bovine Serum Albumin standard from Pierce with dd water.

2.2.8 Flow cytometer analysis of CD36 cell surface expression

Flow cytometry is a technique used to measure the fluorescence of a single cell passing through a laser beam or light source. A fluidics system orders the particles in the sample into a single stream using hydrodynamic focusing (Rahman et al. 2006). The light scattering or fluorescent emissions of the particle reveal information about the particles properties. There are two detectors, one 20° offset from the beams axis called the Forward Scatter Channel (FSC) and the other at 90° to the excitation line is the Side Scatter Channel (SSC). The forward scatter and side scatter patterns are unique for every particle and give information on size, granular content and distinguish between debris and live cells (Rahman et al. 2006). There is also the ability to detect fluorescence with silicon photodiodes or photomultiplier tubes which makes this piece of equipment a very handy tool.

Cell experiments were carried out under aseptic conditions in a Scanlaf Mars Class II biohazard cabinet. Cells were washed with RPMI1640 supplemented with p/s. The cells were then incubated with Accutase™ for 15 minutes at 37° following the Accutase™ protocol from the manufacturer ("Accutase," n.d.). Accutase™ is a protease and collagenase enzyme mix that lifts the adherent cells off the plate. The cells were pipetted to detach and the Accutase™ was neutralised with equal volumes of RPMI1640 supplemented with 10% FCS and p/s. The cells were washed with 1ml PBS and 0.5% BSA and re-suspended in RPMI 1640 supplemented with 10% human serum and p/s. The HMDMs were re-plated in suspension plates and incubated at 37°C for 12 hours. This allowed the CD36 surface protein levels to return to normal (Alessio et al. 1996). At the end of the treatment period, the cells were washed in ice-cold PBS and 0.5% BSA. They were treated on ice with mouse anti-human CD36 for 20 minutes. They were washed with ice-cold PBS and 0.5% BSA and spun in a pre-cooled (4°) centrifuge at 2000rpm for 5 minutes. They were re-suspended in GAM-PE (Polyclonal Goat Anti-Mouse Immunoglobulins/ RPE Goat F(ab')2) for another 20 minutes in the

dark, before being centrifuged at 2000 rpm for 5 minutes at 4°C. The samples were re-suspended in 1ml PBS and 0.5% BSA. A primary antibody control (IgMk BD Biosciences) was used to ensure that the labelling being seen was only due to antibody binding. This avoided indirect staining (Shapiro 2003). 10,000 events were then analysed on the FL2 filter using the BD Biosciences Accuri C6 Flow Cytometer.

2.2.9 Statistical Analysis

Data was graphed and analysed using the GraphPad Prism software program (version 6.0; GraphPad software, Inc. USA). Significance was confirmed by two-way analysis of variance (ANOVA) and Tukey's multiple comparisons test to quantitatively indicate significance.

Results displayed in this thesis were taken from the best experiment, a representative of at least three successful experiments. The means, standard deviations and standard errors of the mean (SEM) are calculated from triplicates.

3 Results

3.1 Standardisation of the cholesteryl ester analysis method.

Commercial standards of cholesterol, cholesteryl arachidonate, cholesteryl palmitate, cholesteryl oleate and cholesteryl linoleate were used to identify these lipids in LDL and oxLDL using a modified version of Kritharides method (L. Kritharides et al. 1993). Figure 1 shows that the commercial standards of cholesterol and the cholesteryl esters all elute off the column at different times. The cholesteryl palmitate peak was not very pronounced. However this was common in all the standard runs performed. The investigation of an LDL sample in figure 2 clearly identified corresponding peaks which eluted off the column at the same time frames as those of the commercial standards. Also present in the LDL sample were other peaks but these were not identified. Figure 3 presents the oxLDL sample which showed a loss of cholesterol and cholesteryl esters. When figure 2 and 3 are compared, not all the lipids seen in figure 2 (LDL) are present in figure 3 (oxLDL). Cholesterol, cholesteryl oleate and cholesteryl palmitate are present but the peaks corresponding to cholesteryl arachidonate and cholesteryl linoleate are not evident in the oxLDL sample. This suggested that the lipids had been altered during oxidation. Literature suggests that much of the cell now contains 7-ketocholesterol (Leonard Kritharides et al. 1996). Cholesteryl arachidonate and -linoleate may also oxidise to hydroperoxides and other oxidation products include isoprostanes and aldehydes (Jessup, Kritharides, and Stocker 2004). Due to the oxidation of these lipids, they will elute off the column at different times. Early elution is likely as the size of the void peak has noticeably increased (figure 3).

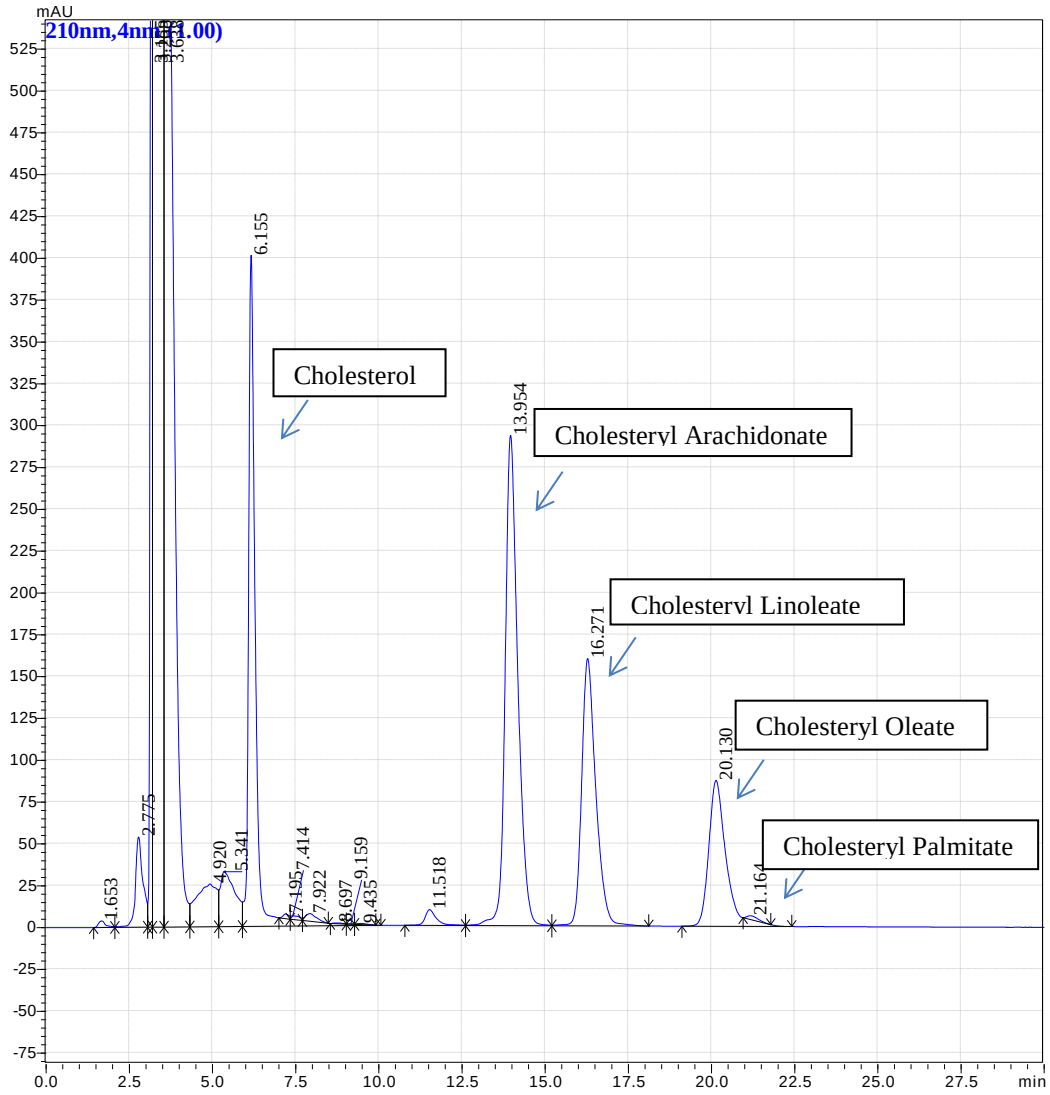

Figure 1. Chromatogram of commercial standards of cholesterol and cholesteryl esters. The above standards are depicted as a chromatogram which have been dissolved in hexane, dried down with nitrogen gas and re-suspended in cholesteryl ester mobile phase. The prepared standards were then run on the HPLC using the cholesteryl ester method.

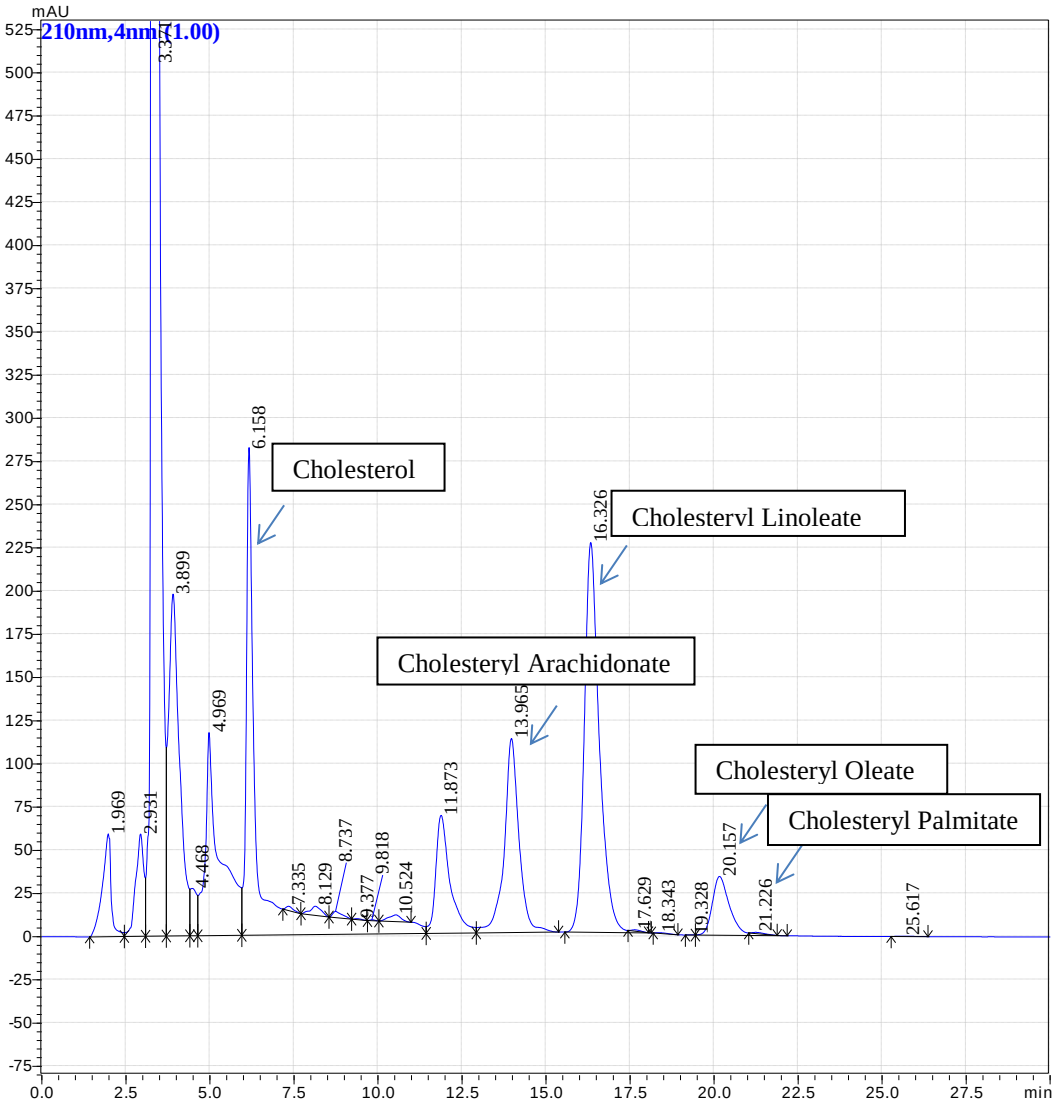

Figure 2. Chromatogram of extracted LDL with cholesterol and cholesteryl esters identified. HPLC analysis of cholesterol and cholesteryl esters in LDL. 0.4mg of LDL was extracted into hexane, dried and dissolved in cholesteryl ester mobile phase as per method. Lipid eluents detected by absorbance at 210nm.

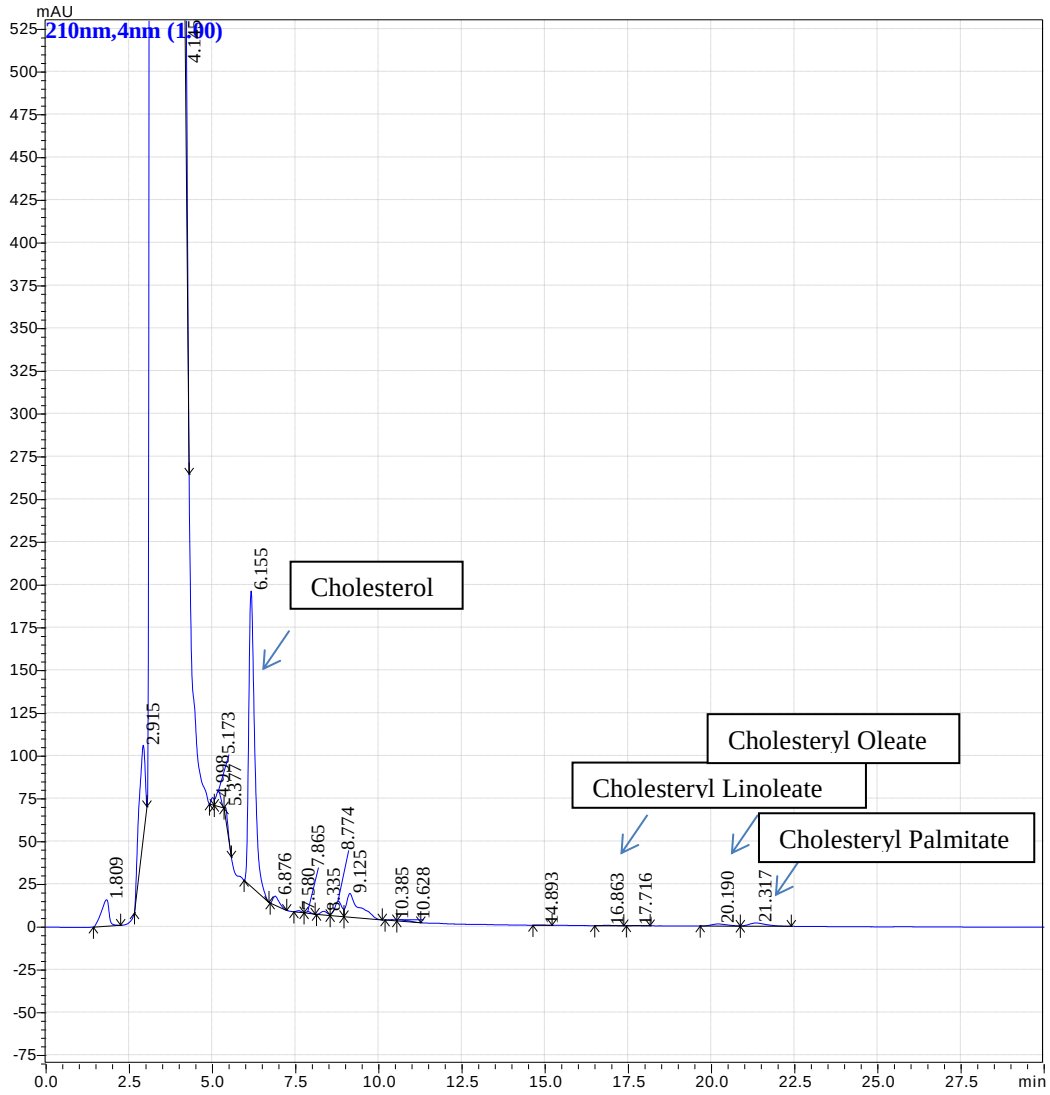

Figure 3. Chromatogram of copper oxidised LDL with cholesterol and cholesteryl esters identified. OxLDL was copper oxidised from the LDL sample (figure 2) at a concentration of 8.2mg/ml. Extracted into hexane, it was then dried under nitrogen and run on the HPLC in cholesteryl ester mobile phase using the cholesteryl ester method.

To further control for the types of lipids the cells were exposed to, the human serum was also analysed for cholesterol and cholesterol esters (figure 4). As was expected, low levels of these various esters were identified in the human serum due to the lipoproteins presence in the serum. Because of the altered lipid profile of oxLDL, if it was the lipid present in the human serum, cholesteryl arachidonate and –linoleate would not be present. As they are, along with cholesteryl oleate and –palmitate the source of these lipids was LDL. This confirmed that the cholesterol ester HPLC method was able to be used to measure cholesterol and cholesteryl esters in the diluted human serum as well as the pure lipoproteins.

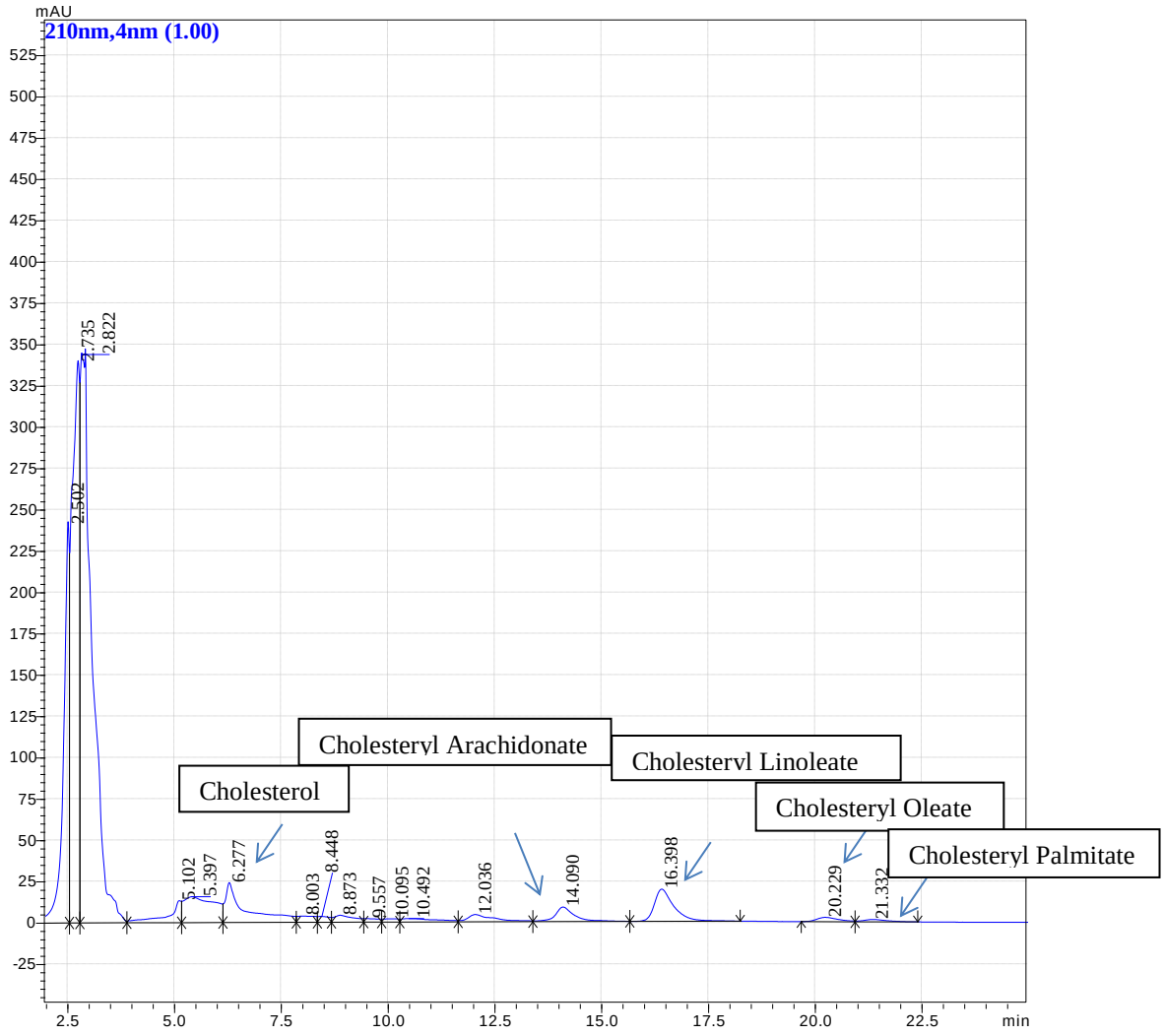

Figure 4. Chromatogram of RPMI 1640 and 10% human serum with cholesterol and cholesteryl esters identified. 200µl of RPMI 1640 and 10% human serum (cell culture media) was extracted into hexane, dried and re-solubilised in cholesteryl ester mobile phase. HPLC analysis used absorbance measured at 210nm.

The resulting data from figures 2 and 3 were analysed to establish how much ester was available (figure 5). LDL had more esters available than oxLDL. This is due to lipids being altered during oxidation.

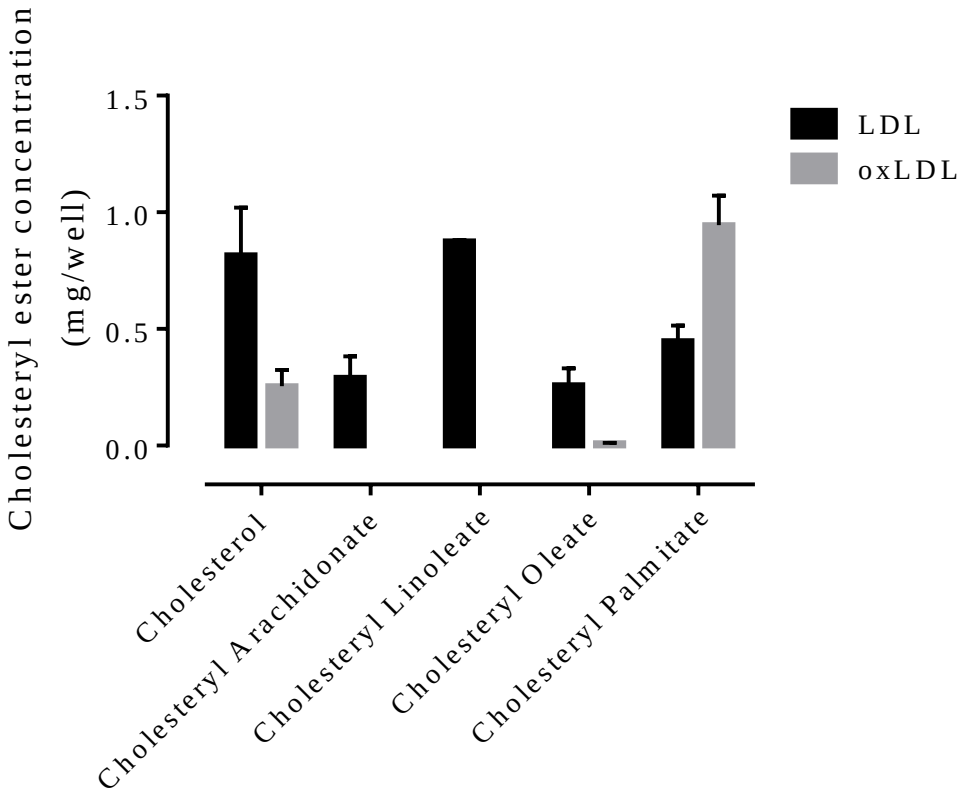

Figure 5. Changes in sterol content during LDL oxidation. LDL isolated from human plasma or oxLDL made by copper oxidation of the LDL sample, was extracted into hexane, dried and re-suspended in cholesteryl ester mobile phase. Samples were processed in triplicate using the Cholesteryl Ester measurement method on the HPLC using absorbance at 210nm to quantify the eluting sterols. Representative chromatograms are shown in figures 2 and 3.

3.2 Determining amount of cells required for analysis

We investigated how many cells would be required to obtain a valid cholesterol and ester signal on the HPLC. One well of a cell culture plate had a seeded concentration of $5x10^6$ cells/ml. In figure 6 the wells of cells were pooled to obtain a clear signal of the cholesterol and esters on the HPLC chromatograms. A clear signal was required to separate the cholesterol and ester peaks from the other peaks on the chromatogram. Once the HPLC signal was acquired, the data was corrected to concentration of cholesterol or ester per well. Figure 6 also demonstrates the variability of the cells within each preparation. Despite the cells being seeded in almost identical environments and the adoption of meticulous handling protocols, the cell response differed. This can be seen in the cholesterol and cholesteryl arachidonate accumulation. The large amount of cholesterol accumulation in 1 well of oxLDL treated cells is

followed by a large drop in the cholesterol accumulation in 2 wells of oxLDL cells. By pooling 3 wells to increase the concentration of cells, the expectation was a stronger signal. While the 3-well-pooled signal was strong, pooling-2-well samples occasionally exhibited higher concentrations of cholesterol and cholesteryl arachidonate as well as 7KC. Only the 2- and 3-well-pooled samples measured cholesteryl linoleate. None of the samples measured a signal for cholesteryl palmitate. Pooling of three wells was chosen as the preferred method on the assumption that if the cells took up higher concentrations of cholesteryl oleate and -palmitate, the higher cell concentration would be more likely to reveal the esters in question. Of note in figure 6 is that none of the cells with oxLDL for 48 hours exhibited signs of cholesterol and ester uptake beyond the control levels. Rather the levels of lipids are below the control cell's levels (figure 6).

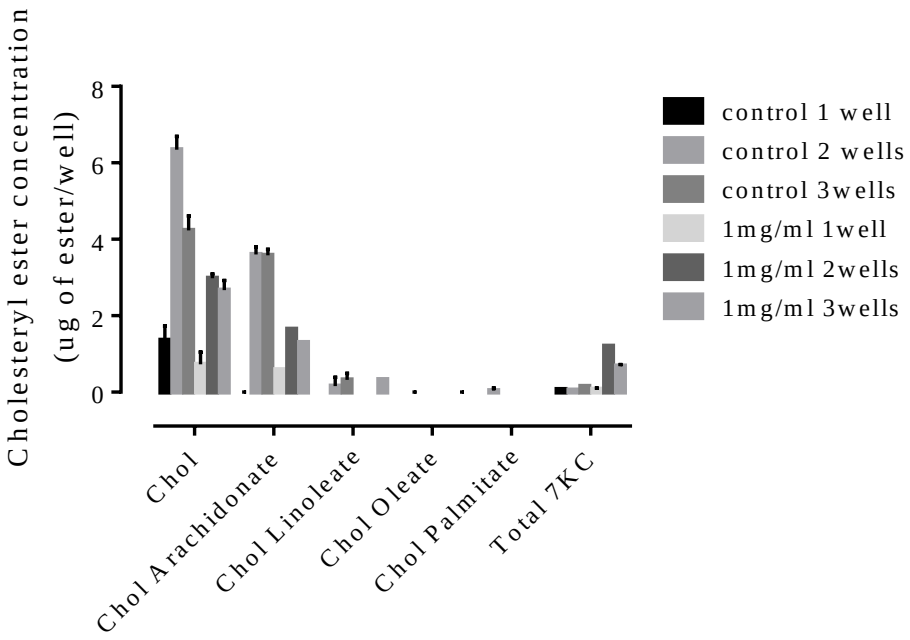

Figure 6. Pooling wells of cells to obtain HPLC signal. 1 well vs. 2 wells vs. 3 wells. Treatment was with 1mg/ml of oxLDL in RPMI 1640 and supplemented with 10% human serum and p/s. Controls were treated with fresh RPMI 1640 and supplemented with 10% human serum and p/s. After 48 hours, cells were pooled and half the sample was extracted into cholesteryl ester mobile phase as per method. The other half was extracted into 7KC mobile phase as per the 7KC method. Samples were analysed by HPLC using the cholesteryl ester method and the 7KC method correspondingly. Cholesterol and cholesteryl esters' absorbance was measured at 210nm and 7KC's absorbance was measured at 234nm. Analysis done by GraphPad Prism

3.3 Effect of the human serum on cholesteryl ester uptake

It was postulated that the lack of cholesterol and ester accumulation in figure 6 was a result of the cell ester uptake being influenced or altered by the concentration of human serum in the RPMI 1640 media. Experiments had been conducted at 10% human serum concentration and this concentration of human serum could provide the cells with enough of the cholesterol or cholesteryl esters to skew the results. The cells cultivated at the higher concentrations showed a healthier morphology but if the higher concentrations altered results, a lower concentration of human serum would have been considered. Figure 4 indicated that LDL is present in human serum and this would be the source of the extra cholesterol and esters. It was deemed prudent to investigate the

human serum concentration. As the U937 cell line flourishes in RPMI supplemented with only 5% foetal calf serum, lower human serum concentrations were expected to keep the macrophages healthy while restricting the amount of extra cholesterol and esters the cells exposed to (figure 7). After 48 hours of incubation in lower human serum concentrations, the uptake was measured using the HPLC (figure 7). No significant differences were evident between serum percentages over the 48 hour trial period. It was concluded that the concentration of human serum has no effect on how much cholesterol or ester the cell consumes during the experiment.

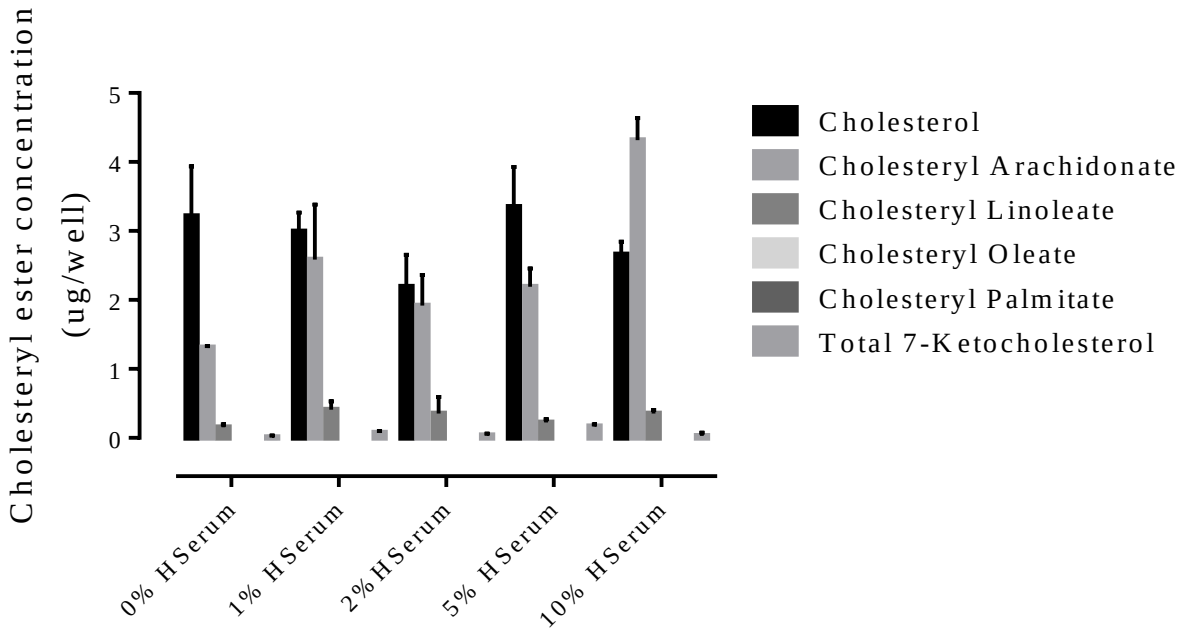

Figure 7. Cholesterol and ester uptake in cells treated with different concentrations of human serum. Macrophages at a concentration of $5x10^6$ cells/ml were treated with 0%, 1%, 2%, 5% and 10% concentrations of human serum in RMPI 1640 for 48 hours. Samples were extracted into cholesteryl ester mobile phase and absorbance was measured at 210nm on the HPLC using the Cholesteryl Ester Method. Data analysed using GraphPad Prism 6.0.

3.4 Cholesteryl ester accumulation

An MTT assay was conducted to determine the LD50 of oxLDL on HMDM cells (figure 8). After 48 hours of incubation with different concentrations of oxLDL, MTT-formazan was added to the cells. The absorbance was read at 570nm and the results calculated as a percent of the control. A sub-toxic concentration of 1.0mg/ml oxLDL was effective because higher concentrations caused cell mortality in 48 hours. Foam cell formation required survival rates beyond 48 hours (Shchepetkina 2013). Because in

figure 6 the oxLDL treatment didn't cause uptake, there was some doubt that we could form foam cells. 0.5mg/ml oxLDL treatments did not cause cholesterol, cholesteryl ester or 7-KC uptake over 48 hours. Figure 9 shows that 1mg/ml oxLDL caused uptake of all the esters as well as free 7-KC. Figure 9 shows an increase in cholesteryl oleate, -palmitate and 7KC uptake in macrophages. This was promising as figure 6 didn't show oxLDL stimulated uptake. This enabled progression onto experimenting with 1.0mg/ml oxLDL as the sub-toxic concentration.

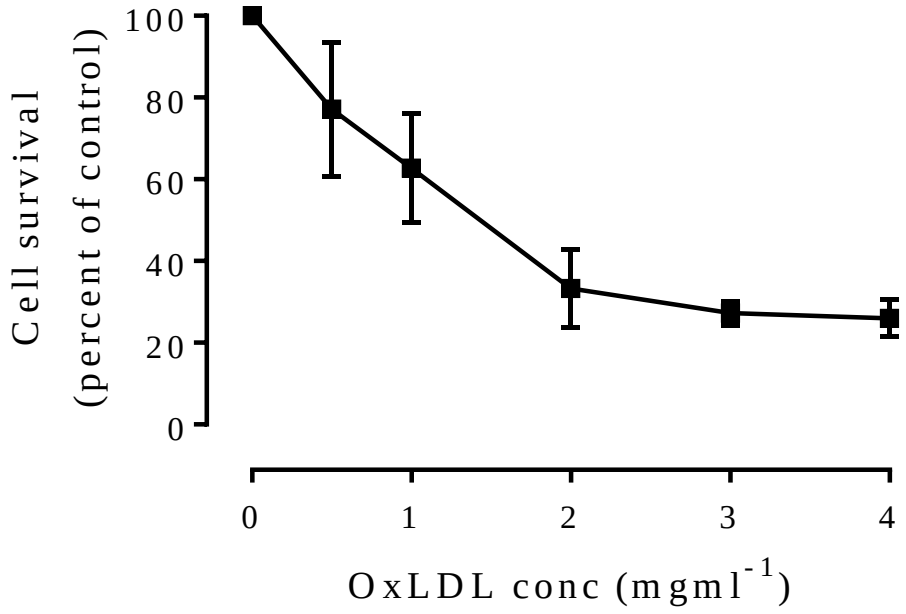

Figure 8. MTT assay of cells treated with oxLDL for 48 hours. HMDM cells Macrophages were treated with different concentrations of oxLDL for 48 hours. Samples in triplicate were washed and the MTT assay was performed to determine cell viability. Absorbance was measured at 570nm. Sub toxic concentrations were determined at 1.0mg/ml which agreed with data shown by this lab previously (Shchepetkina 2013) Data was analysed using second order quadratic polynomial with an R^2 value = 0.9313.

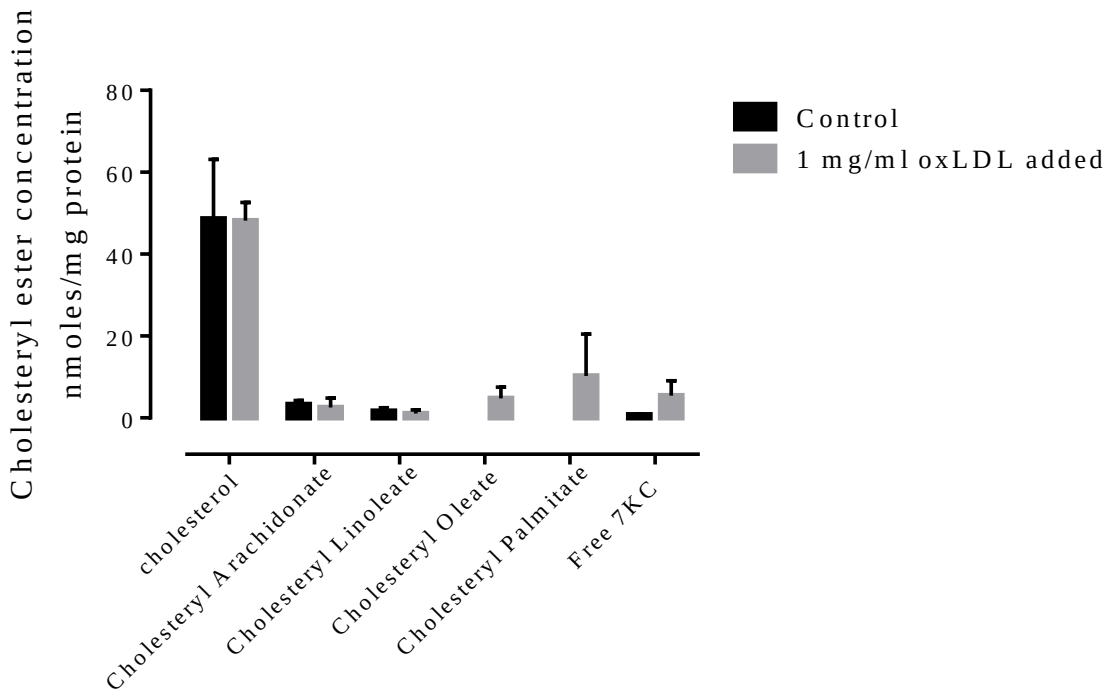

Figure 9. Cholesterol and cholesteryl ester accumulation in cells treated with 1.0mg/ml oxLDL for 48 hours. Macrophages were incubated with 1.0mg/ml oxLDL in RPMI 1640 supplemented with 10% human serum and p/s or fresh RPMI 1640 supplemented with 10% human serum and p/s for 48 hours at 36°C. Cell samples were extracted into cholesteryl ester mobile phase and absorbance was measured at 210nm and 234nm on the HPLC using the cholesteryl ester method. Analysis on GraphPad Prism 6.0.

3.5 Measurement of cellular sterols

After establishing that the cholesteryl ester method reliably measured the presence of cholesterol and cholesterol esters in pure lipoproteins, the loading into cells was examined. Figure 9 had confirmed that cholesteryl ester uptake in macrophages occurs at the sub toxic concentration of 1mg/ml when incubated for 48 hours. However, the amount of the cholesteryl ester accumulation in the macrophages was not very high (figure 10). The only distinct peak in figure 10 is the cholesterol peak. The cholesteryl ester peaks merge with the other peaks seen in cell extracts. This precipitated the decision to focus on cholesterol and 7-ketocholesterol as markers for identifying oxLDL stimulated foam cell formation.

7-ketocholesterol is a major oxidation product of cholesterol in oxLDL and is expected to be a major sterol esterified to fatty acids within oxLDL. In foam cells 7-ketocholesterol also is esterified to fatty acids (Andrew J. Brown, Watts, et al. 2000). We

therefore examined how to measure total cellular 7-ketocholesterol by alkaline hydrolysis of the esters to release the 7-ketocholesterol so it could be measured directly by HPLC (Andrew J. Brown, Watts, et al. 2000). This would also allow the measurement of total cellular cholesterol as the alkaline hydrolysis would also hydrolyse all the other cholesteryl esters.

Using a more polar mobile phase containing a small quantity of water (2%), the elution of cholesterol and 7-ketocholesterol was examined. The commercial cholesterol standard was dissolved in the 7KC mobile phase and run on the HPLC using the 7KC method (figure 11). When comparing the commercial cholesterol standards analysed by the cholesteryl ester measurement method to the 7KC method (figures 1 and 11), it was noted that the differences in mobile phase composition resulted in the cholesterol eluting off the column at different times. In figure 1, the cholesterol standard elutes at 6.1 minutes but in figure 11, when treated with the 7KC method, the cholesterol elutes off at 7.04 minutes. Cell samples were then extracted and run through the HPLC (figure 13) to determine if this change in cholesterol elution time off the column had any adverse effect on the chromatogram peaks, such as overlapping with other peaks. There were no adverse effects from using the 7KC method (figure 13) instead of the cholesteryl ester measurement method. Rather, the cholesterol peak was more clearly delineated and so could be identified with more ease.

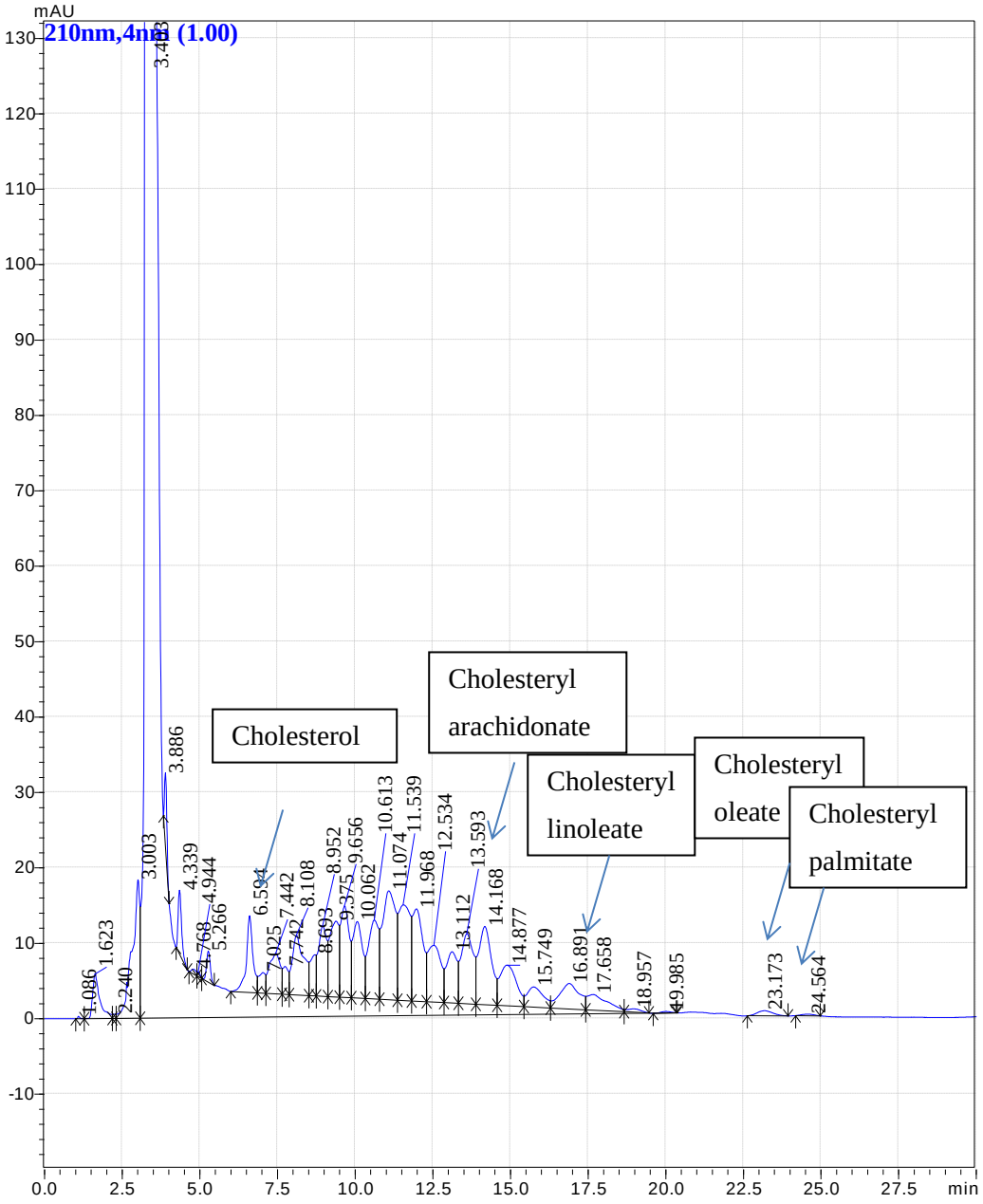

Figure 10. Chromatogram of cholesterol and cholesteryl ester accumulation in macrophages when incubated with 1.0mg/ml oxLDL for 48 hours. Macrophages were treated with 1.0mg/ml oxLDL for 48 hours, then extracted into hexane and re-solubilised in cholesteryl ester mobile phase. Samples were analysed by HPLC using the cholesteryl ester method. Absorbance was measured at 210nm.

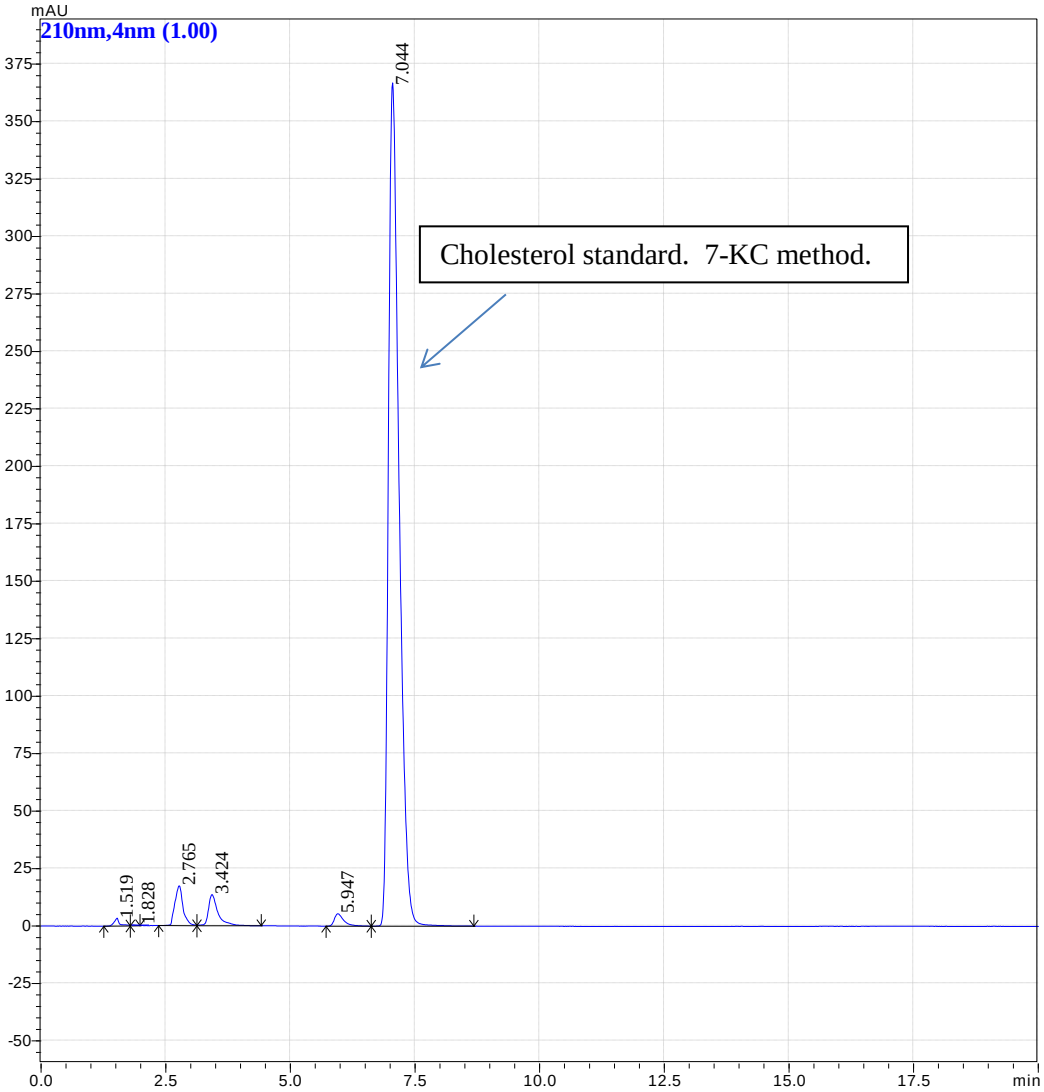

Figure 11. Commercial cholesterol standard processed using 7KC method. Cholesterol standard dissolved in hexane, dried in nitrogen and re-suspended in 7-KC mobile phase as per methods. Processed on the HPLC using 7-KC method and absorbance measured at 210nm.

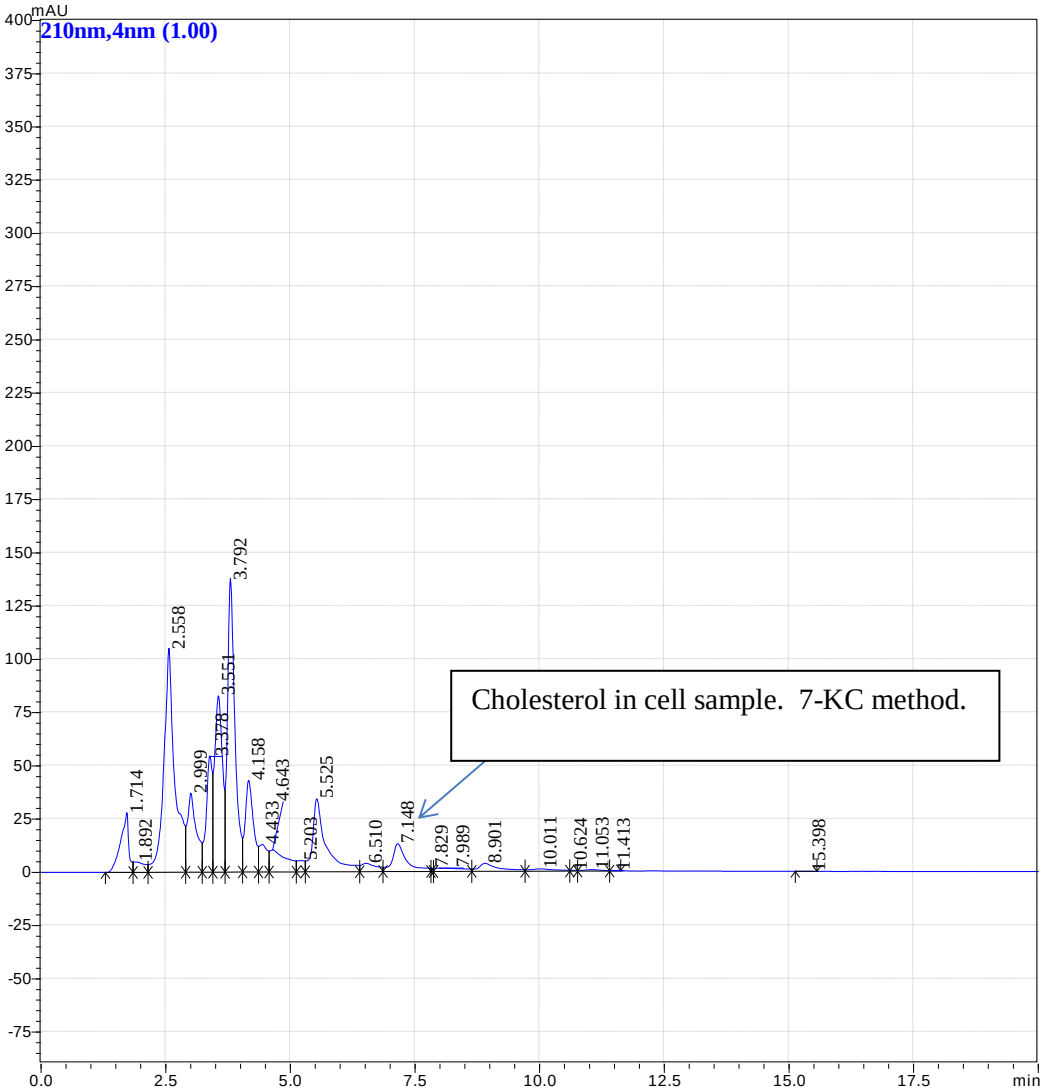

Figure 12. Cell sample analysed using 7KC method. 3 wells of control cell sample from 0 hours extracted into hexane and re-suspended in 7-KC mobile phase as per 7KC method. Processed on the HPLC using the 7-KC method. Cholesterol absorbance was measured at 210nm.

7-ketocholesterol was also analysed using the HPLC. In figure 13, the commercial standard was analysed to determine the time it eluted off the column so that identification of the 7KC in cell samples could occur. Cell samples were then extracted into hexane and hydrolysed using the 7KC method. The 7KC peak in cell samples was identified in figure 14. This resulted in samples which were able to be analysed on the HPLC at both 210 nm for the cholesterol measurement and at 234nm for the 7-KC measurement. Consequently the techniques for confirming foam cell formation were

able to be streamlined into one contiguous method where both 7-ketocholesterol and cholesterol are hydrolysed from the fatty acids and measured in the one HPLC analysis.

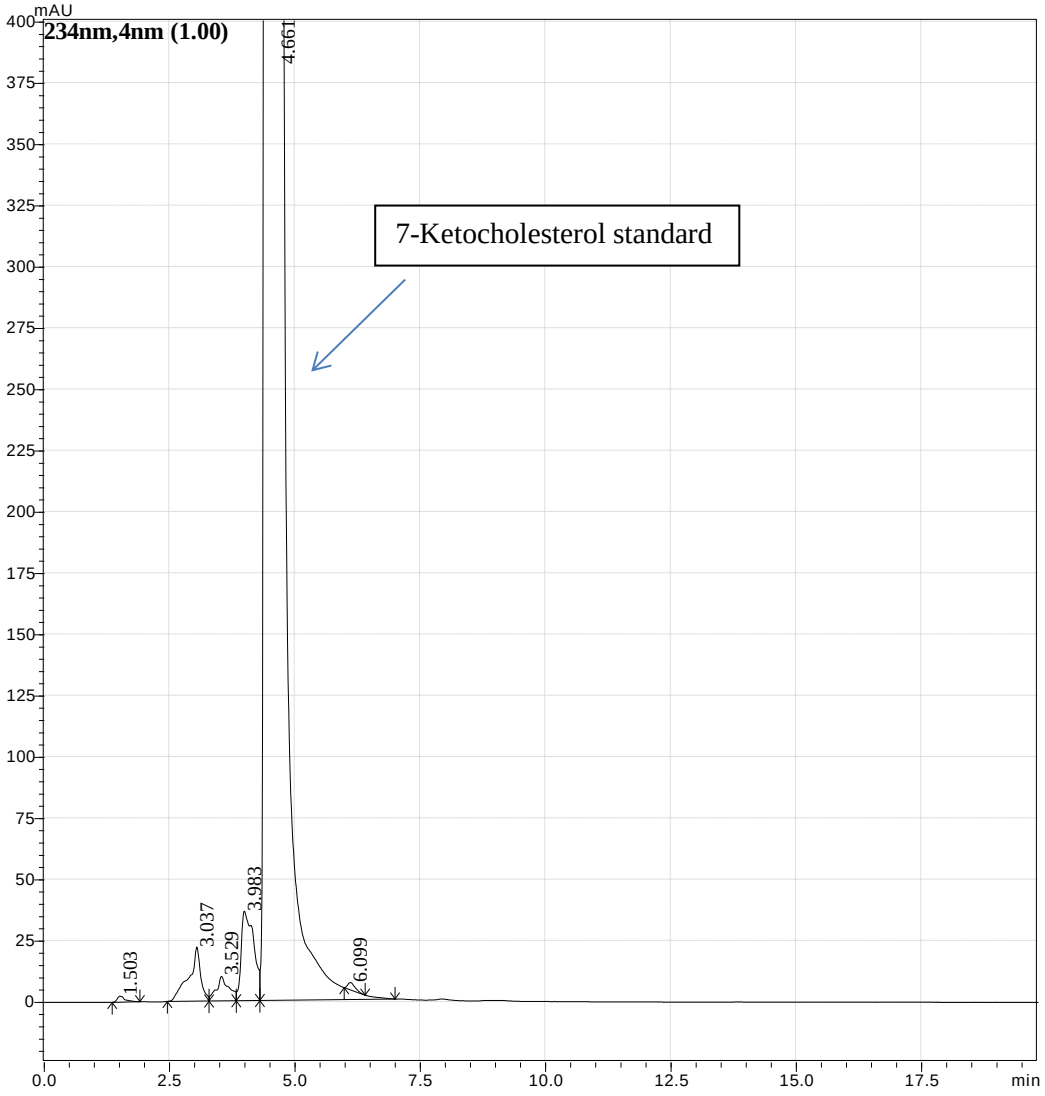

Figure 13. Commercial 7-ketocholesterol standards analysed by HPLC using 7KC method. The commercial 7KC standard was dissolved in the 7KC sample mobile phase (isopropanol/acetonitrile 11:9) and analysed by HPLC. The 7KC method was used to run the standard which called for the new mobile phase (isopropanol, acetonitrile and water as per method). The absorbance was measured at 234nm.

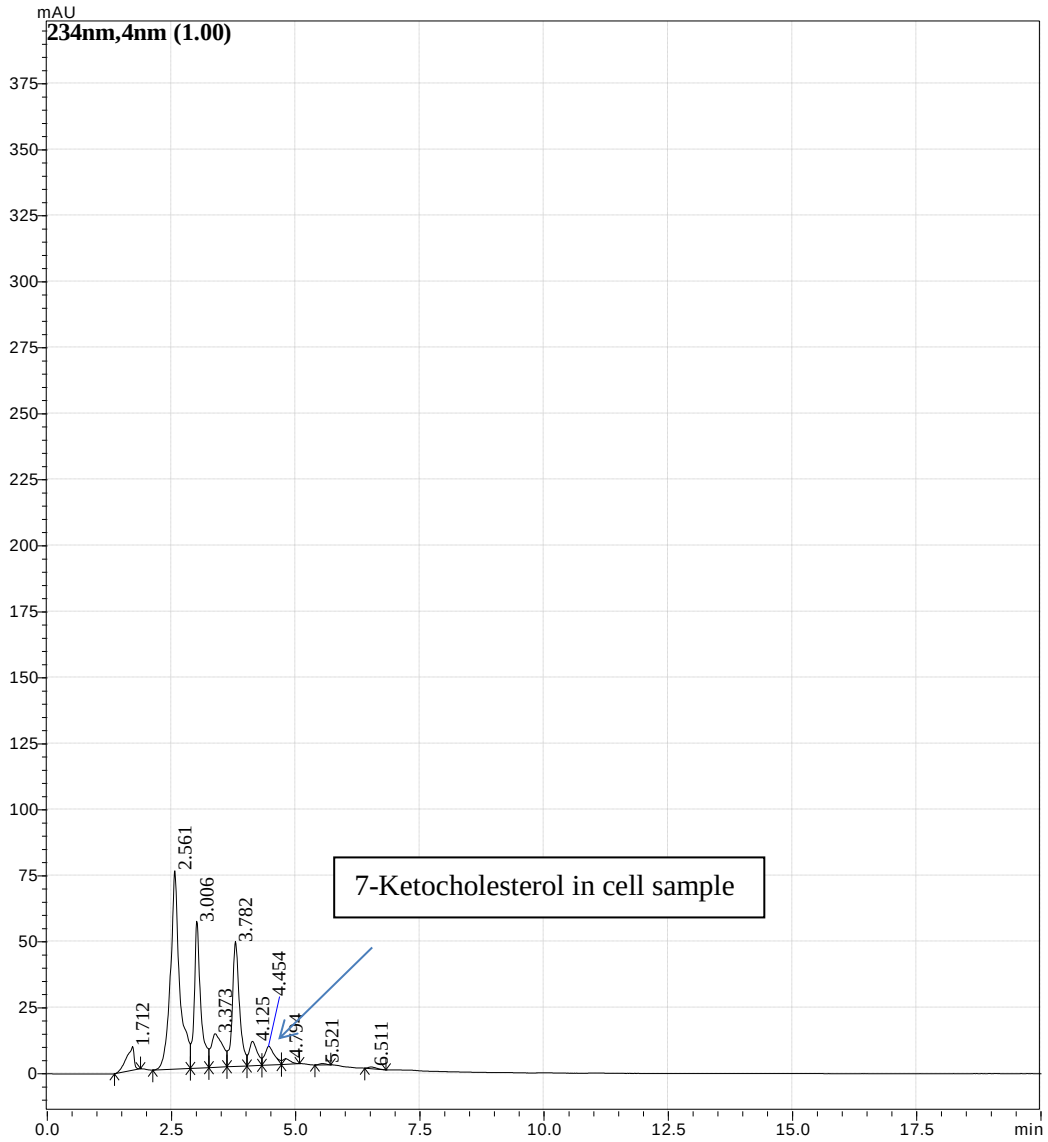

Figure 14. Cell sample from 0 hour control extracted and prepared using the 7KC hydrolysis method. 3 pooled wells of control sample at 0 hours was extracted prepared using the 7KC method with a 3 hour KOH hydrolysis. The sample was re-solubilised using the acetonitrile/isopropanol 9:11 mobile phase and injected and analysed on the HPLC using the 7KC mobile phase and method. Absorbance was measured at 234nm.

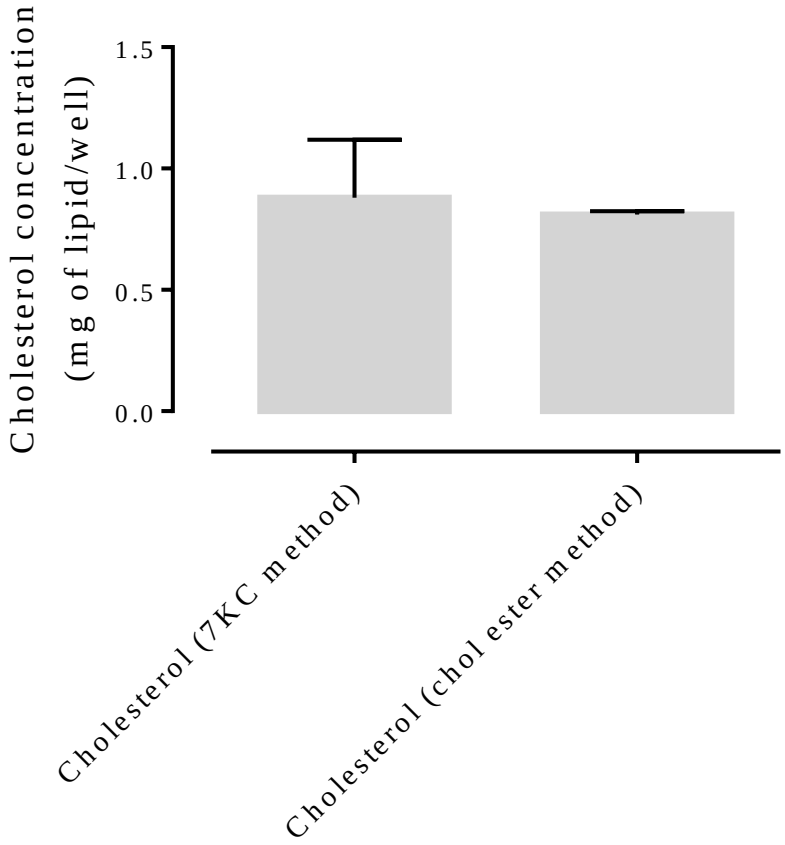

Figure 15. Comparison of cholesterol concentration measured by HPLC using the cholesteryl ester method vs. the 7KC method. Macrophages were incubated with RPMI 1640 supplemented with 10% human serum and p/s. They were extracted in hexane and split into two. Each sample was re-solubilised into respective mobile phases and analysed by HPLC according to their respective methods. Absorbance was measured at 210nm.

Measuring the free cholesterol present using the 7KC HPLC analysis following sterol hydrolysis it was determined that the majority of cholesterol in the cells was as free cholesterol (figure 15). Cholesteryl esters are hydrolysed into free cholesterol but as there was so little cholesteryl ester accumulation (figure 9), we didn't expect a large increase in cholesterol measured by the 7KC method. This confirmed that the hydrolysis method was reliable when measuring markers of foam cell formation.

3.6 Foam cell formation

Foam cells were successfully formed when a conformational change had been seen after 48 hours treatment with sub toxic oxLDL (figure 16)

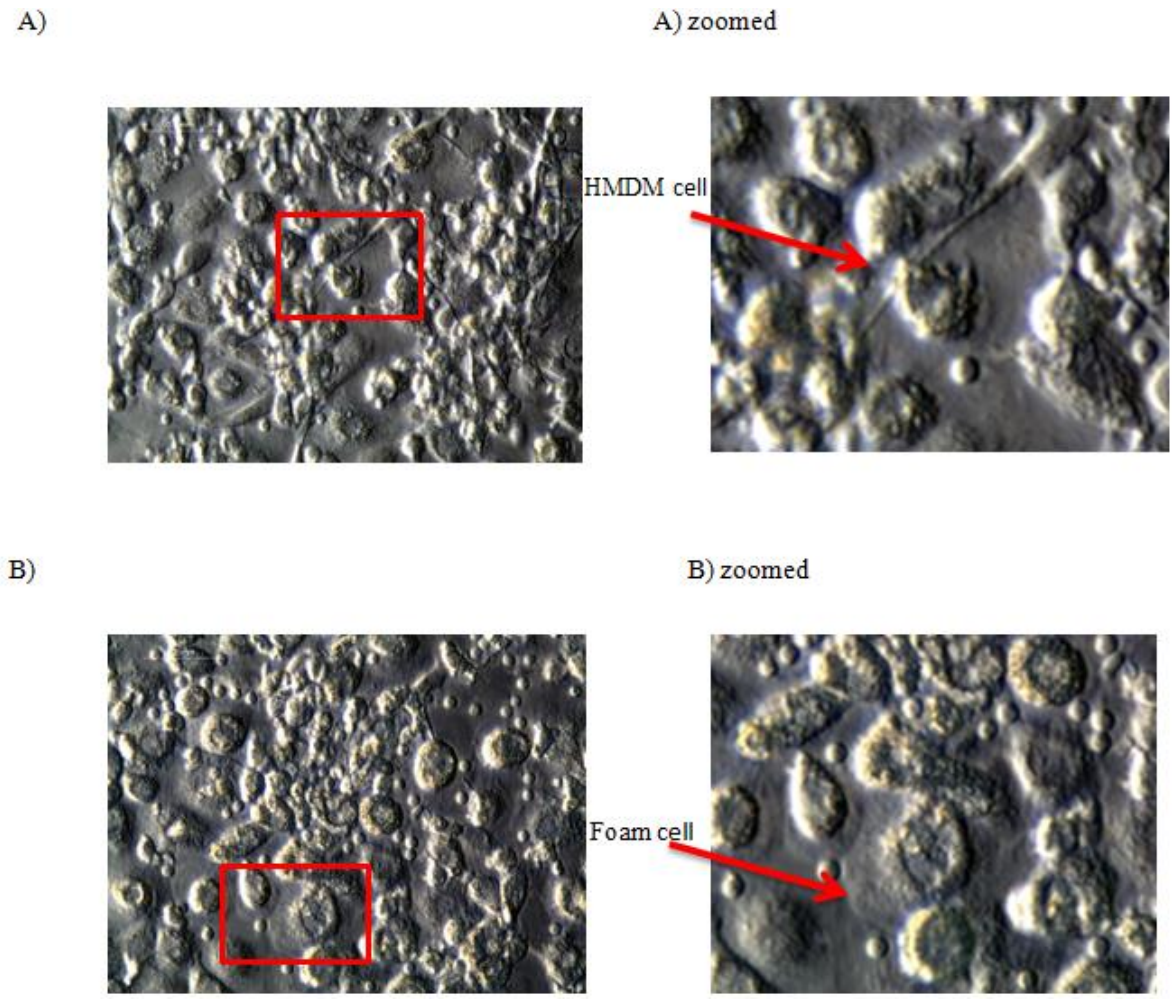

Figure 16. Morphological differences between foam cells and macrophages after 48 hour incubation. Macrophages incubated for 48 hours. A) cells were treated with fresh RPMI 1640 supplemented with 10% human serum and p/s as a control. B) cells were treated with 1mg/ml oxLDL and RPMI 1640 supplemented with 10% human serum and p/s. The morphological changes due to oxLDL treatment are illuminated between A zoomed) and B zoomed). The foam cells in B zoomed) have an engorged cell membrane. Scale bars are 0.1mm.

The cells were analysed using HPLC and uptake of cholesterol, cholesteryl arachidonate, cholesteryl linoleate, cholesteryl oleate, cholesteryl palmitate and 7-ketocholesterol was quantified in figures 17-22. The HMDM cells were treated with 1.0mg/ml oxLDL from an original oxLDL concentration of 10.27mg/ml. The MTT assay (figure 8) had determined that 1.0mg/ml oxLDL was sub-toxic to the macrophages. After 0, 6, 12, 24, 30, 36, 42 and 48 hours the cells were extracted using the cholesteryl ester method. Although the oxLDL only exhibited cholesterol, cholesteryl oleate and cholesteryl palmitate on the HPLC chromatogram (figure 3), it caused macrophages to take up cholesterol, all of the cholesteryl esters and 7-

ketocholesterol. Uptake varied and ranged from a 20nmole/mg of protein uptake in cholesterol (figure 17) to 0.12nmole/mg of protein uptake in cholesteryl linoleate (figure 19). Cholesteryl linoleate is oxidised to hydroperoxides therefore when treated with an oxidised lipoprotein the cholesteryl linoleate uptake was shown to be limited (figure 19), likely due to oxidation. In this experiment, cholesterol oxidation was being measured as 7-ketocholesterol. 7KC is identified as the main oxidation product in atherosclerosis. The trend that cholesterol and all the esters reveal in figures 17-21 is a sharp increase in uptake over the first 24 hours of oxLDL exposure. The uptake slowed in the second 24 hours of oxLDL exposure. The increase in uptake of cholesterol, esters and 7KC indicated that foam cells had been formed.

The original analysis of the data as g of lipid/well showed the trend of the raw data before it was corrected for the amount of protein in the samples. This ensures that the data presented is a product of the oxLDL treatment inducing sterol and ester uptake. It reduced the likelihood of errors in mathematical analysis altering the results when they were corrected for protein expression. Of note, correcting for protein expression reduces the uptake from μmole measurements to nmole measurements. It corrected for varying numbers of cells thereby smoothing out the graphical data.

Figure 17 A)

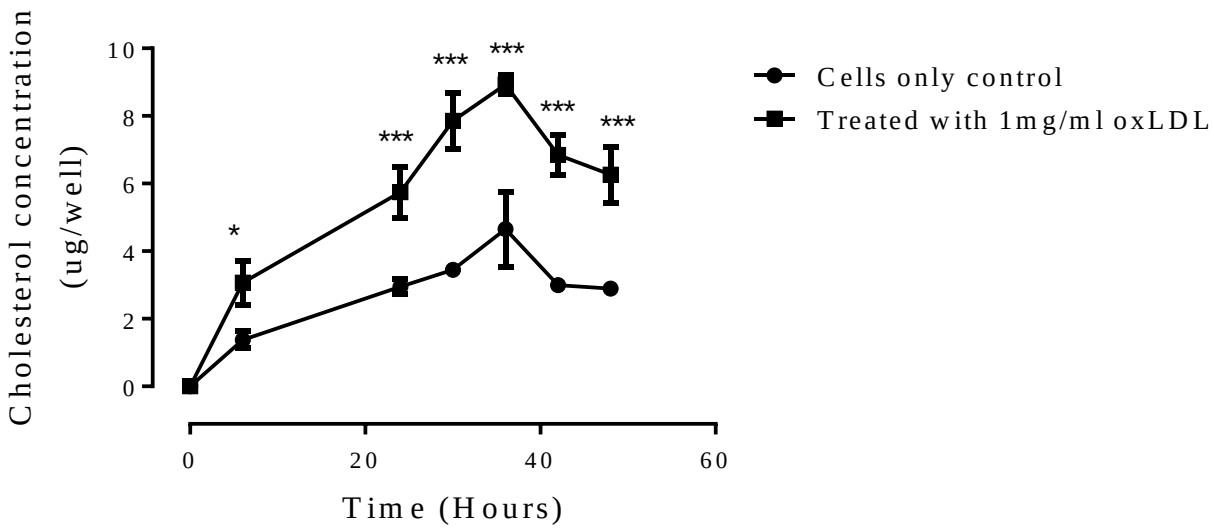

Figure 17 B)

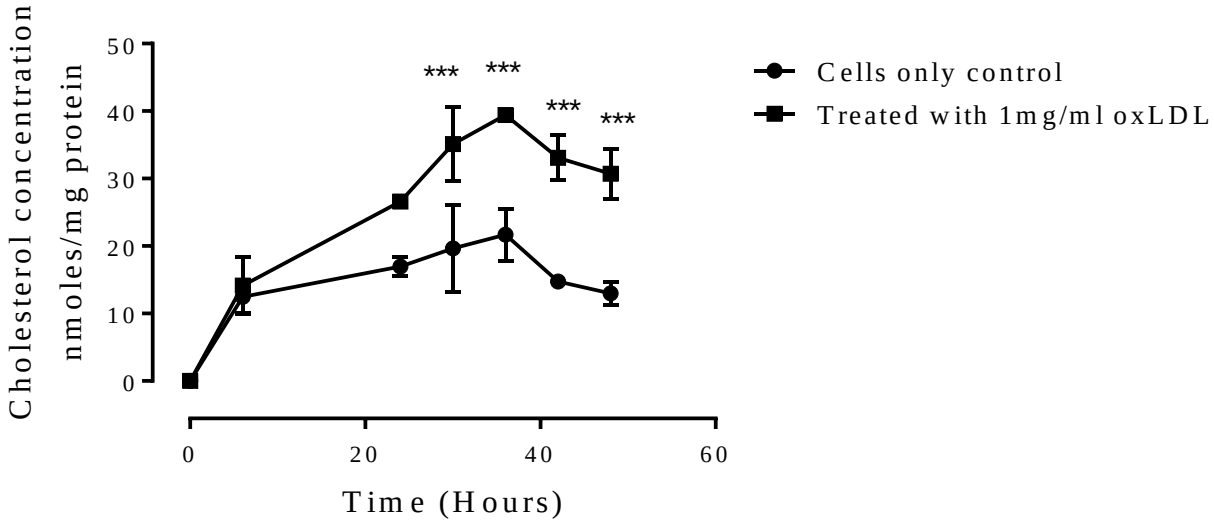

Figure 17. Cholesterol accumulation in macrophages treated with 1mg/ml oxLDL for 48 hours. Macrophages were incubated with 1.0mg/ml oxLDL in RPMI 1640 supplemented with 10% human serum and p/s or RPMI 1640 supplemented with 10% human serum and p/s as a control over 48 hours. Samples were extracted into cholesteryl ester mobile phase and run on the HPLC using the cholesteryl ester method. Absorbance was measured at 210nm. Analysis was corrected for g of lipid/well (15A) and corrected for estimated protein (15B). 2-way ANOVA analysis revealed a p value of *** = 0.001. Analysis using GraphPad Prism 6.0.

Figure 18 A)

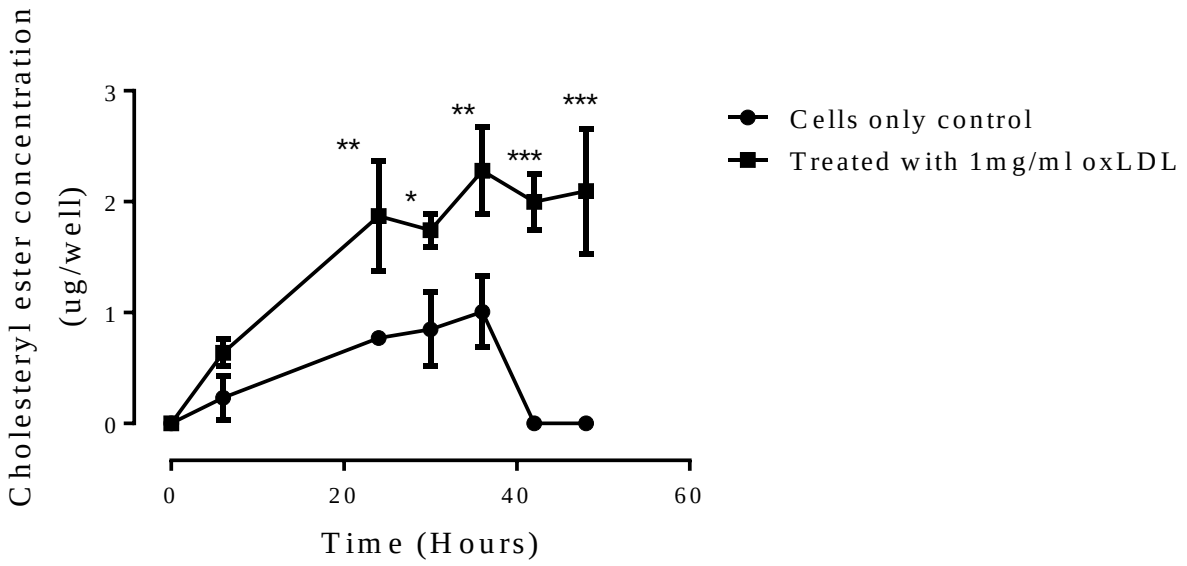

Figure 18 B)

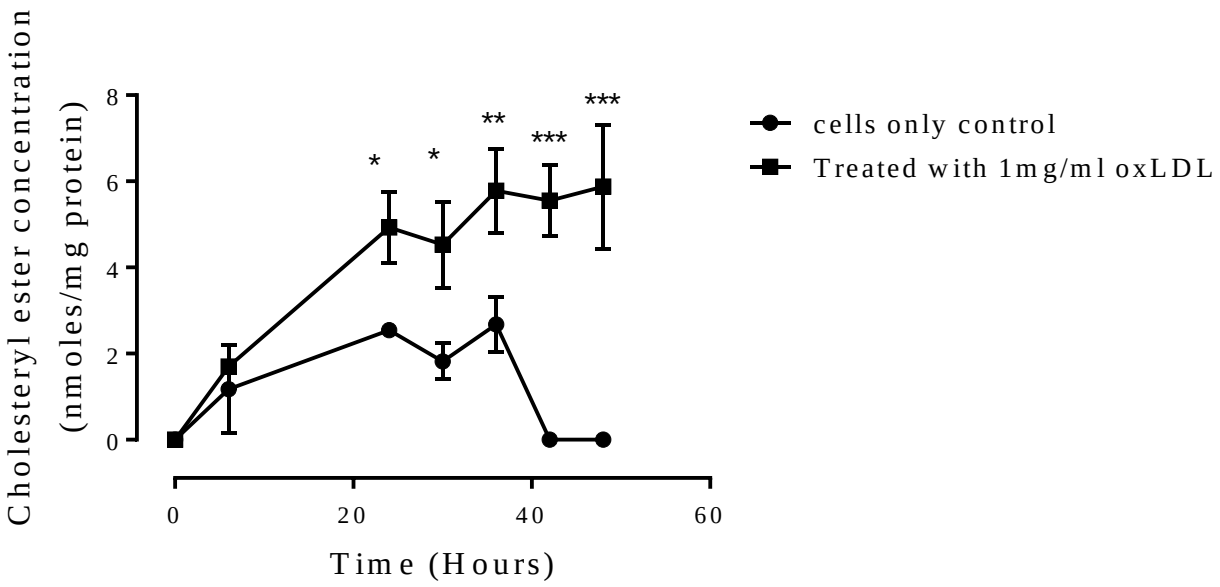

Figure 18. Cholesteryl arachidonate accumulation in macrophages incubated with 1.0 mg/ml oxLDL for 48 hours. Macrophages were incubated with 1.0mg/ml oxLDL in RPMI 1640 supplemented with 10% human serum and p/s or RPMI 1640 supplemented with 10% human serum and p/s as a control over 48 hours. Samples were extracted into cholesteryl ester mobile phase and run on the HPLC using the cholesteryl ester method. Absorbance was measured at 210 nm. Analysis was corrected for g of lipid /well (16A) and corrected for estimated protein (16B). 2-way ANOVA analysis revealed p values of * = 0.5, ** = 0.01 and *** = 0.001. Analysis using GraphPad Prism 6.0.

Figure 19 A)

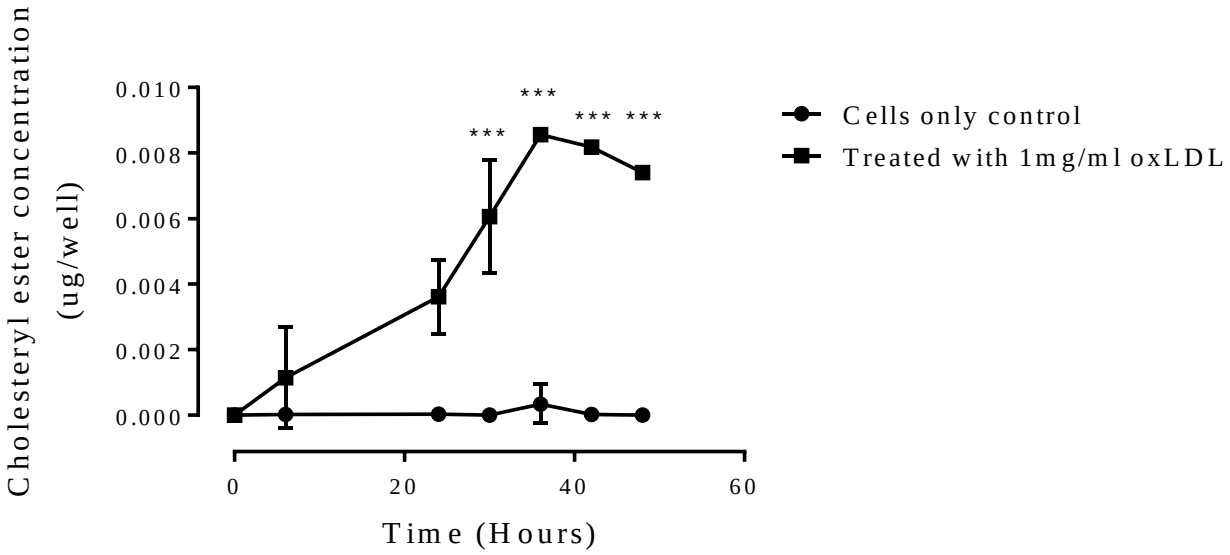

Figure 19 B)

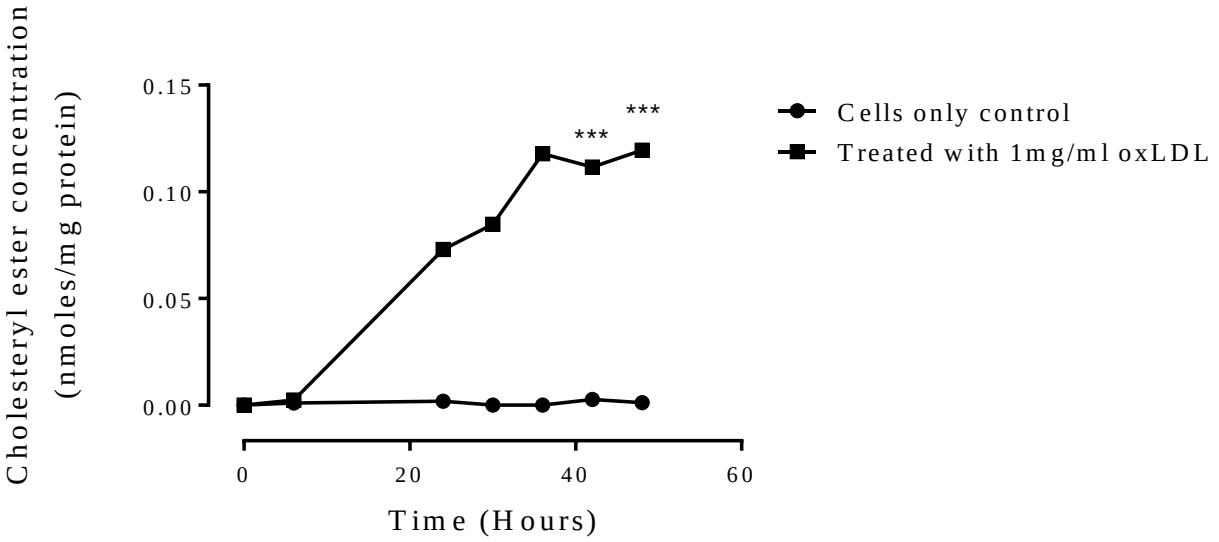

Figure 19. Cholesteryl linoleate accumulation in macrophages treated with 1.0mg/ml oxLDL for 48 hours. Macrophages were incubated with 1.0mg/ml oxLDL in RPMI 1640 and 10% human serum or RPMI 1640 and 10% human serum as a control over 48 hours. Samples were extracted into cholesteryl ester mobile phase and run on the HPLC using the cholesteryl ester method. Absorbance was measured at 210 nm. Analysis was corrected for g of lipid /well (17A) and corrected for estimated protein (17B). 2-way ANOVA analysis revealed a p value of *** = 0.001. Analysis using GraphPad Prism 6.0.

Figure 20 A)

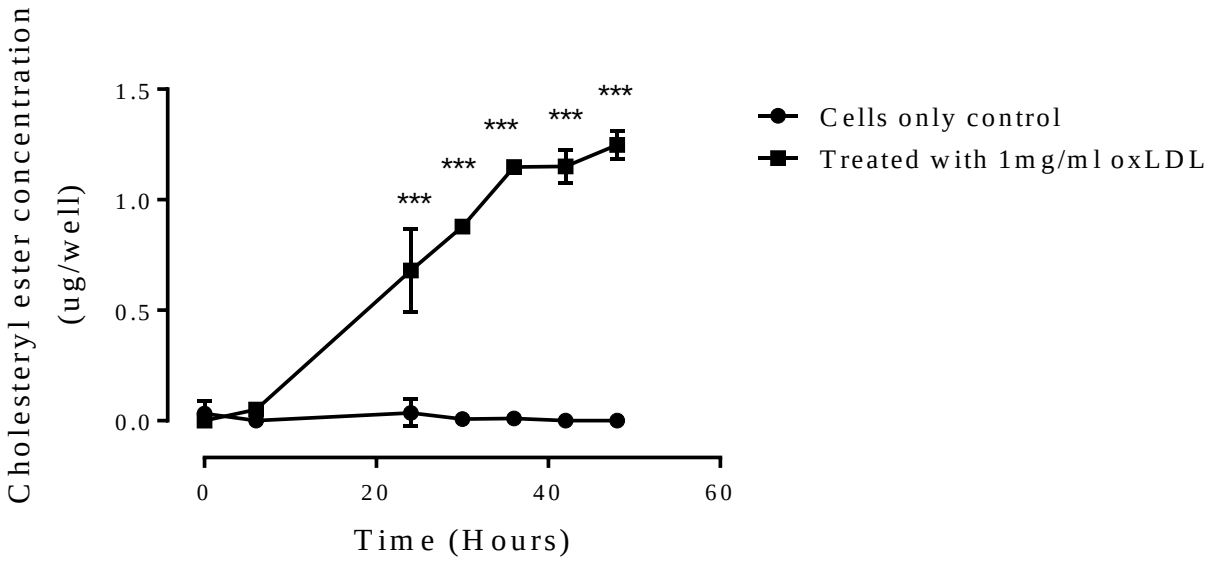

Figure 20 B)

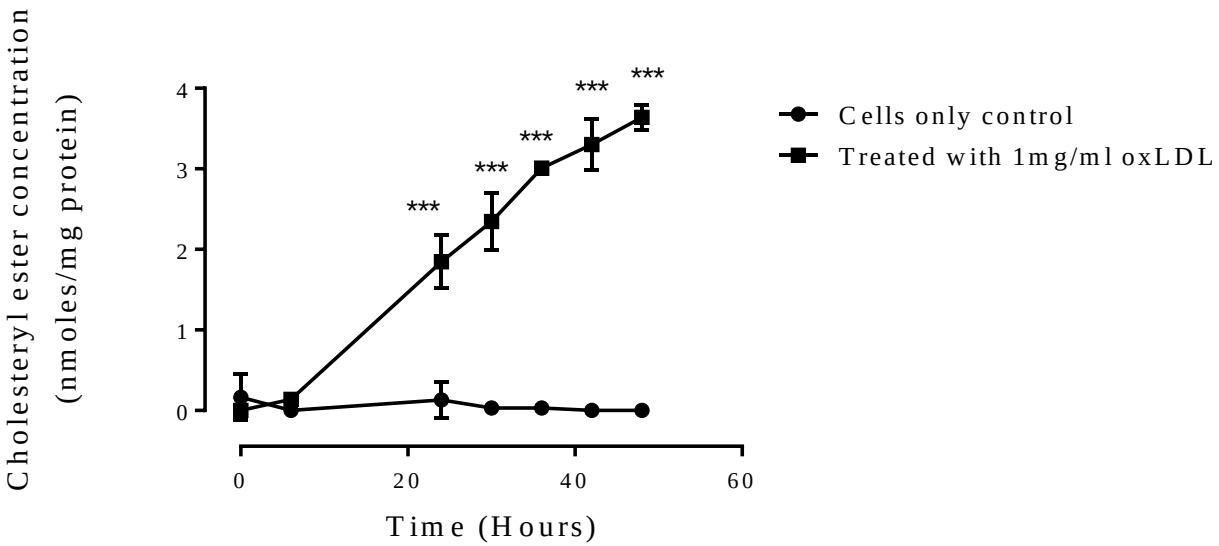

Figure 20. Cholesteryl oleate accumulation in macrophages incubated with 1.0mg/ml oxLDL for 48 hours. Macrophages were incubated with 1.0mg/ml oxLDL in RPMI 1640 supplemented with 10% human serum and p/s or RPMI 1640 supplemented with 10% human serum and p/s as a control over 48 hours. Samples were extracted into cholesteryl ester mobile phase and run on the HPLC using the cholesteryl ester method. Absorbance was measured at 210 nm. Analysis was corrected for g of lipid /well (18A) and corrected for estimated protein (18B). 2-way ANOVA analysis revealed a p value of *** = 0.001. Analysis using GraphPad Prism 6.0

Figure 21 A)

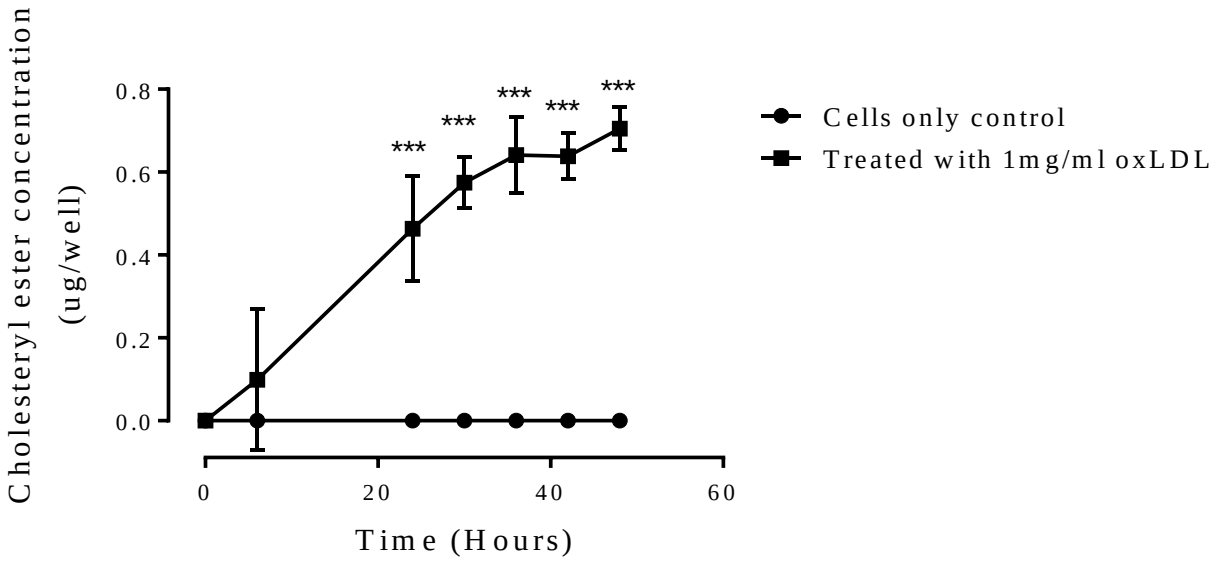

Figure 21 B)

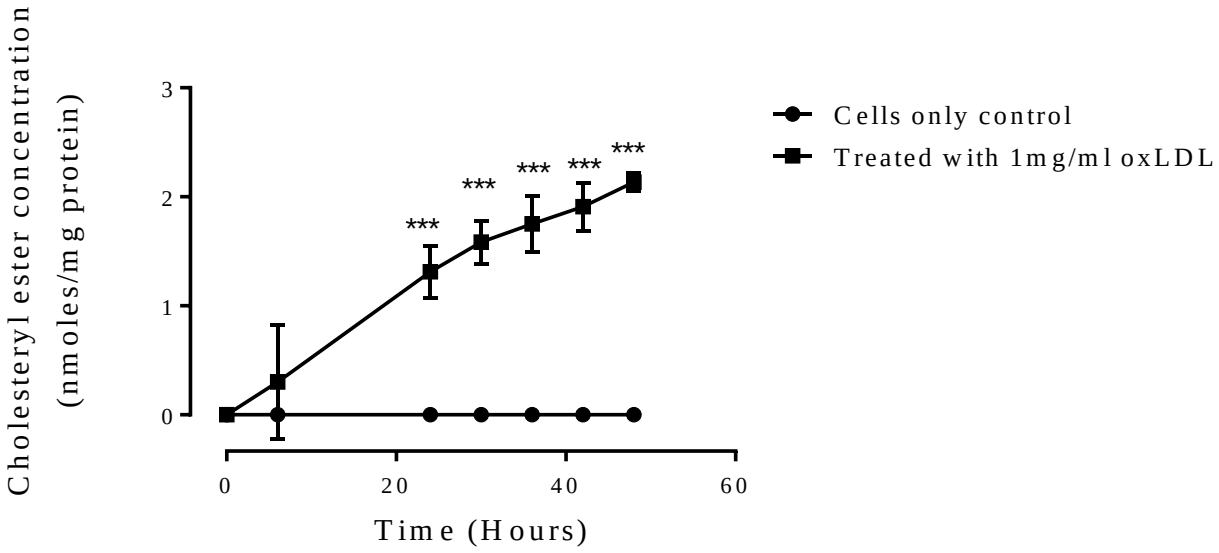

Figure 21. Cholesteryl palmitate accumulation in macrophages incubated with 1.0mg/ml oxLDL for 48 hours. Macrophages were incubated with 1.0mg/ml oxLDL in RPMI 1640 supplemented with 10% human serum with p/s or RPMI 1640 supplemented with 10% human serum and p/s as a control over 48 hours. Samples were extracted into cholesteryl ester mobile phase and run on the HPLC using the cholesteryl ester method. Absorbance was measured at 210 nm. Analysis was corrected for g of lipid /well (19A) and corrected for estimated protein (19B). 2-way ANOVA analysis revealed a p value of *** = 0.001. Analysis using GraphPad Prism 6.0

Figure 22 does not follow the same trend as figures 17-21. This is because the 7-KC uptake in figure 22 was done separately to figures 17-21 and used a preparation of macrophages from a different source. They were incubated for 0, 24, 36 and 48 hours in 1.0mg/ml oxLDL before undergoing 7KC hydrolysis, being re-solubilised in 7KC mobile phase and processed on the HPLC at 234nm using the 7-ketocholesterol method.

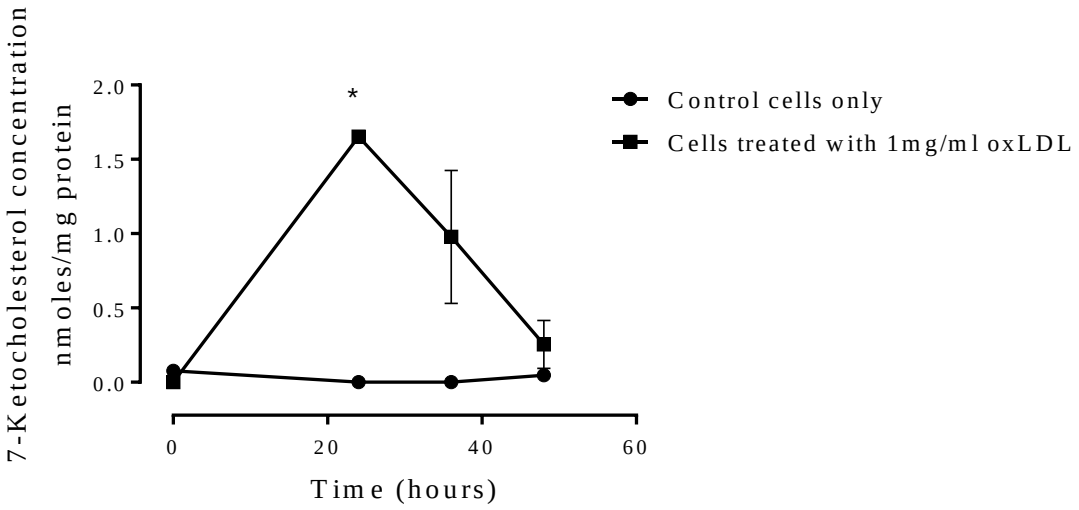

Figure 22. 7-Ketocholesterol accumulation in macrophages incubated with 1.0mg/ml oxLDL for 48 hours. Macrophages were incubated with 1.0mg/ml oxLDL in RPMI 1640 supplemented with 10% human serum and p/s or RPMI 1640 supplemented with 10% human serum and p/s as a control over 48 hours. Samples were extracted into 7-KC mobile phase and run on the HPLC using the 7-KC method. Absorbance was measured at 234 nm. Analysis was corrected for estimated protein. 2-way ANOVA analysis revealed a p value of * = 0.0178. Analysis using GraphPad Prism 6.0.

The initial 24 hour increase of 7KC concentration was expected as it was shown previously in this lab (Shchepetkina 2013), however the drop of 7KC after 24 hours was unexpected and not explained by aberrant protein levels or processing errors. This drop may indicate that in some cells uptake occurs however after 24 hours a blocking mechanism is activated that effluxes 7-KC, possibly the ABC-A1 receptor (Gaus et al. 2001; Karuna et al. 2011). The uptake seen in figure 22 of 1.5nmol/mg protein was considerably less than uptake observed in previous study (Shchepetkina 2013) which saw a 25nmole/mg protein increase in 7-KC in the first 24 hours. This may be explained by the use of macrophages. Macrophages exhibit variability of the results observed depending on the source of the cells. Cells were obtained from different human donors on a weekly basis resulting in a degree of unpredictability which cannot be mitigated.

The interesting trend in figure 22 is not the amount of 7KC uptake, but the decrease in 7-KC seen after 24 hours. This decrease was not seen in previous studies however this may be due to the time period of the experiments which was only 24 hours (Shchepetkina 2013).

3.7 CD36 cell surface expression method development

Once foam cell formation had been observed (figure 16) and measured, the behaviour of CD36 surface expression was focussed on. In order to be able to ensure that the cell population being measured on the flow cytometer was macrophages, a CD16 macrophage phenotypic marker antibody was used (figure 23). The macrophages were treated with antiCD16 primary antibody. This enabled the position of the macrophage population to be identified on the flow cytometer (SSC-A vs. FSC-A) and measured in figure 23. Once the cell population had been confirmed in figure 23 by the CD16 antibody, the correct cells could be studied.

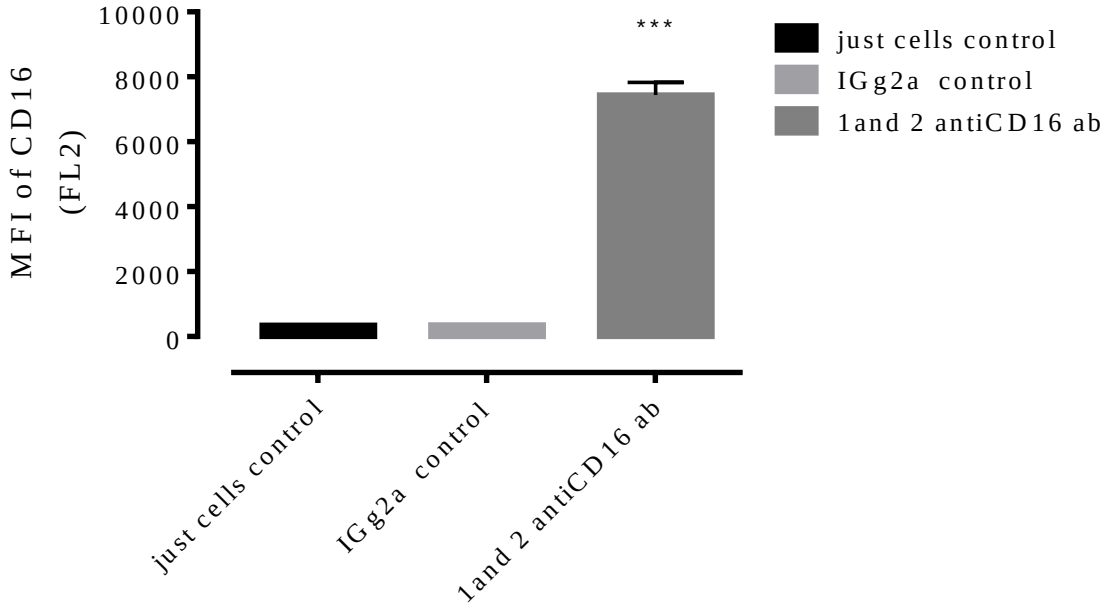

Figure 23. Macrophages treated with the antibody CD16, a macrophage phenotypic marker. HMDM cells Macrophages were washed, lifted up with accutase™ and treated in the dark, on ice with 10mg/ml of a CD16 antibody or a primary antibody control for 30 minutes. Cells were suspended in 1ml PBS and BSA as per method and run through the flow cytometer using the FL2 filter to measure 578nm emission. One-way ANOVA gives a p-value of *** = <0.001. Analysis by GraphPad Prism 6.0.

Initially, the effectiveness of the anti CD36 antibody and PE labelled secondary antibody was determined (figure 24). A titration of CD36 primary antibody was tested on the monocyte-like U937 cell line provided by members of the lab. 1mg/ml, 10mg/ml and 20mg/ml of primary antiCD36 antibody were used on the cells to determine at which concentration the CD36 receptor was saturated with antibody. This also ensured that the anti-CD36 antibody bound to human CD36 receptor. Figure 24 A) depicts the procedure being used is reliable as it shows only one population is present. The presence of only one population is expected when using a cell line as there should only be one type of cell present. The signal can be measured consistently as there are no extraneous interferences from other cell populations. This is why the U937 cells were initially chosen to test on, as a base line for the methodology before moving to testing the macrophage model. The second, smaller population in figure 24 A) is likely cellular debris. Figure 25 is the histogram of figure 24 C) and allows statistical analysis to be done on the data. Figure 25 shows that 10mg/ml of primary antibody is the most effective concentration as 20mg/ml doesn't give a higher mean fluorescence intensity reading. 1mg/ml gives barely more fluorescence than the secondary antibody control. 10mg/ml of primary antibody is therefore ideal as at concentrations higher than that, the receptors become flooded. Using a higher concentration would result in wasting antibody.

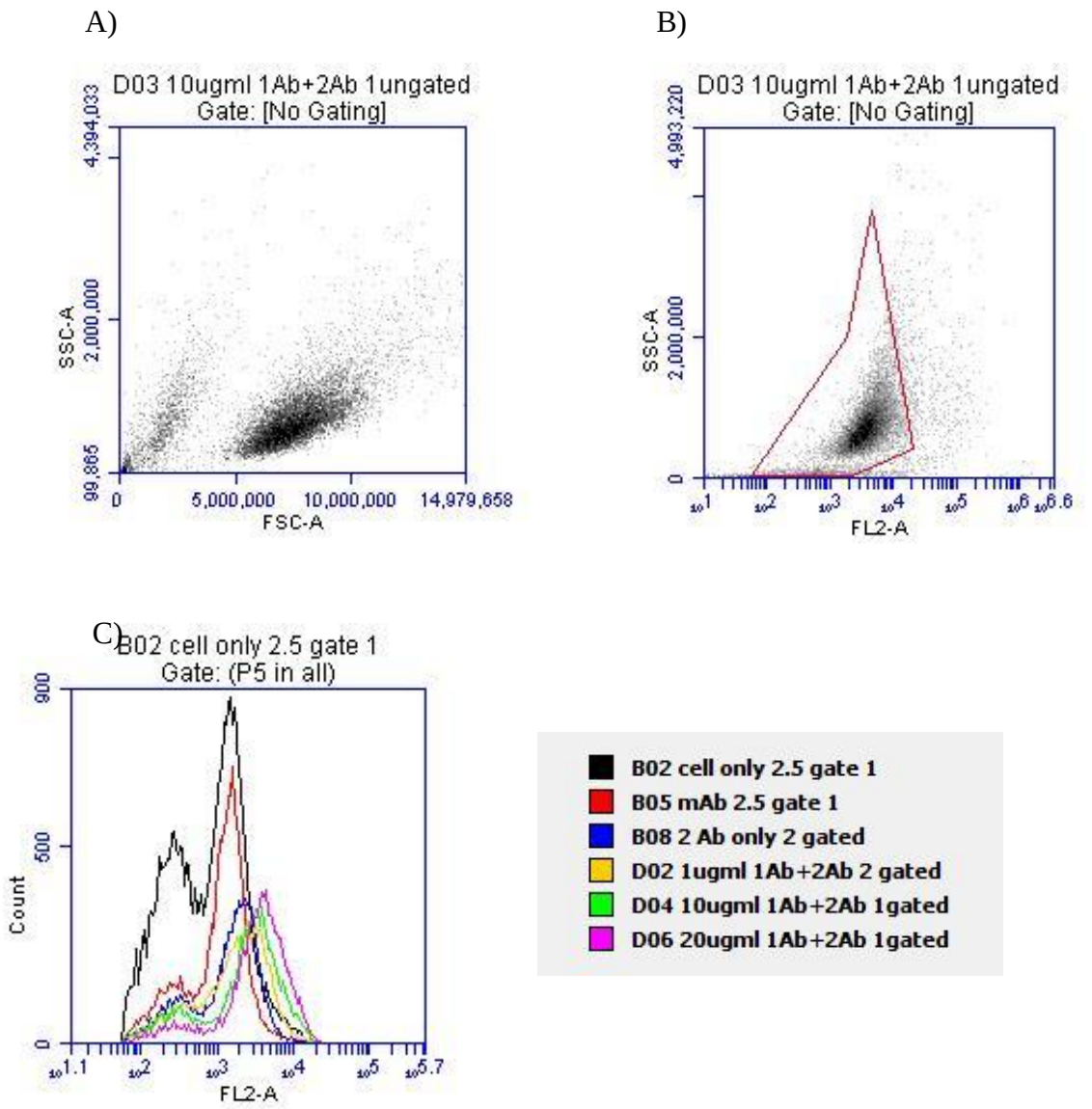

Figure 24. Flow cytometer traces for titration of CD36 antibody concentrations on U937 cells. U937 cells were washed and stained with anti-CD36 primary antibody and secondary antibody on ice, in the dark for 30 minutes as per method. The U937 cancer cell line was processed by the flow cytometer in order to isolate the population. The signal in A) indicates the presence of one dominant population of cells following incubation. Graph B) shows that when gated in FL-2 to measure 578nm emission, the anti CD36 signal was exclusively detected. That signal was transformed into a histogram in graph C). The increase in antiCD36 fluorescence in response to the increase in concentration is seen as a shift of the peak to the right on the x-axis.

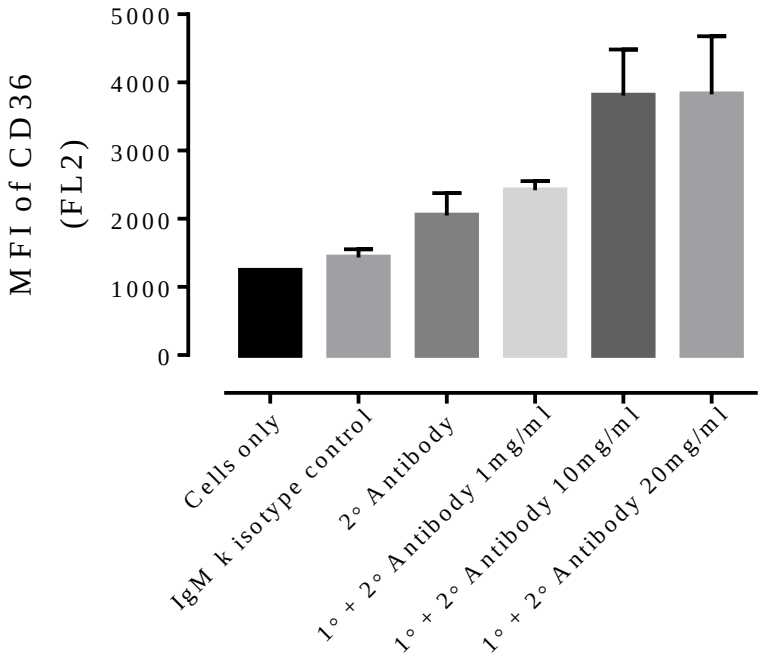

figure 25. CD36 primary antibody concentration titration using the U937 cell line. U937 cancer cell line treated on ice with differing concentrations of primary antibody at 1, 10 and 20 mg/ml. The cells only control was incubated with PBS and Foetal Calf serum as per method, the secondary antibody control and the isotype control cells were all treated for 30 minutes on ice. Cells were analysed on the flow cytometer using the FL2 filter to measure 578nm emission. Primary antibody saturation occurs at 10mg/ml. Analysis done in triplicate by GraphPad Prism 6.0.

Once the efficacy of the primary antibody had been tested on the U937s, titrations of the primary antibody concentration on the macrophage cells were required in order to be able to label the cells (figures 26 and 27). The position of the macrophage population on the flow cytometer trace (figure 26 A) had been identified through using the antiCD16 antibody and was confirmed in figure 26 A) when using the anti CD36 antibody. The cells were lifted off the adherent cell culture plate with accutase™, washed and treated with antibodies on ice. In agreement with the U937 results, the CD36 receptors were flooded with primary antibody at 10mg/ml antiCD36 (figure 26 C) and 27) which produced 4 times more fluorescence than the natural fluorescence of the cells and twice the fluorescence of the secondary antibody control.

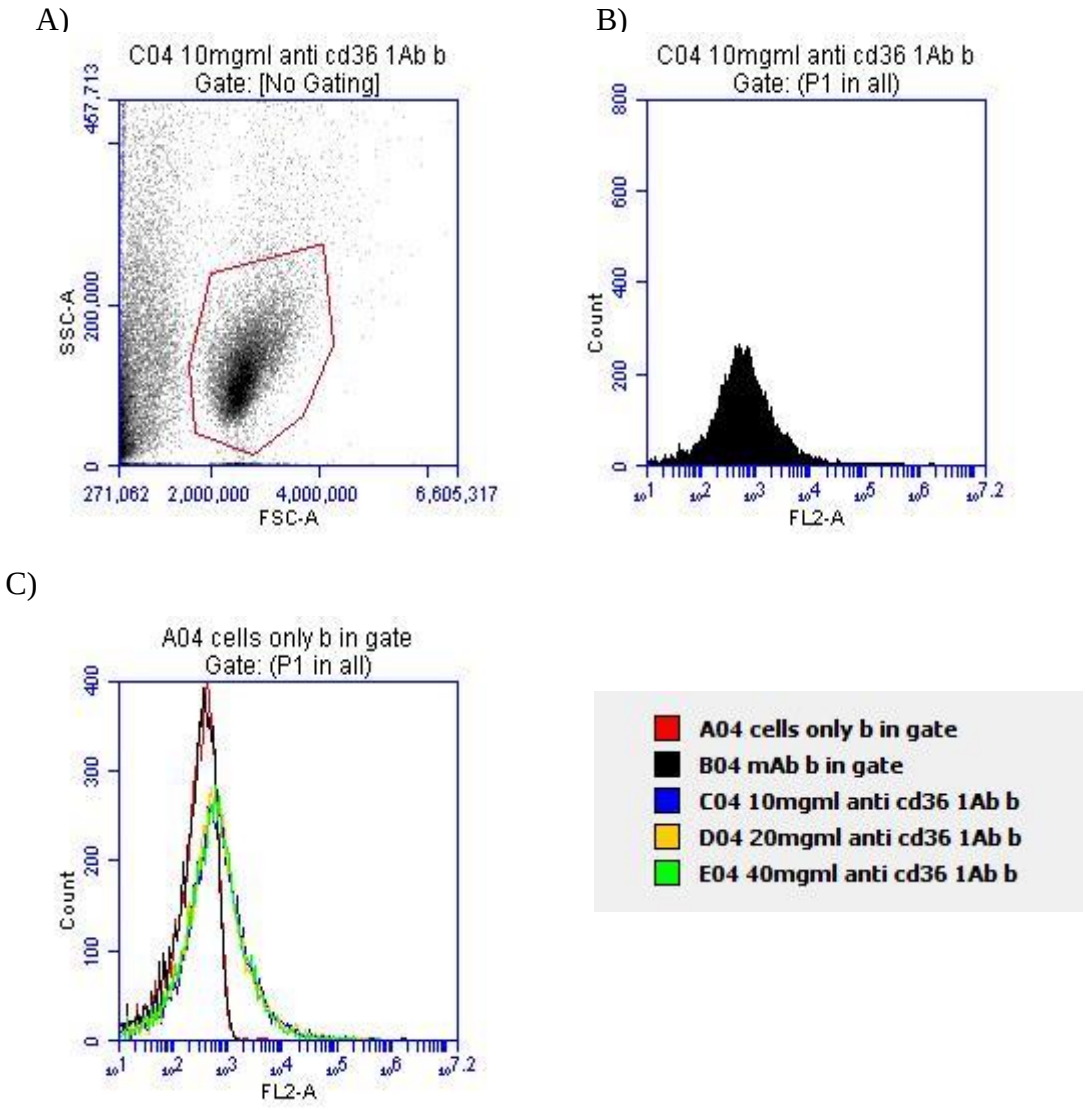

Figure 26. Flow cytometer traces for anti-CD36 concentration titration on macrophages. Macrophages were treated with accutase™ to lift them off adherent wells, washed and treated with anti CD36 primary, secondary and isotype control antibodies on ice for 30 minutes. Cells were washed and processed on the flow cytometer using the FL2 filter. A) Cells processed using forward and side scatter on the flow cytometer to identify the macrophage population. B) and C) are further measurements using the FL2 detector to measure 578nm emission of the PE fluorescent probe on the secondary antibody.

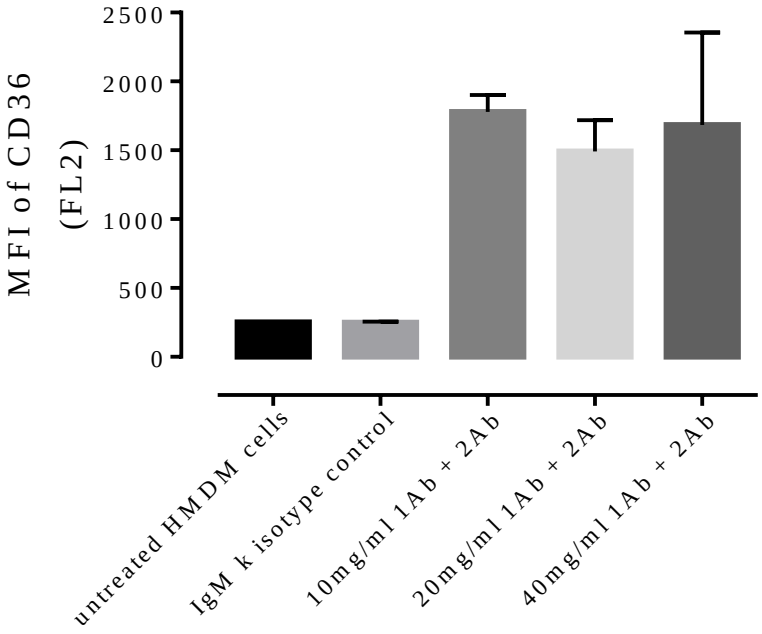

Figure 27. Titration of anti CD36 primary antibody concentrations on macrophages. Macrophages treated with differing concentrations of primary antibody, isotype control antibody and no antibody in the dark, on ice for 30 minutes. Cells were run through the flow cytometer using the FL2 filter to measure 578nm emission. Mean Fluorescence Intensity of triplicates analysed by GraphPad Prism 6.0.

There was an anomaly in the results between the U937 titrations (figure 25) and the macrophage titrations (figure 27). Research in the literature (Venugopal 2004) had indicated that macrophages expressed greater concentrations of surface CD36 than the U937 cell line. However, in figure 25 the mean fluorescence intensity (MFI) from the U937 cells peaked at 4000, whereas in figure 27 the MFI from the macrophages peaked at 1750. Analysis of the protocols used for both cell types indicated that the variance between the two processes involved the accutase™ which was used to lift macrophages off the adherent cell culture plates. Accutase™ is an enzyme solution that has proteolytic and collagenolytic properties. Cells are lifted off adherent wells using this method as it is less disruptive to the cells than methods involving trypsin and unlike scraping, doesn't lyse the cells. To test accutase™ and determine if it was damaging the CD36 receptor, suspension cells were required such as monocytes and U937s. Suspension cells were required because no method of lifting was needed prior to analysis on the flow cytometer. Consequently there was no damage to the receptors from trypsin or damage to the cell from manual manipulation. Both cell lines express CD36 which enabled the effect of accutase™ treatment on the expressed CD36

receptors to be isolated and studied. Figures 28 and 29 show that there is a decrease in CD36 mean fluorescence when treated with accutase™. The monocytes had a ¾ reduction in the MFI of CD36 due to accutase™ (figure 28). The U937 cell line had the CD36 MFI reduced by ½ due to accutase™ (figure 29). Both cell types had the CD36 MFI levels reduced nearly to basal level after a 15 minute incubation with accutase™ as per the protocol ("Accutase," n.d.). Accutase™ was proteolytically removing the CD36 receptor from the surface of the cells.

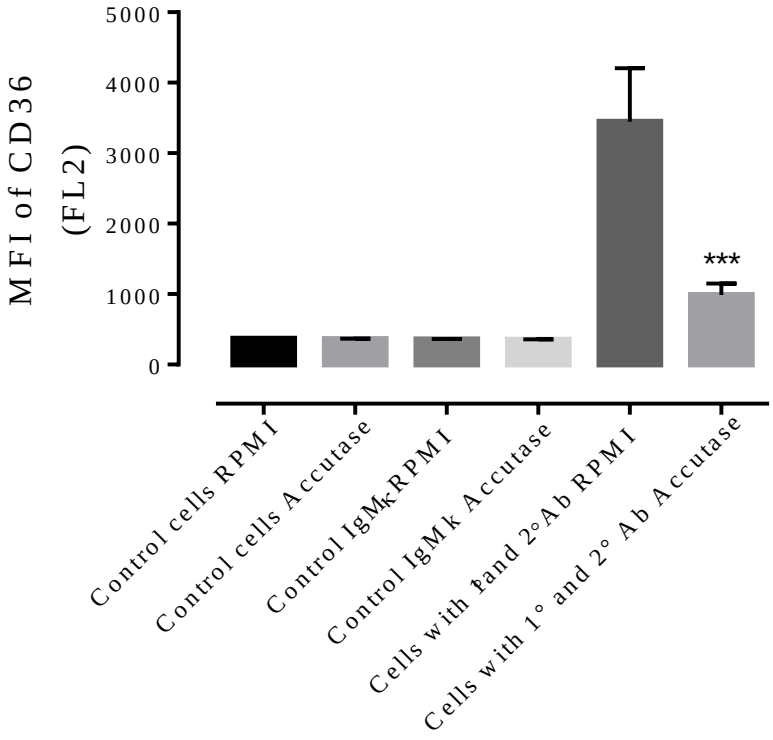

Figure 28. CD36 expression on monocytes treated with accutase™ vs. no accutase™. Monocyte cells were incubated with accutase™ or RPMI 1640 supplemented with p/s as control for 15 minutes at 37°C. After washing, samples treated on ice with anti-CD36 primary and secondary antibodies, the IgMκ isotype control or cells only control for 30 minutes. Cells were analysed using the FL2 filter on the flow cytometer. MFI measured at 578nm. 2-way ANOVA revealed a p- value of *** = <0.001. Triplicates analysed using GraphPad Prism 6.0.

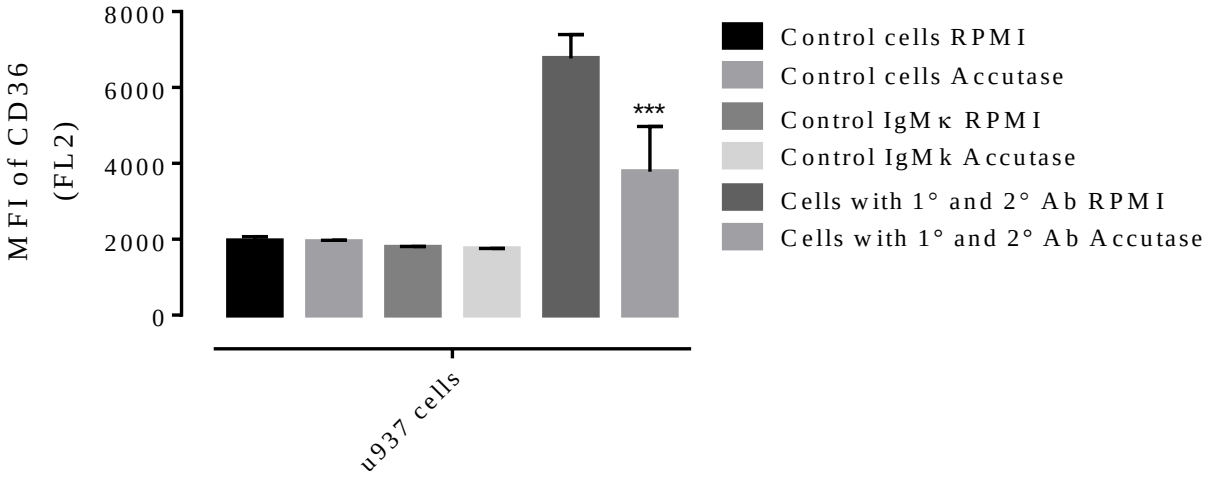

Figure 29. CD36 expression on U937 cells treated with accutase™ vs. RPMI 1640. U937 cells were incubated with accutase™ over 15 minutes at 37°C. After washing, samples treated on ice with anti-CD36 antibodies, the IgMκ isotype control or cells only control for 30 minutes. Cells were analysed using the FL2 filter on the flow cytometer. MFI measured at 578nm. 2-way ANOVA revealed a p- value of *** = <0.001. Triplicates analysed using GraphPad Prism 6.0.

The methodology was altered in an effort to increase the available amount of CD36. Cells were harvested by exposing the cells to accutase™ for differing time intervals (figure 30). The 15 minute incubations with accutase™ were the most successful at lifting cells off the adherent cell culture plates. Reduced incubation time resulted in a reduction in the amount of cells lifted up (figure 30). Figure 30 depicts a sample of the cells treated with RPMI1640 as a control which were able to be dislodged with pipetting, however the number of cells available for measurement on the flow cytometer was below the required 10,000 events per sample. On average, only a quarter of the number of cells was able to be lifted up with RPMI 1640 when compared to using Accutase™ for the full 15 minutes (figure 30). This resulted in a subset of cells being analysed. Further development of the process was required in order to increase the cell numbers in the sample and increase the CD36 cell surface expression.

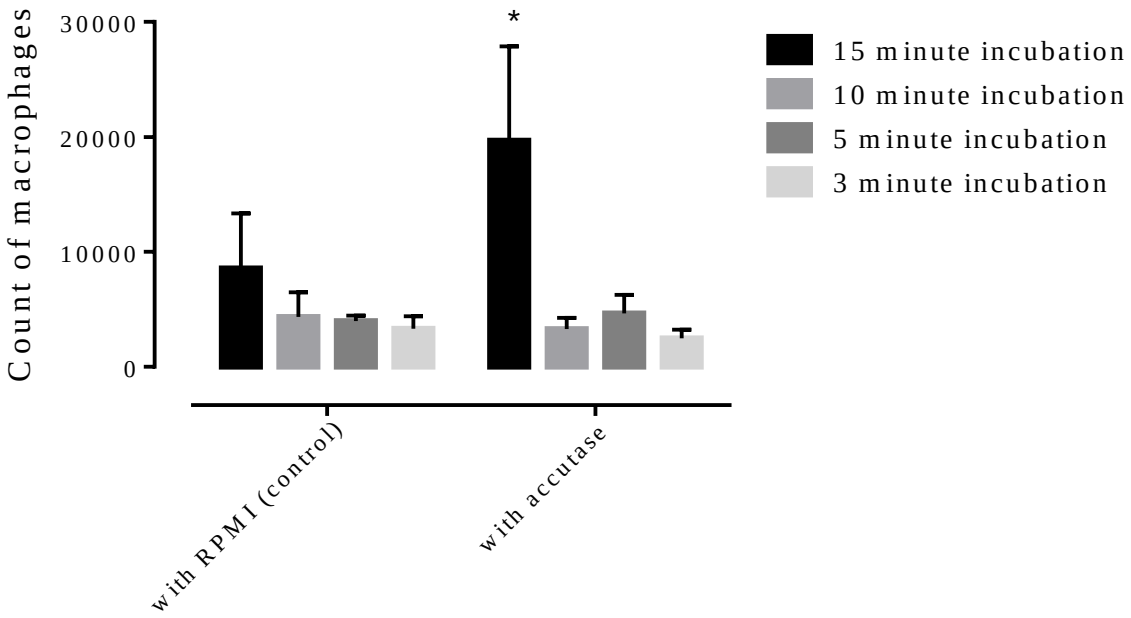

Figure 30. Incubation of macrophages with accutase™ or RPMI 1640 and p/s for 3, 5, 10 or 15 minutes. Macrophages were incubated with accutase™ or RPMI 1640 supplemented with p/s for 15, 10, 5 or 3 minutes. After washing, cells were lifted off the adherent plates and counted with the flow cytometer. Samples were manually counted and cross checked against the flow cytometer using the FL2 filter to measure 578nm emission. 2-way ANOVA gave a p-value of * = 0.05. Data analysed using GraphPad Prism 6.0.

Chu, *et al*, offered an alternative solution through the use of cold PBS (Chu et al. 2013). The cells were washed three times in ice cold PBS and then treated with 10, 7.5 or 5 minutes in accutase™. They were then carefully pipetted to detach them from the substrate. As can be seen from figure 31 C), the antibody treated samples are showing fluorescent traces that line up on top of each other. This result was compared to cells that had been treated with accutase™ only for the full 15 minutes as suggested by Millipore ("Accutase," n.d.). The cells were able to be successfully lifted off after incubations in accutase™ as short as 5 minutes without loss of CD36 fluorescence intensity (figure 32). There was no significant difference in the CD36 fluorescence of the cells treated with accutase™ between the two methodologies, so there was no recovery in the CD36 fluorescence, however the cold wash method produced sufficient numbers of cells to run 10,000 macrophage events on the flow cytometer. This meant that there were enough cells available to present a full cohort of the total cells treated.

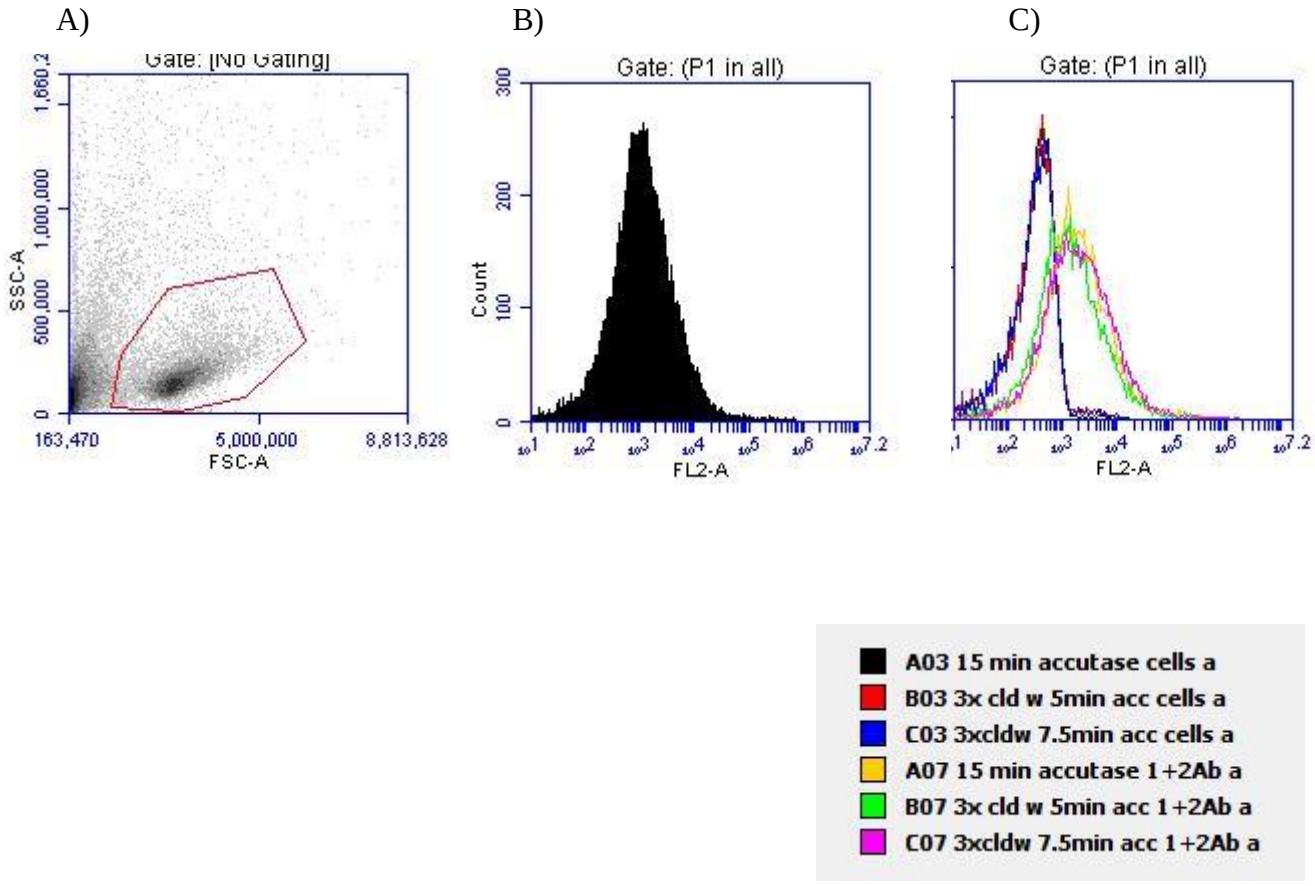

Figure 31. Flow cytometer traces for treatment of macrophages with cold PBS washes before accutase™ for differing time periods. Adherent macrophages were washed three times with ice cold PBS before being incubated with accutase™ at 37°C for 5, 7.5 and 10 minutes. These were compared to cells treated with just accutase™ for 15 minutes. Cells were pipetted to detach and treated with primary and secondary antibodies or a cells only control in the dark, on ice for 30 minutes. Cells were analysed by the flow cytometer using the FL2 filter to measure 578nm emission. A) is gated macrophage population analysed using the flow cytometer. B) fluorescence profile of the cells within the gate were labelled with antibodies. C) fluorescence profile of the antibody treated cells and the cells only control. 10,000 events recorded and the triplicates of each sample analysed with GraphPad Prism 6.0.

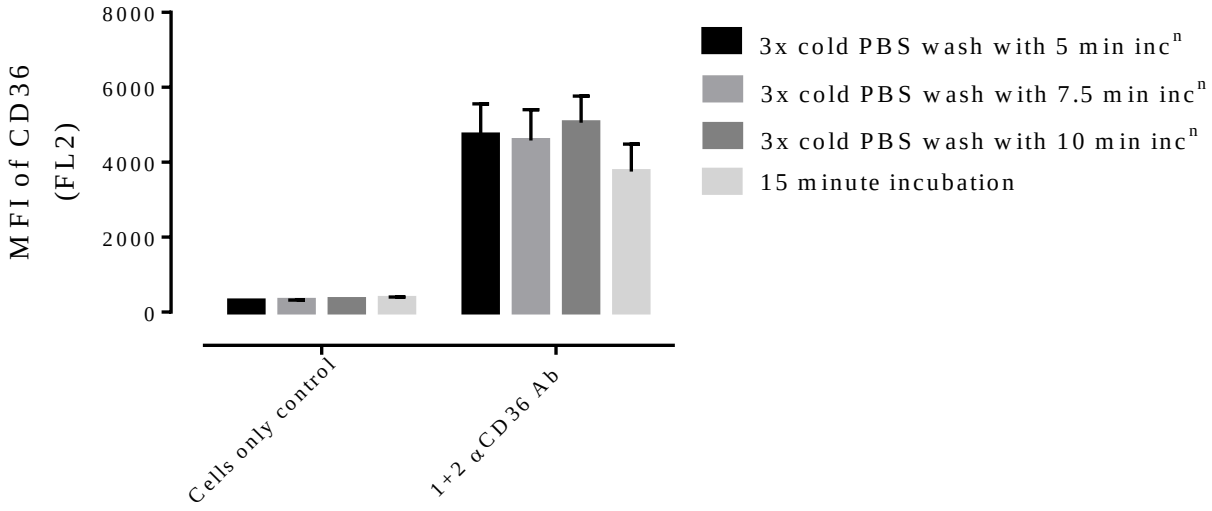

Figure 32. CD36 fluorescence of macrophages treated with cold PBS washes before treatment with accutase™. Macrophages were washed three times with ice-cold PBS before being incubated with accutase™ for 5, 7.5 or 10 minutes. Comparisons were drawn between macrophages incubated with accutase™ for 15 minutes. After pipetting, samples were treated with primary and secondary anti-CD36 antibodies or as a cells only control on ice, in the dark for 30 minutes. Cells were analysed on the flow cytometer using the FL2 filter to measure 578nm emission**.** Analysed using GraphPad Prism 6.0.

Collegial advice was given by Dr. Barry Hock of the University of Otago who suggested running a trial where the cells were first treated with accutase™. Once removed from the adherent plates the cells could be re-suspended in suspension cell culture plates. A recovery period of 12 hours allowed the CD36 surface expression levels to return to normal. The samples were then treated and analysed according to the previous technique. Experimentation could then occur and the results would not be altered by the reduction of the CD36 fluorescence.

3.8 Does 7,8-dihydroneopterin prevent foam cell formation?

Figure 33 indicates that the cells sourced from the suspension cell culture plate following Dr. Hock's advice, express more fluorescence for the 10,000 events recorded than those sourced from an adherent plate per the previous method. The response of the cells also was in line with the descriptions in the literature (Kavanagh et al. 2003). As can be seen in figure 33 A), the treatment of sub-toxic concentrations of oxLDL for 48 hours resulted in an increase in CD36 expression and consequentially an increase in MFI. A resting time of 12 hours before experimenting on the cells enabled them to recover the receptor expression levels from the detachment process involving accutase™. The incubation in suspension culture plates allowed the cells to be obtained for analysis on the flow cytometer without further exposure to accutase™. This recovery and lack of further exposure increased CD36 fluorescence in the control of the suspension macrophages when compared to the adherent macrophages' CD36 MFI (figure 33 A vs. 33 B). The CD36 flow cytometry procedure had been successfully adapted which enabled accurate representation of CD36 surface expression. Experiments could move on to determining whether 7,8-NP could result in a down regulation of the CD36 cell surface expression. The effect on uptake in macrophages when treated with 7,8-NP was able be investigated. To investigate the effect of 7,8-NP on CD36 expression, the recovered, suspension macrophages were treated with 200mM 7,8-NP for 48 hours at 37°C (figure 34). This resulted in a down-regulation of CD36 fluorescence when compared to the control (figure 34). The cells treated with 7,8-NP for 48 hours had less fluorescence compared to the cell-only control as well as the 0 hour sample.

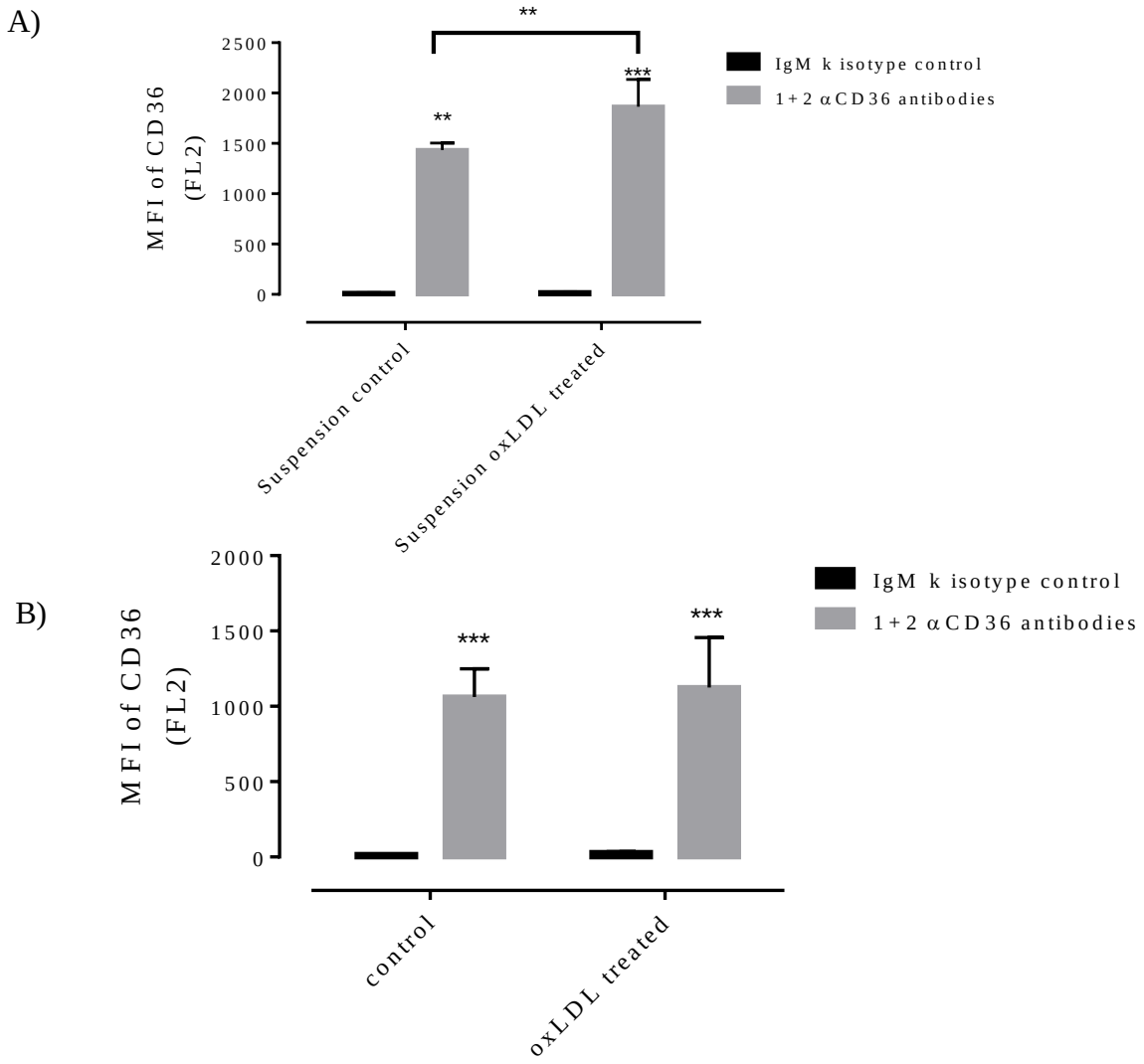

Figure 33. Suspension macrophages and adherent macrophages treated with oxLDL for 48 hours. Cells were divided and treated as suspension cells or adherent cells during treatment and antibody staining. Macrophages in graph A) were incubated with accutase™ for 15 minutes at 37°C, then washed and re-plated in a suspension plate for 12 hours to recover before being treated. Graph B) shows cells that were treated for 48 hours, then washed and incubated with accutase™ for 15 minutes at 37°C. Cells were treated with 0.5 mg/ml oxLDL in RPMI 1640 supplemented with 10% human serum and p/s or fresh RPMI 1640 supplemented with 10% human serum and p/s for 48 hours. Primary and secondary anti-CD36 antibodies and isotype controls were incubated in the dark, on ice for 30 minutes. The cell samples were run through the flow cytometer using the FL2 filter to measure 578nm emission and 10,000 events of each triplicate recorded. 2-way ANOVA reveals p values of ** = 0.05 and ***=<0.001. Analysis of the data done with GraphPad Prism 6.0.

This indicated that when the 7,8-NP was incubated with the cells for extended periods of time it affected a decrease in the cell surface expression of CD36. This conclusion arose because the 7,8-NP did not affect an immediate decrease in CD36. A question arose from the data which showed that the fluorescence for the cells treated with 7,8-NP at 0 hours had increased. Nothing in the literature was found that explained this rise in fluorescence.

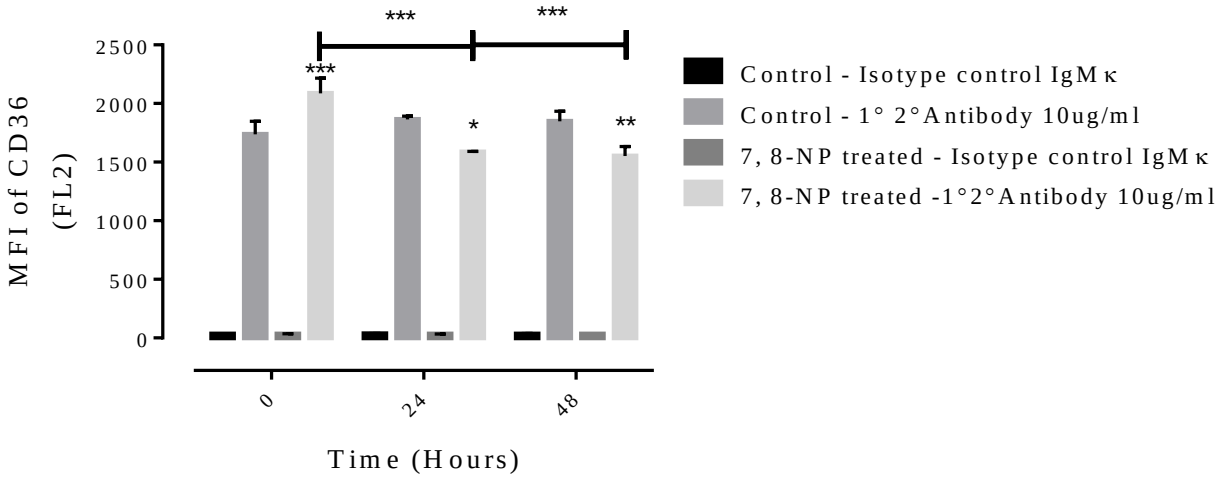

Figure 34. CD36 expression on suspension macrophages' cell surface when treated with 7,8-NP for 48 hours. Cells were lifted up with accutase™ and re-plated in suspension culture plates to recover for 12 hours. Macrophages were treated with 200 mM 7,8-NP or left as they were as a cell only control. After 48 hours of treatment the cells were washed and labelled with primary and secondary anti CD36 antibodies, or isotype controls in the dark, on ice for 30 minutes. The cells were processed using the FL2 filter to measure 578nm emission on the C6 flow cytometer and 10,000 events per triplicate were recorded. 2-way ANOVA revealed p values of * = 0.05, ** = 0.001 and *** = <0.001. Samples were analysed using GraphPad Prism 6.0.

When this 48 hour time-course was repeated with the inclusion of cells treated with oxLDL, the histogram from the C6 flow cytometer revealed very promising results. Figure 35 C) exhibited the fluorescence profile which moves to the right of the cells only control fluorescence with the addition of oxLDL, and to the left of the cells only control fluorescence with the addition of 7,8-NP. The oxLDL induced movement to the right in figure 35 C) indicates an increase in fluorescence, therefore an increase in CD36 expression. The 7,8-NP induced movement to the left indicates a decrease in fluorescence, therefore a decrease in CD36 expression.

A)

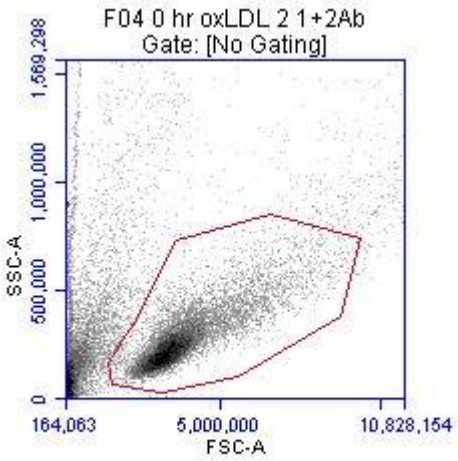

B)

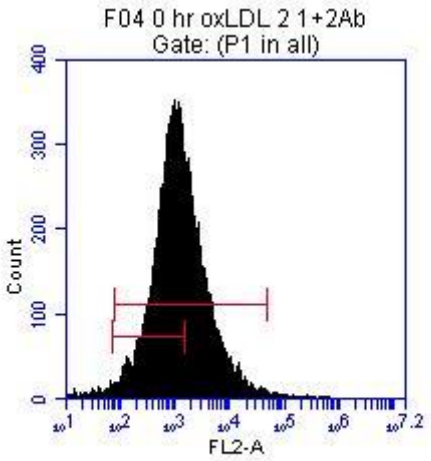

C)

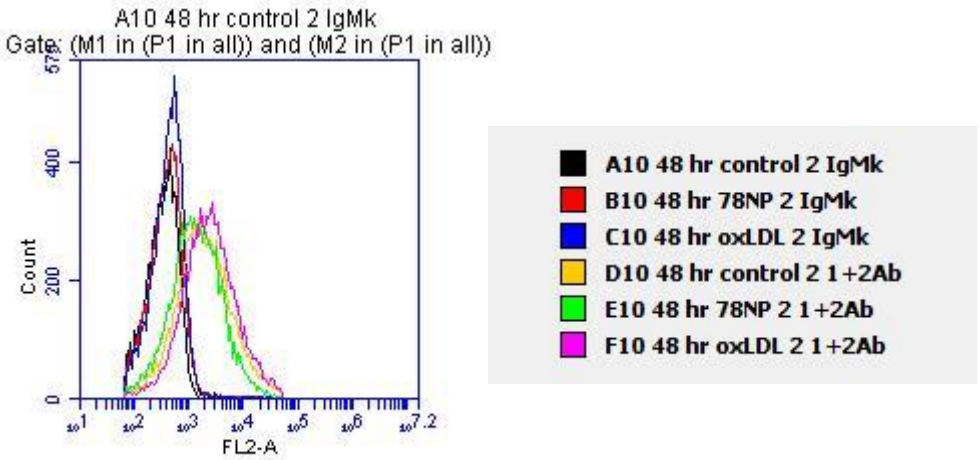

Figure 35. Flow cytometer traces of suspension macrophages treated with 7, 8-NP or oxLDL for 48 hours. Macrophages were lifted with accutase™ and re-plated in suspension plates for 12 hours. They were then treated with 200mM 7, 8-NP or 0.75mg/ml oxLDL or a cells-only control for 48 hours. After treatment the samples were treated with primary and secondary antiCD36 antibodies as per method, or an isotype control on ice, in the dark for 30 minutes. Cells were analysed on the flow cytometer using the FL2 filter. A) presents the macrophage cell population. B) presents the fluorescence measured on FL2 to measure 578nm emission, the bars indicate the width of the primary control compared to the primary and secondary antibody signal. C) presents the 3 treatments and the response of the fluorescence of each treatment compared to the other. 10,000 macrophage events per sample were recorded and each sample recorded in triplicate.

Figure 36 confirms the data from the histogram in figure 35 C) once it was analysed and shows a clear decrease in fluorescence when the cells were treated with 7,8-NP (figure 36 A) and an increase in fluorescence when treated with oxLDL (figure 36 B). There was a slight decrease at 24 hours of the control cells in both the oxLDL and the 7,8-NP treated graphs which at this stage cannot be explained. Experiments ruled out it being the result of interference with the antibody from the accutase™, or the CD36 levels were still recovering. One possible explanation may be that it is a residual effect of the adherent cells becoming suspension cells. However when the 0 hour control is compared to the 24 hour 200mM 7,8-NP treated cells the fluorescence decreases, indicating that the CD36 expression on the surface of the cells has decreased in response to the 7,8-NP.

Alternatively, in figure 36 B) when treated with 0.75mg/ml oxLDL, a sub toxic level, for 48 hours, the fluorescence increases compared to the 0 hour control. The 7,8-NP treated cells decrease significantly and then plateau while the oxLDL treated cells' CD36 expression continues to rise.

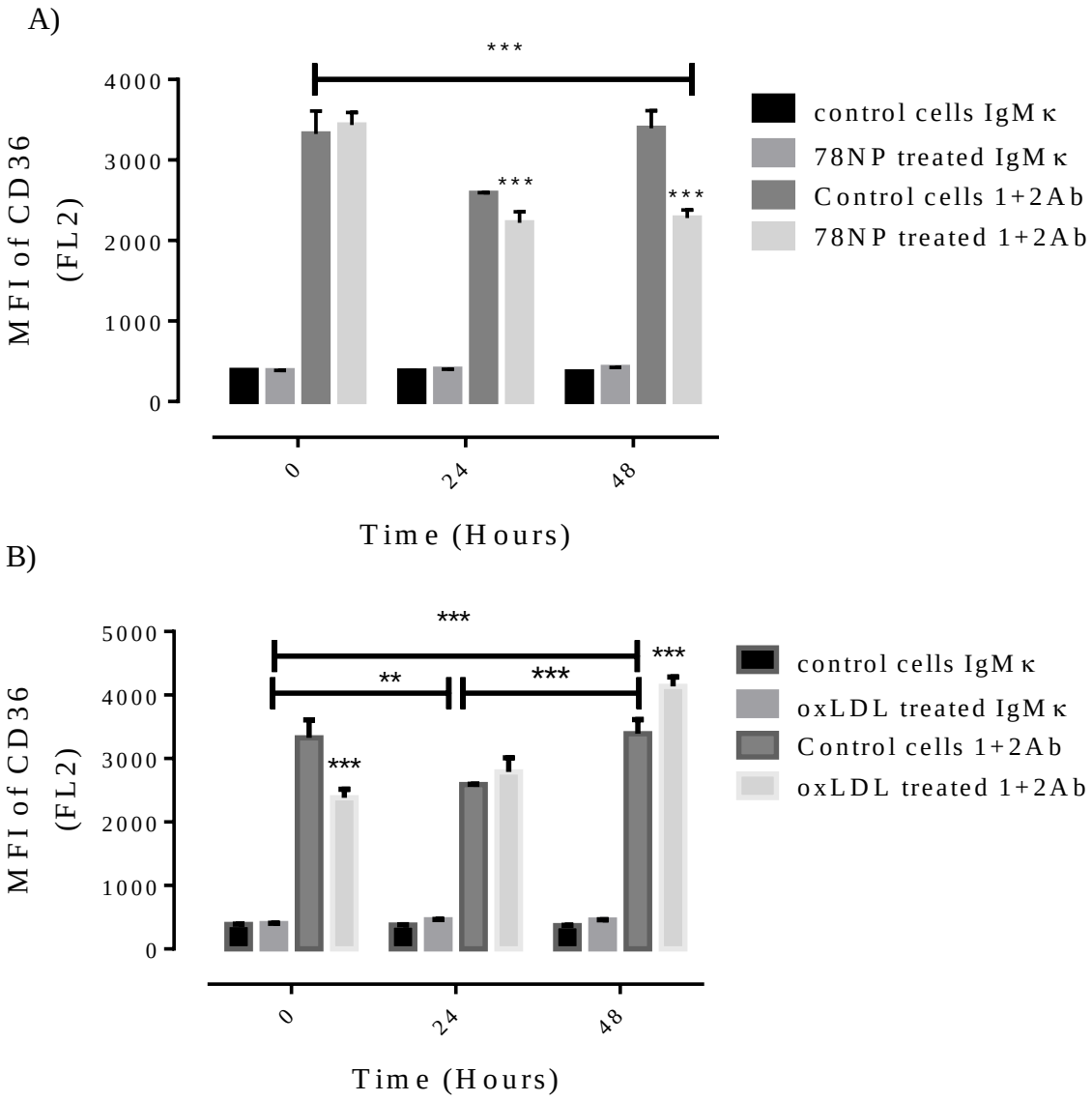

Figure 36. CD36 expression of suspension macrophage cells treated with 7,8-NP or oxLDL for 48 hours. Macrophages lifted up with accutase™ and incubated in suspension plates for 12 hours before treatment. Macrophages were treated with 200mM 7,8-NP in A) or 0.75mg/ml oxLDL in B) over 48 hours. They were then washed and treated on ice, in the dark with CD36 primary and secondary antibody or the primary IgMκ control. Samples processed by the flow cytometer and 10,000 HMDM events recorded using the FL2 gate to measure 578nm emission. 2-way ANOVA shows p-values of ** = 0.001 and *** = <0.001. All experiments replicated in triplicate and data was analysed using GraphPad Prism 6.0.

Once the behaviour of the CD36 receptor when treated with 7,8-NP had been elucidated, interest shifted to the effect of 7,8-NP on foam cell formation as measured by cholesterol and 7KC uptake. Figure 37 presents the 7-KC uptake in macrophage

cells when treated with 1.0mg/ml of oxLDL as a contrast to the uptake when treated with 7,8-NP. The uptake in figure 37 did not have the unusual dip at 36 and 48 hours seen in figure 22. Successful uptake from oxLDL incubation enabled investigation of the proposition that up-regulation could be reversed or prevented with the treatment of the anti-oxidant, 7,8-NP. The uptake in this figure was 2nmol/mg of protein (figure 37 B) and not within the range recorded by A Shchepetkina. However the trend mirrors that of figures 17-21. Previously this lab documented 7-KC uptake of 10-20nmole/mg of protein over 24 hours when the macrophages were treated with 1.0mg/ml of oxLDL (Shchepetkina 2013). The disparity in uptake may be due to the differences in exposure time (24 vs 48 hours). The longer time period may give the cells the opportunity to try to recover by removing the accumulated lipids. It could also be explained by the variability of the cell sources. As previously mentioned, different donors provide the macrophages and therefore the vagaries of genetic disposition and lifestyle choices cannot be mitigated.

Figure 37 A)

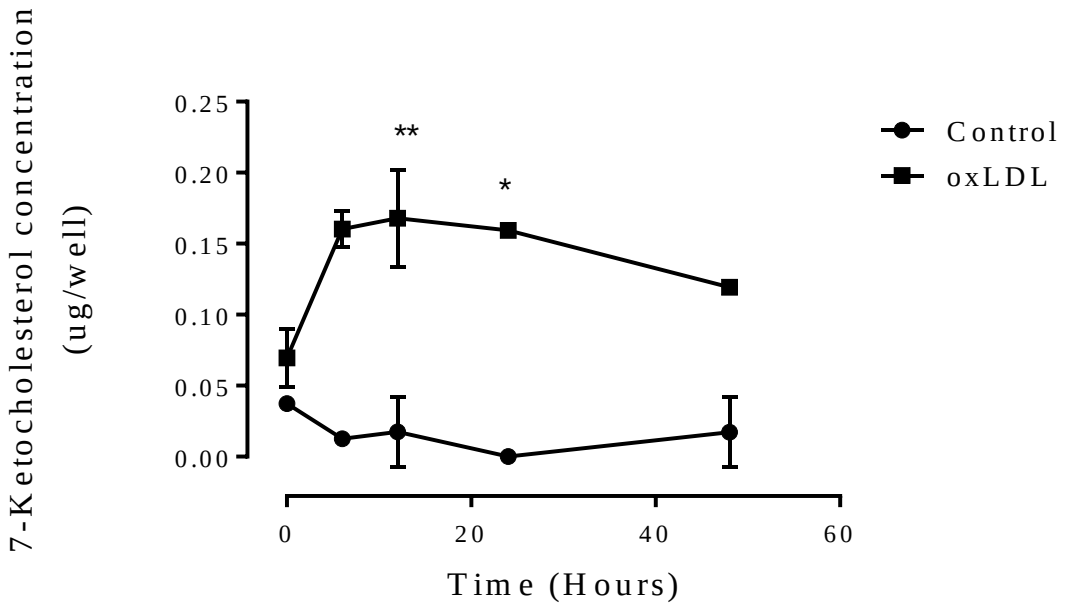

Figure 37 B)

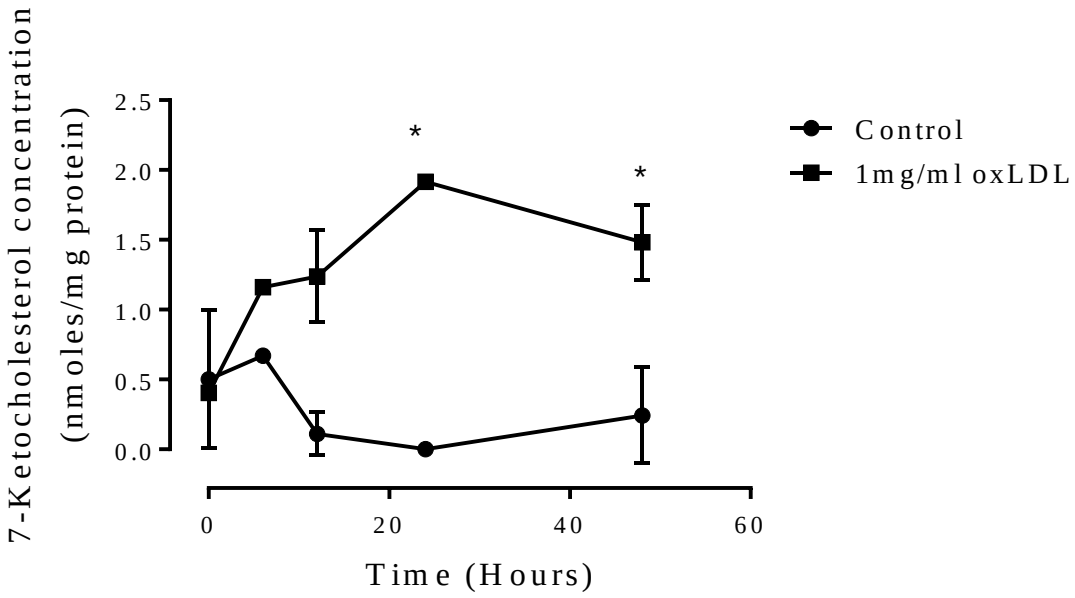

Figure 37. 7-Ketocholesterol uptake in macrophages treated with 1.0mg/ml oxLDL for 48 hours. Macrophages were incubated with 1.0mg/ml oxLDL in RPMI 1640 supplemented by 10% human serum and p/s or RPMI 1640 supplemented by 10% human serum and p/s as a control over 48 hours. Samples were extracted into 7-KC mobile phase and run on the HPLC using the 7-KC method. Absorbance was measured at 234 nm. Analysis was corrected for g/well (36 A) and corrected for estimated protein (36 B). 2-way ANOVA analysis revealed p-values of * = 0.0191 and **=0.001. Analysis using GraphPad Prism 6.0.

Macrophages were also treated with oxLDL for 48 hours and compared to cells pre-treated for 12 hours with 7,8-NP before being incubated with oxLDL + 200mM 7,8-NP. The 7,8-NP was refreshed every 24 hours. The pre-treatment with 7,8-NP ensured that the 7,8-NP was within the cell when the cell was dosed with oxLDL. It also gave the 7,8-NP enough time to down-regulate the CD36 expression which contributed to the result seen in figure 38 A). Both the 7-KC (figure 38 A) and the cholesterol (figure 38 B) uptake was measured on the HPLC. The 7-KC uptake in figure 38 A) was 4μmoles/mg of protein, underscoring the variability between cell preparations. This uptake is much higher than previously documented by this lab (Shchepetkina 2013). Treatment with 7,8-NP + oxLDL prevented the 7-KC uptake, measuring the 7-KC concentration at basal levels. Aberrantly, the 7-KC uptake due to oxLDL didn't occur until after the first 24 hours. Correspondingly, in figure 38 B), the 7,8-NP + oxLDL treated macrophages didn't take up cholesterol beyond control concentrations. The cholesterol accumulation in the oxLDL treated cells was only 5-10 nmole/mg of protein (figure 38 B), rather than the 20 nmole/mg of protein accumulation seen in figure 17 B). The addition of 7,8-NP to macrophages prior to, and during foam cell formation effectively blocked the uptake of cholesterol and 7KC from occurring.

Figure 38 A)

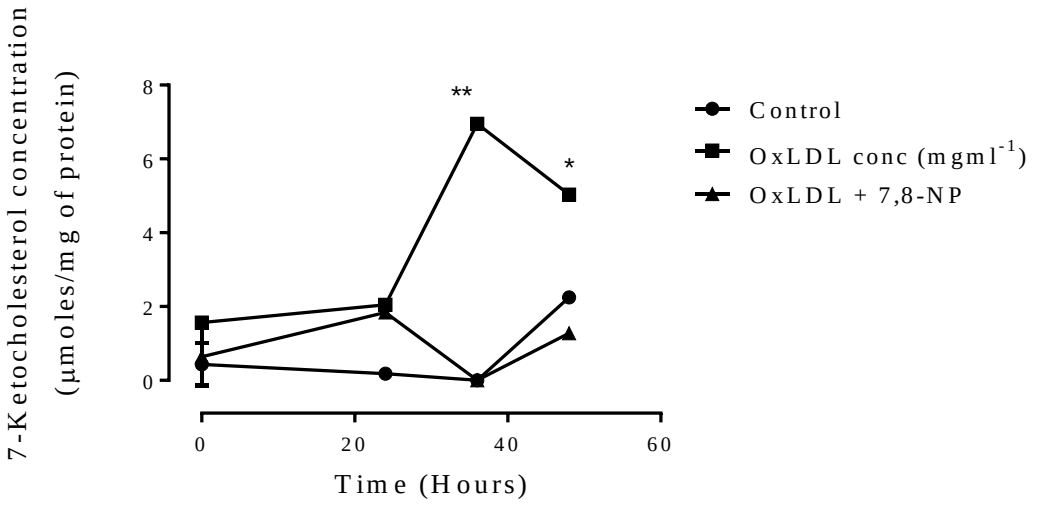

Figure 38 B)

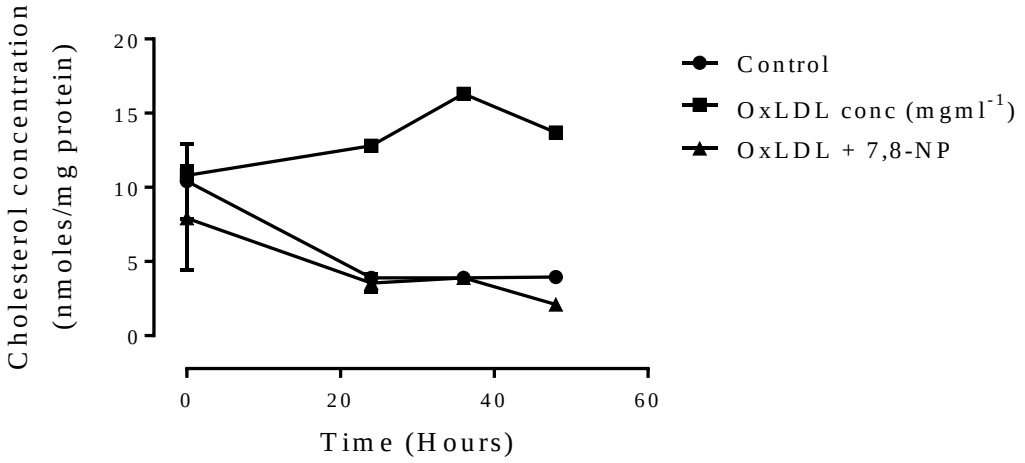

Figure 38. Time course of macrophages treated with oxLDL or oxLDL + 7, 8-NP. Macrophages treated with 1mg/ml oxLDL, 1mg/ml oxLDL and 200mM 7, 8-NP or fresh RPMI 1640 supplemented with 10% human serum and p/s as a cells-only control over 48 hours. After treatment, the cells were extracted into the 7-KC mobile phase and processed on the HPLC using the 7-KC method. A) 7-KC was measured using 234 nm wavelength. B) Cholesterol was measured at 210nm. 2-way ANOVA revealed p values of * = 0.05 ** = 0.0043 between the oxLDL treated cells and the oxLDL and 7, 8-NP treated cells at 36 and 48 hours. Data analysed using GraphPad Prism 6.0.

4 Discussion

4.1 The role of cholesterol and cholesteryl ester accumulation in foam cell formation.

Foam cell formation was quantified from the HPLC method adapted from Kritharides (L. Kritharides et al. 1993) however the cholesterol and cholesteryl ester accumulation in macrophages had to be able to be accurately identified (figure 1). Commercial standards were used to identify the elution time off the HPLC column (figure 1) and this information was used to identify the peaks in the LDL particle (figure 2), and oxLDL (figure 3). The LDL in figure 2 was copper oxidised to give the oxLDL profile in figure 3. Figure 3 displays the absence of peaks from esters in oxLDL such as Cholesteryl Arachidonate. The lower concentration of lipids in oxLDL is because they are being oxidised to oxysterols, hydroperoxides, etc. Cholesteryl Arachidonate and Cholesteryl Linoleate were undetectable after the copper oxidation of LDL. This disappearance suggests they are more easily oxidised than the other esters (Leitinger 2003). These cholesteryl esters are from the core of the lipoprotein and Noguchi proposed that their oxidation occurs before the outer monolayer's oxidation (Noguchi et al. 1998) but that was not addressed by this investigation. Brown identified the loss of cholesteryl ester from LDL during copper oxidation (A. J. Brown, Dean, and Jessup 1996, 199). Cholesteryl arachidonate was identified as the first cholesteryl ester to be oxidised, followed by cholesteryl linoleate, -oleate and finally free cholesterol. This agrees with the peaks seen in figure 3 which does not have a cholesteryl arachidonate peak, and depleted peaks of cholesterol, and cholesteryl esters when compared to figure 2. This was represented in figure 5 and the reduction in cholesterol, cholesteryl arachidonate, -linoleate, and –oleate is marked.

A diluted sample of RPMI supplemented with 10% human serum in figure 4 has much smaller peaks than the pure lipoprotein samples in figures 2 and 3. The amount and identity of cholesterol and cholesteryl esters present indicates the human serum has LDL present in the sample. The effect of this exposure of LDL to the cells during experimentation needed to be investigated. However, in order to investigate the effect of lipoprotein on macrophages, the method of measuring cell extracts had to be further adapted.

4.2 Cholesteryl ester method development

Pooling cell culture plate wells was undertaken to determine and standardise the number of cells needed for a useful signal on the HPLC. In figure 6 one, two or three wells of $5x10^6$ cells/well were pooled and analysed for cholesterol and cholesteryl ester content. The most notable result in figure 6 is the variability of macrophages within preparations. It is expected that cells from multiple donors will react with greater irregularity, based on the donor's health, immune responses, age, and food intake at the time of donation. Figure 6 shows that cells from the same person will also react with high degrees of variability. The cells from the same donor being cultivated in separate wells must expose them to slightly different micro-environments. This variation had been studied by Wintergest, who had found different subsets with varied receptor expression and a 2.5 fold variation in cholesterol mass in untreated macrophages (Wintergerst, Jelk, and Asmis 1998). Therefore the variation seen in figure 6 was a well-established limitation of the human macrophage model.

Although the higher concentration of cells is in the 3 well sample, the 2 well sample's cells took up cholesterol and cholesteryl arachidonate and 7KC more efficiently. However for the purpose of this study the 3 well combined sample is the only one that showed signal for cholesteryl linoleate. None of the cells treated with oxLDL showed a deviation from the control loading, indicating no foam cell formation. Once it was decided that pooling three wells would give the strongest and most encompassing signals on the HPLC chromatograms, the effect of human serum on macrophages could be investigated.

The presence of LDL particles in human serum posed the possibility that the LDL could alter the oxLDL stimulated cholesterol and ester uptake. Garner had established that the supplementation of RPMI 1640 with 10% human serum increased the triglyceride content by exposure to LDL in the human serum (Garner et al. 1997, 199). However as our definition of foam cells was reliant on cholesterol and cholesteryl ester uptake, which Garner reported as not significant due to exposure to human serum, we had to investigate the cholesterol and ester accumulation ourselves (figure 7). Figure 7 graphs the cells which were incubated using different percentages of human serum. There was no evidence that the LDL particle availability affected the cell's cholesterol and ester uptake. All the cells took up cholesterol, cholesteryl arachidonate, cholesteryl linoleate and 7-

ketocholesterol. However the uptake did not correspond to the percentage of human serum the cells were exposed to. For example, the 1% human serum cells took up more cholesterol than the 2% and 10% human serum cells. Despite the variation between cell uptakes, analysis by 2-way ANOVA suggests there are no significant differences between any of the different human serum percentages and the cell uptake responses.

With the lack of interference from the human serum established, an MTT assay indicated that 2.0mg/ml was the LD50 for HMDMs. Figure 8 depicts the toxicity of oxLDL to macrophages. A 1.0mg/ml concentration of oxLDL was decided upon as the sub-toxic concentration that would be used because 0.5mg/ml oxLDL did not cause the cells to uptake cholesterol and esters. Figure 6 indicated that 1.0mg/ml was not enough to ensure oxLDL uptake in all cases. Standard toxicity concentrations were unable to be obtained which may be explained by the variability of the blood donations.

While the macrophage preparations are stimulated with GM-CSF to encourage the macrophages to become a M1, pro-inflammatory phenotype, they are able to switch to the M2, anti-inflammatory phenotype, and back again. Rios found that oxLDL exposure encouraged the switch to the M2 phenotype (Rios et al. 2013). This may account for the lack of foam cell formation seen in figure 6, as the M2 macrophage is less likely to load cholesterol and esters and become a foam cell (Ravi et al. 2014). For the majority of MTT assays, 1.0mg/ml oxLDL was an effective sub-toxic concentration.

Figure 9 confirms that 1.0mg/ml oxLDL treated cells accumulate cholesteryl esters. This accumulation of cholesteryl and esters is what defines a foam cell according to Mattsson who isolated foam cells from an aortic atherosclerotic lesion (Mattsson et al. 1993). Because this cholesteryl ester accumulation was slight in cell extracts (figure 10), the oxysterol (7-ketocholesterol) and cholesterol accumulation was focussed on as markers for foam cell formation.

4.3 7-Ketocholesterol method development for sterol measurement

Peroxidation of cholesteryl esters and oxidation of cholesterol yields the oxysterol, 7-ketocholesterol (Leitinger 2003) which is the major ester formed during copper oxidation of LDL (Andrew J and Jessup 1999). As 7-KC is the main oxysterol found in foam cells

in vitro, studying the loading of macrophages with 7-KC was another aspect by which we could define foam cells.

The ability to measure total 7-KC and cholesterol using one method decreased any anomalies due to handler error. Consequently the cholesterol and 7-KC uptake could be directly compared because they are from the same cell source and have been treated using the same process with minimal handling. Figure 12 demonstrates the cholesterol being measured from cell samples using the 7KC hydrolysis method. The commercial standard used to identify the cholesterol peak is in figure 11. Using one method ensures the total amounts of both cholesterol (figure 15) and 7-ketocholesterol are present. The hydrolysis released both cholesterol from cholesteryl esters and 7-ketocholesterol from fatty acids within the foam cell (Andrew J. Brown, Watts, et al. 2000). Otherwise, because the samples would not be processed identically, the researcher would be reliant on comparing trends, not empirical data. Figure 13 depicts the commercial standard used to identify the 7-ketocholesterol and figure 14 identifies the 7-KC within the cell sample.

4.4 Foam cell formation measured by cholesteryl ester and 7-KC methods

Confirmation that oxLDL uptake was occurring at 1.0mg/ml (figure 9) resulted in a series of tests being undertaken to investigate cell activity over a 48 hour time frame (figures 17-22). Further investigation showed loading of individual esters, cholesterol and 7-KC. The control cells depicted in figures 17 and 18 indicated that the natural response of the cells is to take up esters. After 40 hours, it was noted that there was a drop in ester uptake which may be explained by the presence of the ABC/A1 receptor. It is known that LDL is delivered to the cell and the excess FFA, TAG and cholesterol is removed via the ABCA1 receptor and the HDL particle. It is reasonable to suggest that this may also be an explanation for the drop in ester uptake as the cell tries to efflux the ester (Gaus et al. 2001; Greig, Kennedy, and Spickett 2012).

The process of cholesterol homeostasis is complex as the cell is able to produce its own cholesterol if none is available from the diet. In the absence of cholesterol via the LDL delivery system, enzymes HMG-CoA synthase and HMG-CoA reductase produce mevalonate, which is synthesized via a negative feedback loop resulting in the production of cholesterol. LDL reduces the activity of the enzymes by 90%

(Goldstein and Brown 1990). This may explain why the control cells also show evidence of taking up cholesterol. Due to this difficulty in limiting the source of cholesterol in a human system, there are complications in measuring the oxLDL stimulated uptake.

Each pair of graphs consists of a graph where the data was corrected for protein in the cell samples. Data corrected for g/well of ester was included so that any large deviations in the data due to protein amounts in the sample were evident. Despite the differences in amount of each sterol taken up, the trend is similar for all.

Figure 22 depicts the 7KC uptake using a different preparation of cells and while uptake did occur, the amount was slight. After 24 hours, the amount of 7KC in the cells dropped. This was not due to aberrant cell protein levels, therefore may be due to internal cell protection. The drop in the 7KC uptake indicates that this cell batch has up-regulated the ABC-A1/G1 receptors via stimulation with cAMP to help expel the oxysterol. This drop is seen before the results are altered for protein content which indicates that some cells have the ability to protect themselves. Cell protection may contribute to the length of time before the atherosclerotic plaque and disease progresses inside the artery.

This quantifiable definition of foam cells is compared to that within the literature, where many authors are still using lipid dyes (Chávez-Sánchez et al. 2014; Lee et al. 2014; Ouchi et al. 2001). Our definition of foam cells allows standardisation *in vitro,* while being applicable *in vivo* (Mattsson et al. 1993; Hegyi et al. 1996) based on studies done on atherosclerotic lesions. OxLDL has been proven to be taken up by macrophages (Endemann et al. 1993) through the scavenger receptor CD36 and results in the loading of macrophages with cholesterol, cholesteryl ester, oxysterol and triacylglycerides. This results in lipid loaded cells, that are ubiquitously named foam cells (Kruth 2001). Macrophages that are incubated with oxLDL have an increased cellular content of both cholesterol and 7-KC (Andrew J. Brown, Mander, et al. 2000) and accurately measuring this increased content was the purpose of developing the HPLC method.

4.5 Accutase effect on CD36 cell surface expression

Visual confirmation of foam cell formation (figure 16) as well as fulfilling the foam cell definition of cells (Mattsson et al. 1993) loaded with cholesterol, cholesteryl esters and 7-KC (figures 17-22) enabled the next phase of testing investigating the

cell surface CD36 expression. CD36 is a main altered LDL scavenger receptor, and credited with 60-70% of oxLDL uptake into cells (Febbraio et al. 2000). Of interest was the cholesterol and cholesteryl ester uptake from oxLDL and CD36's influence in that process. Figure 23 confirmed that the population being gated and investigated was HMDM cells. Confirmation was important because despite preparations being encouraged to differentiate into M1 type macrophages (Chu et al. 2013; Greig, Kennedy, and Spickett 2012) by the cytokine, GM-CSF, this does not always happen. Upon occasion the monocytes do not differentiate, and differentiation into macrophages is not guaranteed, instead muscle cells, dendritic cells and more have been identified in preparations. While these preparations are not typically used, occasionally the macrophage population is large enough to excuse use in experimentation. Consequently not all the cells run through the C6 flow cytometer are the cells under investigation. Using CD16 as a macrophage label ensures that future analysis of experiments is correct.

Figures 24 and 25 graphed titration levels of primary antibody concentrations which enabled observation of which concentrations inundate the receptors on the surface of the cells. U937 cells were tested as they also express CD36 (Alessio et al. 1996). This enabled the focus to narrow and identify which concentrations performed best on HMDM cells. If the theory was correct, then an increase in fluorescence would be depicted by the histogram moving to the right (figure 24C). A higher harvesting ratio of HMDM cells required higher concentrations of primary antibody. Higher harvesting ratios also have higher numbers of CD36 expressed on the cell surface. However it was discovered that the 10mg/ml concentration of primary antibody was enough to inundate the receptors fully (figure 26B) which is indicated by the colours representing the fluorescence being directly on top of each other. Figure 27 indicated that there is no benefit to adding more than 10mg/ml primary antibody to the cell preparations.

The HMDM fluorescence intensity was lower than the fluorescence expressed by the U937 cells by about a ratio of half which contradicted the literature (Venugopal 2004). Figures 28 and 29 suggest that the Accutase™ was removing the CD36 from the surface of the cells, but not down to basal levels. This placed the model in doubt as the receptors being studied were being removed during the process. Other procedures used to remove the HMDM cells from the cell culture plates were too harsh and destructive, resulting in limited cells being available for testing.

In an effort to lessen the effect of Accutase™, shorter incubation times were trialled. Figure 30 shows that not all of the cells were lifted off the culture plates. Shorter incubation times also proved limited as the cohort was inadequate. The literature suggested ice cold sterile PBS washes before treating with Accutase™ (Chu et al. 2013). Testing this method showed that three ice cold PBS washes before Accutase™ treatment allowed for shorter incubation periods. This method produced similar amounts of recovered cells to the full 15 minute incubation. The assumption that short incubation times would result in improved CD36 fluorescence had to be confirmed. Figure 32 indicated that even though the incubation periods were as short as 5 minutes, the CD36 fluorescence wasn't significantly different to a full 15 minute incubation with accutase™.

In the absence of published work on this topic, Dr. Barry Hock of the University of Otago was consulted. His suggestion to model accurately the CD36 response to oxLDL or 7,8-NP was to lift the cells off the plate with Accutase™. He then suggested a recovery time to let CD36 levels come back to normal (figure 33). Questions remained around turning an adherent cell line into a suspension model; however work proceeded using the new protocol.

Because CD36 and SR-A are responsible for 90% of altered LDL uptake into cells, the development of a method to measure CD36 surface expression and its correlation to foam cell formation enabled more of the mechanism to be understood. Viana reported that oxLDL and aldehydes increase the CD36 cell surface expression as measured by flow cytometry, however their work was done on a suspension cell line (Viana et al. 2005). Thorne also used flow cytometry on a human suspension cell line to measure the effect of oxHDL on the CD36 expression (Thorne et al. 2007). Flow cytometry is a versatile technique that has been useful in previous studies of CD36. CD36 expression on macrophages is especially important, not only because CD36 cell signalling has deleterious effects on cell motility (Park et al. 2012) but also for its role in oxLDL binding (Nguyen-Khoa et al. 1999; Rusiñol et al. 2000; Febbraio, Hajjar, and Silverstein 2001; Han 1997). OxLDL also results in increase in cell surface CD36 expression (Han 1997). Therefore analysis of CD36 cell surface expression by flow cytometer was a valuable tool.

4.6 7,8-Dihydroneopterin effect on CD36 cell surface expression

The suspension HMDMs in the control samples had more mean fluorescence intensity than the adherent HMDMs by 500 units (figure 33). The suspension HMDMs that had been treated with oxLDL had more mean fluorescent intensity than the adherent HMDM cells by 1000 units. This was a successful result in that the CD36 expression was now being accurately represented in the data which corresponded to the literature (Kavanagh et al. 2003), but also the cells' response to treatments could now be seen more clearly. CD36 expression levels increasing when exposed to oxLDL was a response confirmed by the literature. Of special note was the degree of the increase particularly when the cells were treated with 7,8-dihydroneopterin (7,8-NP). When comparing this newly developed method with the western blotting technique (Shchepetkina 2013), it became evident that there were multiple advantages. The suspension flow cytometry method did not destroy the cells and enabled the receptors to recover their fluorescence, giving almost 500 times the fluorescence. The technique for recovering treated cells off the culture plate was quicker and more straightforward. A third extremely important advantage was that the cells were not lysed which enabled accurate measurement of the receptor activity at the surface of the cell.

Cells treated with 7,8-NP over a 48 hour time period decreased fluorescence compared to the control at each time point (figure 34). At 24 hours the rate of decrease of fluorescence slows. The 0 hour time point that had been treated with 7,8-NP had fluorescence above the control which was unexpected. This anomaly with extra CD36 on the cell surface is difficult to explain and is subject to small error bars. Multiple tests were carried out which eliminated human error however cell variability may be a possible explanation. The decrease of fluorescence on cells treated at time point 24 and 48 hours compared with the 0 hour control indicates that the decrease in CD36 cell surface expression is a significant result.

Anastasia Shchepetkina found a 40% decrease of relative CD36 expression after 24 hours using Western blotting technique (Shchepetkina 2013). The surface expression measured in figure 34 does not align with the reduction indicated by western blotting technique. This may be due to the recycling system inherent in the cells. There is a significant amount of CD36 in vacuoles, waiting for the cell to require their presence on the cell surface (Huh et al. 1996; Febbraio and Silverstein 2007) and this difference in CD36 may have been measured by the western blot. The western

blotting technique relies on cell lysis and measures the total cell content of the protein in question however the flow cytometry technique only measures the protein on the cell's surface. This may account for the differences in CD36 expression between the two techniques.

When cells from the same preparation were treated with oxLDL or 7,8NP the shift of fluorescence was quite evident, although not large, on the flow cytometer histogram in figure 35 C). Figure 36 A depicts the 7,8-NP inducing a dramatic drop in CD36 fluorescence and the maximum rate of decrease is reached at 24 hours and plateaus for the following 24 hours. At 24 hours for the antibody labelled control cells there was a large, un-induced drop in CD36 fluorescence. This isn't the case with any other time points. Therefore it's possible that compared to 0 and 48 hour control cells, the 24 hour antibody labelled control cells produced a limited amount of CD36. In contrast the 7,8-NP treated cells exhibit a drop in fluorescence at the 24 and 48 hour time points which is significant. This drop in fluorescence is supported by the literature (Gieseg et al. 2010). OxLDL was tested in this experiment (fig 36B). The 0 hour and 24 hour time points showed a reduction from 0 hour control in CD36 which may be due to oxLDL bound on the receptors and preventing the CD36 antibody from binding. At 48 hours there was a large increase in CD36 fluorescence which was in line with data from the literature (Han 1997; Nicholson and Hajjar 2004) and with figure 32. Figure 36B also indicated that the CD36 receptors take 24 hours for the oxLDL to be taken up enough to interact with the transcription of the CD36 receptor.

4.7 7,8-Dihydroneopterin effect on foam cell formation

Figure 37 documents 7-KC uptake and the trend of the uptake mirrors similar work also undertaken at the University of Canterbury FRB lab (Shchepetkina 2013). This data doesn't show the drop in 7-KC uptake at 24 hours shown in figure 22. The sample reaches a plateau much earlier than cholesterol and cholesteryl ester uptake. The cells continue to take cholesterol and esters up for 40 hours while the 7-KC peaks at 24 hours and plateaus from then on. This may be due to the nature of the cholesterol-7KC relationship. During incubation, the oxidants available from the oxLDL particle are able to oxidise cholesterol for the first 24 hours. In the second

24 hour period the amount of oxidant does not increase, therefor it has all transferred to the HMDM cell and the amount of cholesterol that can be oxidised is limited by the available oxidants. Comparatively the amount of cholesterol in the cell continues to increase, indicating that the cellular mechanism for cholesterol synthesis has been stimulated or that there is more cholesterol in the oxLDL particle than there is oxidant.

Figure 38 answers the question "Does 7,8-NP down-regulate foam cell formation?" This graph shows that when cells were treated with 7,8-NP as well as oxLDL the uptake doesn't go beyond basal levels. The oxLDL treated cells confirm that the cells were able to become foam cells as they had become loaded with 7-KC and cholesterol. Figure 38A portrays the cells in this preparation taking up a significant amount of 7-KC, 4-5µmoles/ mg of protein. The cholesterol was taken up in concentrations of 7nmoles/mg of protein, rather than the 20nmoles/mg of protein seen in figure 17. However in both instances, the 7,8-NP prevented the oxLDL stimulated uptake from occurring.

The research confirms that 7 8-NP decreases CD36 surface expression. Thus there is a reduction in the amount of oxLDL that can bind to cells. A reduction in oxLDL binding results in no ester uptake beyond control levels. This behavioural change in the macrophages indicated that 7,8-NP blocked the formation of foam cells.

While the literature is full of compounds that down regulate CD36 expression and foam cell formation, very few of these compounds are produced by the cells that express CD36 and are turned into foam cells. Febbraio showed that CD36-apoE double-null mice had 77% less lesion area, as well as a decrease in the binding of copper oxidised LDL to CD36 (Febbraio et al. 2000). Pietsch used lovastatin to effectively reduce CD36 cell surface expression in a human cell line (Pietsch, Erl, and Lorenz 1996). Zamora demonstrated that toll like receptor ligands can down regulate CD36 (Zamora et al. 2012). Luan demonstrated that C_2-ceramides can also down regulated CD36 (Luan and Griffiths 2006) but these are not physiological, nor are the statins. The benefit of 7,8-Dihydroneopterin as a CD36 and foam cell regulator is its protection and native proximity to the affected area (Gieseg et al. 2010).

4.8 Future Research and Summary

The aim of this thesis was to measure the intracellular lipid accumulation in HMDMs and define the "foam cell". CD36 cell surface expression was measured by flow cytometer to investigate the relationship between lipid accumulation and CD36 expression in HMDM cells. The protective ability of 7,8-NP and its effect on the CD36 expression and lipid accumulation was studied using the HPLC and flow cytometer.

A method using the HPLC was elucidated in the current study to measure the sterol ester content of the cells along with 7KC. Treatment of HMDM cells with sub toxic concentrations of oxLDL over a 48 hour period produced lipid uptake and foam cell formation. This method was developed in order to reliably and reproducibly measure foam cell formation in a human cell model.

Use of the flow cytometer to measure CD36 surface expression was key to probing the role of the receptor. Modification of published protocols was necessary due to the discovery that CD36 was not immune to Accutase™ activity. Accutase™ is an enzymatic mix with proteolytic and collagenolytic properties. Treatment of the HMDM cells with Accutase™ resulted in the reduction of the CD36 signal leading to the belief that CD36 was being removed by the Accutase™. An eventual solution treating the HMDM cells with Accutase™ and allowing them to recover for 12 hours in a suspension cell culture plate before experimenting enabled collection of CD36 data. Further research into the procedure may yield a different solution as there are unknown consequences in treating an adherent model like a suspension cell line.

Treatment of the cells with 7,8-NP resulted in a decrease in the CD36 fluorescence beyond the control levels. CD36 fluorescence levels went up when treated with oxLDL, which agreed with literature. Comparatively, chromatograms from the HPLC showed the normal uptake when treated with oxLDL and treatment with 7,8-NP retards that uptake. These two sets of data confirm that 7,8-NP reduces foam cell formation.

Future research should investigate the protective properties of 7,8-NP on organelles within the cell. Study into the exact relationship between CD36 down regulation and cholesterol and oxysterol uptake will also be refined. This will determine the reduction in CD36 surface expression that is necessary for a reduction in uptake. Focussing on the affected structures within the cell will enable the isolation of the pathway that is responsible for the protection. Once this pathway is identified, long term inhibition

studies could determine if the formation of the foam cell can be reduced in clinical settings.

The effect of oxLDL on the M1 state of the macrophages during incubation should also be investigated. Rios has shown that oxLDL treatment of M1 macrophages induces change to the M2 state. M2 macrophages are more phagocytotic and express more CD36 however are not as prone to development into foam cells (Ravi et al. 2014; Rios et al. 2013). Further study should look at incubation of macrophages with oxLDL and pro-inflammatory cytokines such as IFN-ɣ to ensure the continued pro-inflammatory, M1 state of the macrophages (Rios et al. 2013; Fenyo and Gafencu 2013).

Additional studies could probe the effect of reduction of foam cell formation on the resultant plaque formation. With the reduction in foam cell presence, the cell accumulation would be decreased and the plaque development slowed.

5 Bibliography

"Accutase." n.d. Millipore. https://www.emdmillipore.com/INTL/en/product/Accutase-cell-detachment-solution,MM_NF-SCR005.

Adachi, T., T. Naruko, A. Itoh, R. Komatsu, Y. Abe, N. Shirai, H. Yamashita, et al. 2007. "Neopterin Is Associated with Plaque Inflammation and Destabilisation in Human Coronary Atherosclerotic Lesions." *Heart (British Cardiac Society)* 93 (12): 1537–41. doi:10.1136/hrt.2006.109736.

Aldred, Sarah, and Helen R. Griffiths. 2004. "Oxidation of Protein in Human Low-Density Lipoprotein Exposed to Peroxyl Radicals Facilitates Uptake by Monocytes; Protection by Antioxidants in Vitro." *Environmental Toxicology and Pharmacology* 15 (2–3): 111–17. doi:10.1016/j.etap.2003.11.006.

Alessio, Massimo, Lucia De Monte, Alessandra Scirea, Paola Gruarin, Narendra N. Tandon, and Roberto Sitia. 1996. "Synthesis, Processing, and Intracellular Transport of CD36 during Monocytic Differentiation." *Journal of Biological Chemistry* 271 (3): 1770–75. doi:10.1074/jbc.271.3.1770.

Amit, Zunika. 2008. "A Model of Complex Plaque Formation: 7, 8-Dihydroneopterin Protects Human Monocyte-Derived Macrophages from Oxidised Low Density Lipoprotein-Induced Death." http://ir.canterbury.ac.nz/handle/10092/2328.

Andrew J, and Wendy Jessup. 1999. "Oxysterols and Atherosclerosis." *Atherosclerosis* 142 (1): 1–28. doi:10.1016/S0021-9150(98)00196-8.

Aviram, M. 1992. "Low Density Lipoprotein Modification by Cholesterol Oxidase Induces Enhanced Uptake and Cholesterol Accumulation in Cells." *Journal of Biological Chemistry* 267 (1): 218–25.

Baird, Sarah K., Linzi Reid, Mark B. Hampton, and Steven P. Gieseg. 2005. "OxLDL Induced Cell Death Is Inhibited by the Macrophage Synthesised Pterin, 7,8-Dihydroneopterin, in U937 Cells but Not THP-1 Cells." *Biochimica et Biophysica Acta (BBA) - Molecular Cell Research* 1745 (3): 361–69. doi:10.1016/j.bbamcr.2005.07.001.

Berdowska, A., and K. Zwirska-Korczala. 2001. "Neopterin Measurement in Clinical Diagnosis." *Journal of Clinical Pharmacy and Therapeutics* 26 (5): 319–29. doi:10.1046/j.1365-2710.2001.00358.x.

Brown, A. J., R. T. Dean, and W. Jessup. 1996. "Free and Esterified Oxysterol: Formation during Copper-Oxidation of Low Density Lipoprotein and Uptake by Macrophages." *Journal of Lipid Research* 37 (2): 320–35.

Brown, Andrew J., Erin L. Mander, Ingrid C. Gelissen, Leonard Kritharides, Roger T. Dean, and Wendy Jessup. 2000. "Cholesterol and Oxysterol Metabolism and Subcellular Distribution in Macrophage Foam Cells: Accumulation of Oxidized Esters in Lysosomes." *Journal of Lipid Research* 41 (2): 226–36.

Brown, Andrew J., Gerald F. Watts, John R. Burnett, Roger T. Dean, and Wendy Jessup. 2000. "Sterol 27-Hydroxylase Acts on 7-Ketocholesterol in Human Atherosclerotic Lesions and Macrophages in Culture." *Journal of Biological Chemistry* 275 (36): 27627–33. doi:10.1074/jbc.M004060200.

Chávez-Sánchez, Luis, Montserrat Guadalupe Garza-Reyes, José Esteban Espinosa-Luna, Karina Chávez-Rueda, María Victoria Legorreta-Haquet, and Francisco Blanco-Favela. 2014. "The Role of TLR2, TLR4 and CD36 in Macrophage Activation and Foam Cell Formation in Response to oxLDL in Humans." *Human Immunology* 75 (4): 322–29. doi:10.1016/j.humimm.2014.01.012.

Chu, Eugene M., Daven C. Tai, Jennifer L. Beer, and John S. Hill. 2013. "Macrophage Heterogeneity and Cholesterol Homeostasis: Classically-Activated Macrophages Are Associated with Reduced Cholesterol Accumulation Following Treatment with Oxidized LDL." *Biochimica et Biophysica Acta (BBA) - Molecular and Cell Biology of Lipids* 1831 (2): 378–86. doi:10.1016/j.bbalip.2012.10.009.

Collot-Teixeira, Sophie, Juliette Martin, Chris McDermott-Roe, Robin Poston, and John Louis McGregor. 2007. “CD36 and Macrophages in Atherosclerosis.” *Cardiovascular Research* 75 (3): 468–77. doi:10.1016/j.cardiores.2007.03.010.

Cookson, F. B. 1971. “The Origin of Foam Cells in Atherosclerosis.” *British Journal of Experimental Pathology* 52 (1): 62–69.

Dean, R. T., S. Fu, R. Stocker, and M. J. Davies. 1997. “Biochemistry and Pathology of Radical-Mediated Protein Oxidation.” *Biochemical Journal* 324 (Pt 1): 1.

Dotan, Y, D Lichtenberg, and I Pinchuk. 2004. “Lipid Peroxidation Cannot Be Used as a Universal Criterion of Oxidative Stress.” *Progress in Lipid Research* 43 (3): 200–227. doi:10.1016/j.plipres.2003.10.001.

Endemann, Gerda, Lawrence Stanton, Kip Madden, Carmen Bryant, R. Tyler White, and Andrew Protter. 1993. “CD36 Is a Receptor for Oxidized Low Density Lipoprotein.” *The Journal of Biological Chemistry* 268 (June 5): 11811–16.

Febbraio, Maria, David P. Hajjar, and Roy L. Silverstein. 2001. “CD36: A Class B Scavenger Receptor Involved in Angiogenesis, Atherosclerosis, Inflammation, and Lipid Metabolism.” *Journal of Clinical Investigation* 108 (6): 785–91. doi:10.1172/JCI200114006.

Febbraio, Maria, Eugene A. Podrez, Jonathan D. Smith, David P. Hajjar, Stanley L. Hazen, Henry F. Hoff, Kavita Sharma, and Roy L. Silverstein. 2000. “Targeted Disruption of the Class B Scavenger Receptor CD36 Protects against Atherosclerotic Lesion Development in Mice.” *Journal of Clinical Investigation* 105 (8): 1049–56.

Febbraio, Maria, and Roy L. Silverstein. 2007. “CD36: Implications in Cardiovascular Disease.” *The International Journal of Biochemistry & Cell Biology* 39 (11): 2012–30. doi:10.1016/j.biocel.2007.03.012.

Fenyo, Ioana Madalina, and Anca Violeta Gafencu. 2013. “The Involvement of the Monocytes/macrophages in Chronic Inflammation Associated with Atherosclerosis.” *Immunobiology* 218 (11): 1376–84. doi:10.1016/j.imbio.2013.06.005.

Firth, Carole A., Elizabeth M. Crone, Elizabeth A. Flavall, Justin A. Roake, and Steven P. Gieseg. 2008. “Macrophage Mediated Protein Hydroperoxide Formation and Lipid Oxidation in Low Density Lipoprotein Are Inhibited by the Inflammation Marker 7,8-Dihydroneopterin.” *Biochimica et Biophysica Acta (BBA) - Molecular Cell Research* 1783 (6): 1095–1101. doi:10.1016/j.bbamcr.2008.02.010.

Firth, Carole A., Andrew D. Laing, Sarah K. Baird, Joseph Pearson, and Steven P. Gieseg. 2008. “Inflammatory Sites as a Source of Plasma Neopterin: Measurement of High Levels of Neopterin and Markers of Oxidative Stress in Pus Drained from Human Abscesses.” *Clinical Biochemistry* 41 (13): 1078–83. doi:10.1016/j.clinbiochem.2008.06.008.

Flavall, Elizabeth A., Elizabeth M. Crone, Grant A. Moore, and Steven P. Gieseg. 2008. “Dissociation of Neopterin and 7,8-Dihydroneopterin from Plasma Components before HPLC Analysis.” *Journal of Chromatography B* 863 (1): 167–71. doi:10.1016/j.jchromb.2007.12.019.

Gardner, Malcolm J., Neil Hall, Eula Fung, Owen White, Matthew Berriman, Richard W. Hyman, Jane M. Carlton, et al. 2002. “Genome Sequence of the Human Malaria Parasite Plasmodium Falciparum.” *Nature* 419 (6906): 498–511. doi:10.1038/nature01097.

Garner, Brett, Anna Baoutina, Roger T Dean, and Wendy Jessup. 1997. “Regulation of Serum-Induced Lipid Accumulation in Human Monocyte-Derived Macrophages by Interferon-γ. Correlations with Apolipoprotein E Production, Lipoprotein Lipase Activity and LDL Receptor-Related Protein Expression.” *Atherosclerosis* 128 (1): 47–58. doi:10.1016/S0021-9150(96)05979-5.

Gaus, Katharina, J. Justin Gooding, Roger T. Dean, Leonard Kritharides, and Wendy Jessup. 2001. “A Kinetic Model to Evaluate Cholesterol Efflux from THP-1 Macrophages to Apolipoprotein A-1 †.” *Biochemistry* 40 (31): 9363–73. doi:10.1021/bi010323n.

Genet, Rebecca May. 2010. “A Study of Oxidation and Inflammation Using Plaque and Plasma of Vascular Disease Patients.” http://ir.canterbury.ac.nz/handle/10092/5809.

Gieseg, Steven P., Zunika Amit, Ya-Ting Yang, Anastasia Shchepetkina, and Hanadi Katouah. 2010. “Oxidant Production, oxLDL Uptake, and CD36 Levels in Human Monocyte–derived Macrophages Are Downregulated by the Macrophage-Generated Antioxidant 7, 8-Dihydroneopterin.” *Antioxidants & Redox Signaling* 13 (10): 1525–34.

Gieseg, Steven P., and Hermann Esterbauer. 1994. “Low Density Lipoprotein Is Saturable by pro-Oxidant Copper.” *FEBS Letters* 343 (3): 188–94. doi:10.1016/0014-5793(94)80553-9.

Gieseg, Steven P., Gilbert Reibnegger, Helmut Wachter, and Hermann Esterbauer. 1995. “7,8 Dihydroneopterin Inhibits Low Density Lipoprotein Oxidation in Vitro. Evidence That This Macrophage Secreted Pteridine Is an Anti-Oxidant.” *Free Radical Research* 23 (2): 123–36. doi:10.3109/10715769509064027.

Gieseg, Steven P., Jacqueline Whybrow, Dylan Glubb, and Chris Rait. 2001. “Protection of U937 Cells from Free Radical Damage by the Macrophage Synthesized Antioxidant 7, 8-Dihydroneopterin.” *Free Radical Research* 35 (3): 311–18.

Goldin, Alison, Joshua A. Beckman, Ann Marie Schmidt, and Mark A. Creager. 2006. “Advanced Glycation End Products Sparking the Development of Diabetic Vascular Injury.” *Circulation* 114 (6): 597–605. doi:10.1161/CIRCULATIONAHA.106.621854.

Goldstein, Joseph L., and Michael S. Brown. 1990. “Regulation of the Mevalonate Pathway.” *Nature* 343 (6257): 425–30. doi:10.1038/343425a0.

Gordon, Siamon, and Philip R. Taylor. 2005. “Monocyte and Macrophage Heterogeneity.” *Nature Reviews Immunology* 5 (12): 953–64. doi:10.1038/nri1733.

Greig, Fiona H., Simon Kennedy, and Corinne M. Spickett. 2012. “Physiological Effects of Oxidized Phospholipids and Their Cellular Signaling Mechanisms in Inflammation.” *Free Radical Biology and Medicine* 52 (2): 266–80. doi:10.1016/j.freeradbiomed.2011.10.481.

Han, J. 1997. “Native and Modified Low Density Lipoproteins Increase the Functional Expression of the Macrophage Class B Scavenger Receptor, CD36.” *Journal of Biological Chemistry* 272 (34): 21654–59. doi:10.1074/jbc.272.34.21654.

Hegyi, Laszlo, Jeremy N. Skepper, Nat R. B. Cary, and Malcolm J. Mitchinson. 1996. “Foam Cell Apoptosis and the Development of the Lipid Core of Human Atherosclerosis.” *The Journal of Pathology* 180 (4): 423–29. doi:10.1002/(SICI)1096-9896(199612)180:4<423::AID-PATH677>3.0.CO;2-1.

Huh, H. Y., S. F. Pearce, L. M. Yesner, J. L. Schindler, and R. L. Silverstein. 1996. “Regulated Expression of CD36 during Monocyte-to-Macrophage Differentiation: Potential Role of CD36 in Foam Cell Formation.” *Blood* 87 (5): 2020–28.

Jessup, W., L. Kritharides, and R. Stocker. 2004. “Lipid Oxidation in Atherogenesis: An Overview.” *Biochemical Society Transactions* 32 (1): 134–38.

Karuna, Ratna, Adriaan G. Holleboom, Mohammad M. Motazacker, Jan Albert Kuivenhoven, Ruth Frikke-Schmidt, Anne Tybjaerg-Hansen, Spiros Georgopoulos, et al. 2011. “Plasma Levels of 27-Hydroxycholesterol in Humans and Mice with Monogenic Disturbances of High Density Lipoprotein Metabolism.” *Atherosclerosis* 214 (2): 448–55. doi:10.1016/j.atherosclerosis.2010.10.042.

Kavanagh, Ian C., Carole E. Symes, Pauline Renaudin, Esther Nova, Maria Dolores Mesa, George Boukouvalas, David S. Leake, and Parveen Yaqoob. 2003. “Degree of Oxidation of Low Density Lipoprotein Affects Expression of CD36 and PPARγ, but Not Cytokine Production, by Human Monocyte-Macrophages.” *Atherosclerosis* 168 (2): 271–82. doi:10.1016/S0021-9150(03)00148-5.

Kerr, Mary E., Catherine M. Bender, and Elizabeth J. Monti. 1996. “An Introduction to Oxygen Free Radicals.” *Heart & Lung: The Journal of Acute and Critical Care* 25 (3): 200–209. doi:10.1016/S0147-9563(96)80030-6.

Kritharides, Leonard, Michele Kus, Andrew J. Brown, Wendy Jessup, and Roger T. Dean. 1996. “Hydroxypropyl-β-Cyclodextrin-Mediated Efflux of 7-Ketocholesterol from Macrophage Foam Cells.” *Journal of Biological Chemistry* 271 (44): 27450–55.

Kritharides, L., W. Jessup, J. Gifford, and R.T. Dean. 1993. “A Method for Defining the Stages of Low-Density Lipoprotein Oxidation by the Separation of Cholesterol and Cholesteryl Ester-Oxidation Products Using HPLC.” *Analytical Biochemistry* 213 (1): 79–89. doi:10.1006/abio.1993.1389.

Kruth, Howard S. 2001. “1. Abstract 2. Introduction 3. Nature of Lipid in Foam Cells 4. Sources of Cholesterol That Accumulates in Foam Cells 5. Significance of Foam Cell Formation 5.1. Trapping Lipid in Lesions versus Removing Lipid from Lesions.” *Frontiers in Bioscience* 6: d429–55.

Lee, Ha Young, Eunseo Oh, Sang Doo Kim, Jeong Kon Seo, and Yoe-Sik Bae. 2014. “Oxidized Low-Density Lipoprotein-Induced Foam Cell Formation Is Mediated by Formyl Peptide Receptor 2.” *Biochemical and Biophysical Research Communications* 443 (3): 1003–7. doi:10.1016/j.bbrc.2013.12.082.

Legein, Bart, Lieve Temmerman, Erik A. L. Biessen, and Esther Lutgens. 2013. “Inflammation and Immune System Interactions in Atherosclerosis.” *Cellular and Molecular Life Sciences* 70 (20): 3847–69. doi:10.1007/s00018-013-1289-1.

Leitinger, Norbert. 2003. “Cholesteryl Ester Oxidation Products in Atherosclerosis.” *Molecular Aspects of Medicine* 24 (4–5): 239–50. doi:10.1016/S0098-2997(03)00019-0.

Libby, P. 2002. “Inflammation and Atherosclerosis.” *Circulation* 105 (9): 1135–43. doi:10.1161/hc0902.104353.

Luan, Yingjun, and Helen R. Griffiths. 2006. “Ceramides Reduce CD36 Cell Surface Expression and Oxidised LDL Uptake by Monocytes and Macrophages.” *Archives of Biochemistry and Biophysics* 450 (1): 89–99. doi:10.1016/j.abb.2006.03.016.

Lugrin, Jérôme, Nathalie Rosenblatt-Velin, Roumen Parapanov, and Lucas Liaudet. 2014. “The Role of Oxidative Stress during Inflammatory Processes.” *Biological Chemistry* 395 (2): 203–30. doi:10.1515/hsz-2013-0241.

Martin, Céline, Michael Chevrot, Hélène Poirier, Patricia Passilly-Degrace, Isabelle Niot, and Philippe Besnard. 2011. “CD36 as a Lipid Sensor.” *Physiology & Behavior* 105 (1): 36–42. doi:10.1016/j.physbeh.2011.02.029.

Mattsson, L, H Johansson, M Ottosson, G Bondjers, and O Wiklund. 1993. “Expression of Lipoprotein Lipase mRNA and Secretion in Macrophages Isolated from Human Atherosclerotic Aorta.” *Journal of Clinical Investigation* 92 (4): 1759–65. doi:10.1172/JCI116764.

Maxwell, Simon R. J., and Gregory Y. H. Lip. 2003. “Free Radicals and Antioxidants in Cardiovascular Disease.” *British Journal of Clinical Pharmacology* 44 (4): 307–17. doi:10.1046/j.1365-2125.1997.t01-1-00594.x.

Moore, Kathryn J., Vidya V. Kunjathoor, Stephanie L. Koehn, Jennifer J. Manning, Anita A. Tseng, Jessica M. Silver, Mary McKee, and Mason W. Freeman. 2005. “Loss of Receptor-Mediated Lipid Uptake via Scavenger Receptor A or CD36 Pathways Does Not Ameliorate Atherosclerosis in Hyperlipidemic Mice.” *Journal of Clinical Investigation* 115 (8): 2192–2201. doi:10.1172/JCI24061.

Morris, Devin, Melissa Khurasany, Thien Nguyen, John Kim, Frederick Guilford, Rucha Mehta, Dennis Gray, Beatrice Saviola, and Vishwanath Venketaraman. 2013. “Glutathione and Infection.” *Biochimica et Biophysica Acta (BBA) - General Subjects*, Cellular functions of glutathione, 1830 (5): 3329–49. doi:10.1016/j.bbagen.2012.10.012.

Nagano, Yutaka, Hidenori Arai, and Toru Kita. 1991. “High Density Lipoprotein Loses Its Effect to Stimulate Efflux of Cholesterol from Foam Cells after Oxidative Modification.” *Proceedings of the National Academy of Sciences* 88 (15): 6457–61.

Nguyen-Khoa, Thao, Ziad A. Massy, Véronique Witko-Sarsat, Sandrine Canteloup, Messeret Kebede, Bernard Lacour, Tilman Drüeke, and Béatrice Descamps-Latscha. 1999. “Oxidized Low-Density Lipoprotein Induces Macrophage Respiratory Burst via Its Protein Moiety: A Novel Pathway in Atherogenesis?” *Biochemical and Biophysical Research Communications* 263 (3): 804–9.

Nicholson, Andrew C., and David P. Hajjar. 2004. “CD36, Oxidized LDL and PPARγ: Pathological Interactions in Macrophages and Atherosclerosis.” *Vascular Pharmacology* 41 (4-5): 139–46. doi:10.1016/j.vph.2004.08.003.

Noguchi, Noriko, Rika Numano, Hajime Kaneda, and Etsuo Niki. 1998. “Oxidation of Lipids in Low Density Lipoprotein Particles.” *Free Radical Research* 29 (1): 43–52. doi:10.1080/10715769800300061.

Oettl, Karl, Sergey Dikalov, Hans-Joachim Freisleben, Walter Mlekusch, and Gilbert Reibnegger. 1997. “Spin Trapping Study of Antioxidant Properties of Neopterin and 7,8-Dihydroneopterin.” *Biochemical and Biophysical Research Communications* 234 (3): 774–78. doi:10.1006/bbrc.1997.6712.

Ouchi, Noriyuki, Shinji Kihara, Yukio Arita, Makoto Nishida, Akifumi Matsuyama, Yoshihisa Okamoto, Masato Ishigami, et al. 2001. “Adipocyte-Derived Plasma Protein, Adiponectin, Suppresses Lipid Accumulation and Class A Scavenger Receptor Expression in Human Monocyte-Derived Macrophages.” *Circulation* 103 (8): 1057–63. doi:10.1161/01.CIR.103.8.1057.

Özer, Nesrin Kartal, Yesim Negis, Nurgül Aytan, Luis Villacorta, Roberta Ricciarelli, Jean-Marc Zingg, and Angelo Azzi. 2006. “Vitamin E Inhibits CD36 Scavenger Receptor Expression in Hypercholesterolemic Rabbits.” *Atherosclerosis* 184 (1): 15–20. doi:10.1016/j.atherosclerosis.2005.03.050.

Park, Young Mi, Judith A. Drazba, Amit Vasanji, Thomas Egelhoff, Maria Febbraio, and Roy L. Silverstein. 2012. “Oxidized LDL/CD36 Interaction Induces Loss of Cell Polarity and Inhibits Macrophage Locomotion.” *Molecular Biology of the Cell* 23 (16): 3057–68.

Pietsch, Angelika, Wolfgang Erl, and Reinhard L Lorenz. 1996. “Lovastatin Reduces Expression of the Combined Adhesion and Scavenger Receptor CD36 in Human Monocytic Cells.” *Biochemical Pharmacology* 52 (3): 433–39. doi:10.1016/0006-2952(96)00245-6.

Podrez, Eugene A., David Schmitt, Henry F. Hoff, and Stanley L. Hazen. 1999. “Myeloperoxidase-Generated Reactive Nitrogen Species Convert LDL into an Atherogenic Form in Vitro.” *Journal of Clinical Investigation* 103 (11): 1547–60. doi:10.1172/JCI5549.

Rahman, Misha, Andy Lane, Angie Swindell, and Sarah Bartram. 2006. “Introduction to Flow Cytometry.” Serotec Ltd.

Ravi, Saranya, Tanecia Mitchell, Philip A. Kramer, Balu Chacko, and Victor M. Darley-Usmar. 2014. “Mitochondria in Monocytes and Macrophages-Implications for Translational and Basic Research.” *The International Journal of Biochemistry & Cell Biology* 53 (August): 202–7. doi:10.1016/j.biocel.2014.05.019.

Rhainds, David, and Louise Brissette. 2004. “The Role of Scavenger Receptor Class B Type I (SR-BI) in Lipid Trafficking. Defining the Rules for Lipid Traders.” *The International Journal of Biochemistry & Cell Biology* 36 (1): 39–77.

Rios, Francisco J., Marianna M. Koga, Mateus Pecenin, Matheus Ferracini, Magnus Gidlund, and S. Jancar. 2013. “Oxidized LDL Induces Alternative Macrophage Phenotype through Activation of CD36 and PAFR.” *Mediators of Inflammation* 2013: 1–8. doi:10.1155/2013/198193.

Roger, Véronique L., Alan S. Go, Donald M. Lloyd-Jones, Emelia J. Benjamin, Jarett D. Berry, William B. Borden, Dawn M. Bravata, et al. 2012. “Heart Disease and Stroke Statistics—2012 Update A Report From the American Heart Association.” *Circulation* 125 (1): e2–220. doi:10.1161/CIR.0b013e31823ac046.

Rusiñol, Antonio E., Lin Yang, Douglas Thewke, Sankhavaram R. Panini, Marianne F. Kramer, and Michael S. Sinensky. 2000. “Isolation of a Somatic Cell Mutant Resistant to the Induction of Apoptosis by Oxidized Low Density Lipoprotein.” *Journal of Biological Chemistry* 275 (10): 7296–7303.

Saha, Prakash, Bijan Modarai, Julia Humphries, Katherine Mattock, Matthew Waltham, Kevin G Burnand, and Alberto Smith. 2009. “The Monocyte/macrophage as a Therapeutic Target in Atherosclerosis.” *Current Opinion in Pharmacology* 9 (2): 109–18. doi:10.1016/j.coph.2008.12.017.

Schumacher, Martin, Gabriele Halwachs, Franz Tatzber, Friedrich M Fruhwald, Robert Zweiker, Norbert Watzinger, Bernd Eber, Martie Wilders-Truschnig, Hermann Esterbauer, and Werner Klein. 1997. “Increased Neopterin in Patients With Chronic and Acute Coronary Syndromes.” *Journal of the American College of Cardiology* 30 (3): 703–7. doi:10.1016/S0735-1097(97)00172-1.

Shapiro, Howard. 2003. *Practical Flow Cytometry*. Fourth. Wiley-Liss.

Shchepetkina, Anastasia. 2013. “Mechanisms of 7, 8-Dihydroneopterin Protection of Macrophages from Cytotoxicity.” Christchurch: Canterbury.

Silverstein, Roy L., Wei Li, Young Mi Park, and S. Ohidar Rahaman. 2010. “Mechanisms of Cell Signaling by the Scavenger Receptor CD36: Implications in Atherosclerosis and Thrombosis.” *Transactions of the American Clinical and Climatological Association* 121: 206.

Sugioka, Kenichi, Takahiko Naruko, Yoshiki Matsumura, Nobuyuki Shirai, Takeshi Hozumi, Minoru Yoshiyama, and Makiko Ueda. 2010. “Neopterin and Atherosclerotic Plaque Instability in Coronary and Carotid Arteries.” *Journal of Atherosclerosis and Thrombosis* 17 (11): 1115–21. doi:10.5551/jat.4606.

Thorne, Rick F., Nizar M. Mhaidat, Kylie J. Ralston, and Gordon F. Burns. 2007. “CD36 Is a Receptor for Oxidized High Density Lipoprotein: Implications for the Development of Atherosclerosis.” *Febs Letters* 581 (6): 1227–32. doi:10.1016/j.febslet.2007.02.043.

Tiwari, R.l., V. Singh, and M.k. Barthwal. 2008. “Macrophages: An Elusive yet Emerging Therapeutic Target of Atherosclerosis.” *Medicinal Research Reviews* 28 (4): 483–544. doi:10.1002/med.20118.

Venugopal, S. 2004. “RRR-?-Tocopherol Decreases the Expression of the Major Scavenger Receptor, CD36, in Human Macrophages via Inhibition of Tyrosine Kinase (Tyk2).” *Atherosclerosis* 175 (2): 213–20. doi:10.1016/j.atherosclerosis.2004.03.012.

Viana, M., L. Villacorta, B. Bonet, A. Indart, A. Munteanu, I. Sánchez-Vera, A. Azzi, and J.M. Zingg. 2005. “Effects of Aldehydes on CD36 Expression.” *Free Radical Research* 39 (9): 973–77. doi:10.1080/10715760500073758.

Widner, Bernhard, Christiane Mayr, Barbara Wirleitner, and Dietmar Fuchs. 2000. “Oxidation of 7,8-Dihydroneopterin by Hypochlorous Acid Yields Neopterin.” *Biochemical and Biophysical Research Communications* 275 (2): 307–11. doi:10.1006/bbrc.2000.3323.

Wintergerst, E. S., J. Jelk, and R. Asmis. 1998. “Differential Expression of CD14, CD36 and the LDL Receptor on Human Monocyte-Derived Macrophages.” *Histochemistry and Cell Biology* 110 (3): 231–41. doi:10.1007/s004180050285.

Yu, Xiao-Hua, Yu-Chang Fu, Da-Wei Zhang, Kai Yin, and Chao-Ke Tang. 2013. “Foam Cells in Atherosclerosis.” *Clinica Chimica Acta* 424 (September): 245–52. doi:10.1016/j.cca.2013.06.006.

Zamora, Carlos, Elisabet Cantó, Juan C. Nieto, M. Angels Ortiz, Candido Juarez, and Sílvia Vidal. 2012. "Functional Consequences of CD36 Downregulation by TLR Signals." *Cytokine* 60 (1): 257–65. doi:10.1016/j.cyto.2012.06.020.

6 Acknowledgments

I would like to sincerely and comprehensively thank my supervisor, Associate Professor Steven Gieseg for all his help, advice, faith and support. His guidance and the environment he created in his lab were critical in finishing this thesis. I would also like to thank my associate supervisors, Professor Barry Hock and Professor Grant Pearce, for their advice when I was at a loss.

Thanks go to the Biochemistry Department, the School of Biology and the University of Canterbury for enabling me to do this research. Thanks must also be given to the Hemochromatosis patients and the NZ Blood Bank for providing cells on a weekly basis for me to study.

I would like to thank past PhD students from the Free Radical Lab, Anastasia Shchepetkina and Tejraj Janmale who willingly and kindly passed on the knowledge gained during their PhDs. I also thank Izani Othman and Angus Lindsay who have been very wise sounding boards during my time in the lab. Of course, my sanity is completely due to the support of Craig Galilee who mitigated my slightly more insane moments in the lab and worked tirelessly to keep the FRB lab running year long. The FRB lab group members have my undying gratitude for enduring my quirks and supporting me, especially with rechecking my maths.

Finally thanks go to my family, friends and God. You pulled me through this master of biochemistry, kicking and screaming at times, so this thesis is partially your responsibility. Thanks especially to my parents who wouldn't let me wallow and to Letitia, Emma and Brian who listened endlessly to biochemistry details and didn't complain.